8

CELLULAR ENERGETICS

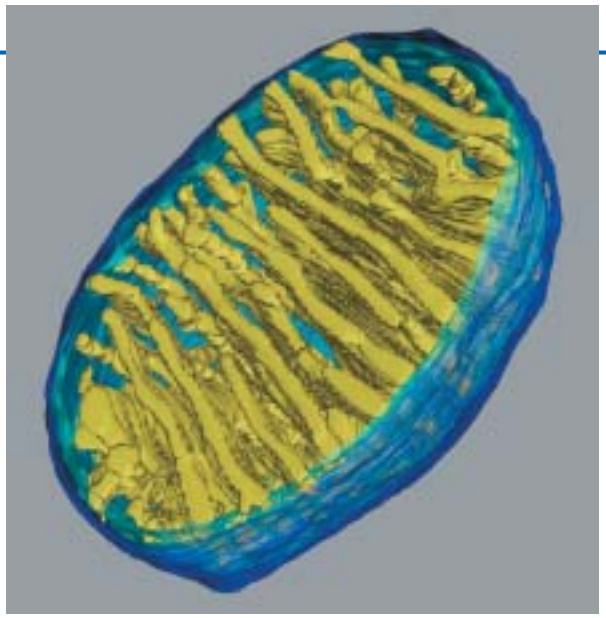

Computer-generated model of a section of a mitochondrion from chicken brain, based on a three-dimensional electron tomogram. [T. Frey and C. Mannella, 2000, *Trends Biochem. Sci.* **25:**319.]

The most important molecule for capturing and transferring free energy in biological systems is **adenosine triphosphate,** or **ATP** (see Figure 2-24). Cells use the energy released during hydrolysis of the terminal "high-energy" phosphoanhydride bond in ATP to power many energetically unfavorable processes. Examples include the synthesis of proteins from amino acids and of nucleic acids from nucleotides (Chapter 4), transport of molecules against a concentration gradient by ATP-powered pumps (Chapter 7), contraction of muscle (Chapter 19), and movement (beating) of cilia (Chapter 20). Although other high-energy molecules occur in cells, ATP is the universal "currency" of chemical energy; it is found in all types of organisms and must have occurred in the earliest life-forms.

This chapter focuses on how cells generate the high-energy phosphoanhydride bond of ATP from ADP and inorganic phosphate (HPO_4^{2-}). This endergonic reaction, which is the reverse of ATP hydrolysis and requires an input of 7.3 kcal/mol to proceed, can be written as

$$P_i^{2-} + H^+ + ADP^{3-} \longrightarrow ATP^{4-} + H_2O$$

where P_i^{2-} represents inorganic phosphate (HPO_4^{2-}). The energy to drive this reaction is produced primarily by two main processes: **aerobic oxidation,** which occurs in nearly all cells, and **photosynthesis,** which occurs only in leaf cells of plants and certain single-celled organisms.

In aerobic oxidation, fatty acids and sugars, principally glucose, are metabolized to carbon dioxide (CO_2) and water (H_2O), and the released energy is converted to the chemical energy of phosphoanhydride bonds in ATP. In animal cells and most other nonphotosynthetic cells, ATP is generated mainly by this process. The initial steps in the oxidation of glucose, called **glycolysis,** occur in the cytosol in both eukaryotes and prokaryotes and do not require oxygen (O_2). The final steps, which require oxygen, generate most of the ATP. In eukaryotes, these later stages of aerobic oxidation occur in **mitochondria;** in prokaryotes, which contain only a plasma membrane and lack internal organelles, many of the final steps occur on the plasma membrane. The final stages of fatty acid metabolism sometimes occur in mitochondria and generate ATP; in most eukaryotic cells, however, fatty acids are metabolized to CO_2 and H_2O in **peroxisomes** without production of ATP.

In photosynthesis, light energy is converted to the chemical energy of phosphoanhydride bonds in ATP and stored in the chemical bonds of carbohydrates (primarily sucrose and starch). Oxygen also is formed during photosynthesis. In

OUTLINE

plants and eukaryotic single-celled algae, photosynthesis occurs in **chloroplasts**. Several prokaryotes also carry out photosynthesis on their plasma membrane or its invaginations by a mechanism similar to that in chloroplasts. The oxygen generated during photosynthesis is the source of virtually all the oxygen in the air, and the carbohydrates produced are the ultimate source of energy for virtually all nonphotosynthetic organisms. Bacteria living in deep ocean vents, where there is no sunlight, disprove the popular view that sunlight is the ultimate source of energy for all organisms on earth. These bacteria obtain energy for converting carbon dioxide into carbohydrates and other cellular constituents by oxidation of reduced inorganic compounds in dissolved vent gas.

At first glance, photosynthesis and aerobic oxidation appear to have little in common. However, a revolutionary discovery in cell biology is that bacteria, mitochondria, and chloroplasts all use the same basic mechanism, called **chemiosmosis** (or chemiosmotic coupling), to generate ATP from ADP and P_i. In chemiosmosis, a proton (H^+) concentration gradient and an electric potential (voltage gradient) across the membrane, collectively termed the **proton-motive force,** drive an energy-requiring process such as ATP synthesis (Figure 8-1, *bottom*).

Chemiosmosis can occur only in sealed, membrane-limited compartments that are impermeable to H^+. The proton-motive force is generated by the stepwise movement of electrons from higher to lower energy states via membrane-bound **electron carriers**. In mitochondria and nonphotosynthetic bacterial cells, electrons from NADH (produced during the metabolism of sugars, fatty acids, and other substances) are transferred to O_2, the ultimate electron acceptor. In the thylakoid membrane of chloroplasts, energy absorbed from light strips electrons from water (forming O_2) and powers their movement to other electron carriers, particularly $NADP^+$; eventually these electrons are donated to CO_2 to synthesize carbohydrates. All these systems, however, contain some similar carriers that couple **electron transport** to the pumping of protons across the membrane—always from the **cytosolic face** to the **exoplasmic face** of the membrane—thereby generating the proton-motive force (Figure 8-1, *top*). Invariably, the cytosolic face has a negative electric potential relative to the exoplasmic face.

Moreover, mitochondria, chloroplasts, and bacteria utilize essentially the same kind of membrane protein, the **F_0F_1 complex,** to synthesize ATP. The F_0F_1 complex, now commonly called **ATP synthase,** is a member of the F class of ATP-powered proton pumps (see Figure 7-6). In all cases, ATP synthase is positioned with the globular F_1 domain, which catalyzes ATP synthesis, on the cytosolic face of the membrane, so ATP is always formed on the cytosolic face of the membrane (Figure 8-2). Protons always flow through ATP synthase from the exoplasmic to the cytosolic face of the membrane, driven by a combination of the proton concentration gradient ($[H^+]_{exoplasmic} > [H^+]_{cytosolic}$) and the membrane electric potential (exoplasmic face positive with respect to the cytosolic face).

These commonalities between mitochondria, chloroplasts, and bacteria undoubtedly have an evolutionary origin. In bacteria both photosynthesis and oxidative phosphorylation occur on the plasma membrane. Analysis of the sequences and transcription of mitochondrial and chloroplast DNAs (Chapters 10 and 11) has given rise to the popular hypothesis that these organelles arose early in the evolution of eukaryotic cells by endocytosis of bacteria capable of oxidative phosphorylation or photosynthesis, respectively (Figure 8-3). According to this *endosymbiont*

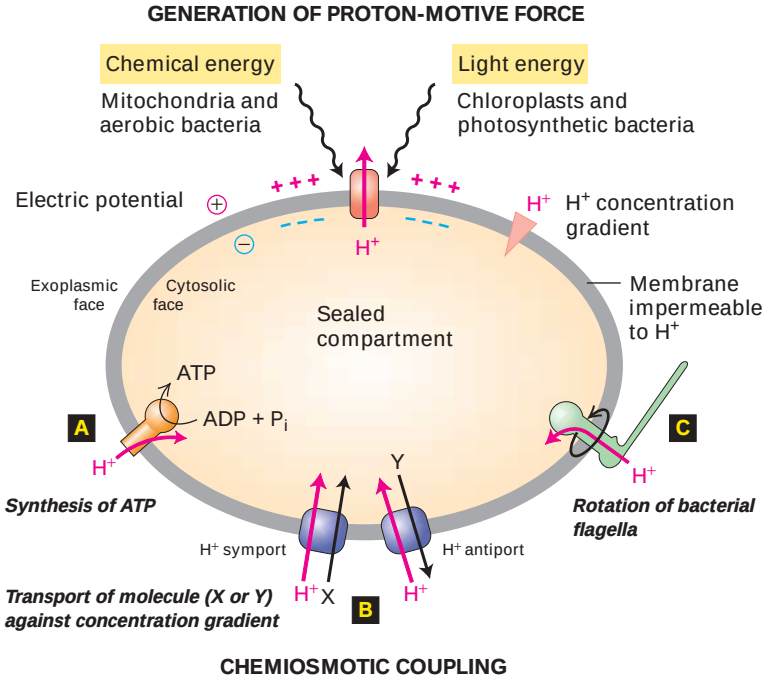

▶ FIGURE 8-1 **Overview of the generation and utilization of a proton-motive force.** A transmembrane proton concentration gradient and a voltage gradient, collectively called the *proton-motive force,* are generated during photosynthesis and the aerobic oxidation of carbon compounds in mitochondria and aerobic bacteria. In chemiosmotic coupling, a proton-motive force powers an energy-requiring process such as ATP synthesis (A), transport of metabolites across the membrane against their concentration gradient (B), or rotation of bacterial flagella (C).

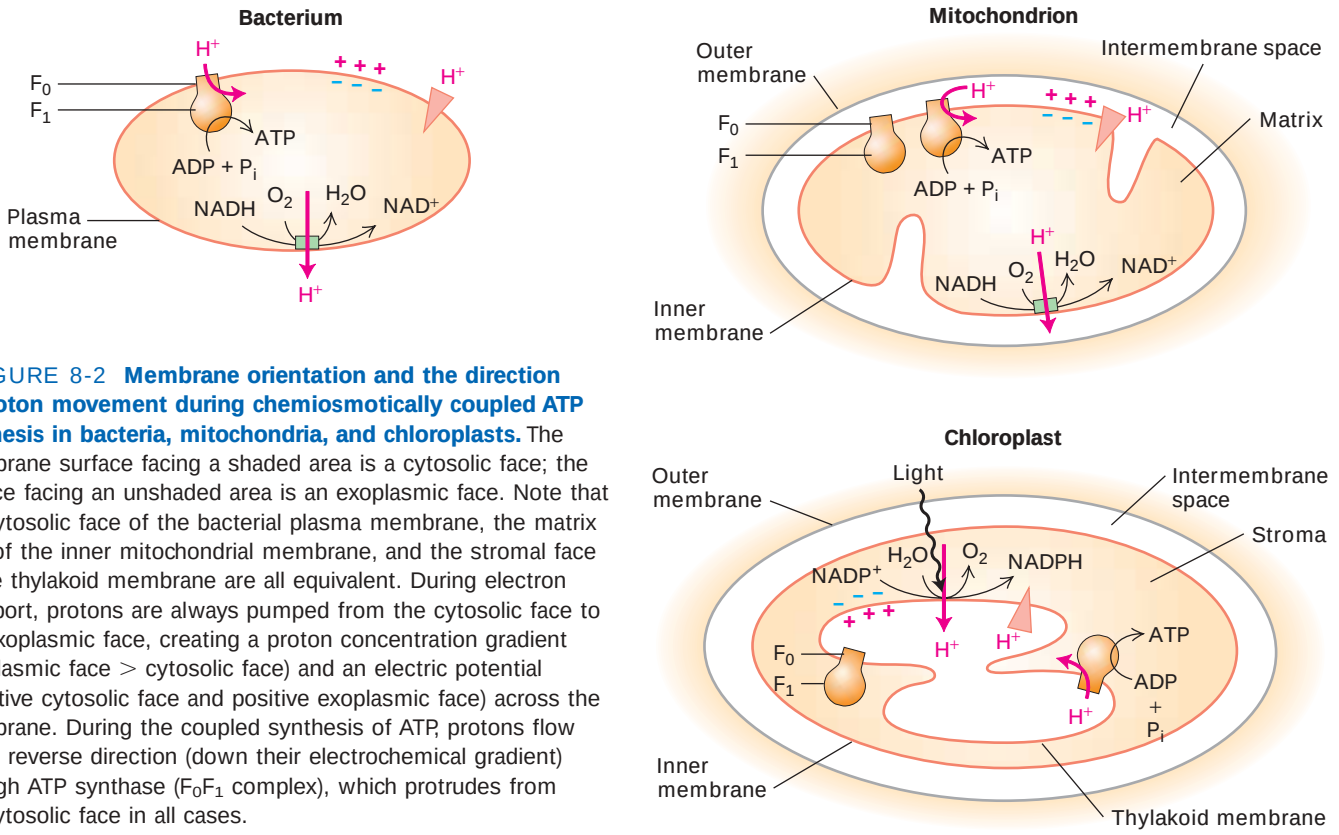

▲ FIGURE 8-2 **Membrane orientation and the direction of proton movement during chemiosmotically coupled ATP synthesis in bacteria, mitochondria, and chloroplasts.** The membrane surface facing a shaded area is a cytosolic face; the surface facing an unshaded area is an exoplasmic face. Note that the cytosolic face of the bacterial plasma membrane, the matrix face of the inner mitochondrial membrane, and the stromal face of the thylakoid membrane are all equivalent. During electron transport, protons are always pumped from the cytosolic face to the exoplasmic face, creating a proton concentration gradient (exoplasmic face > cytosolic face) and an electric potential (negative cytosolic face and positive exoplasmic face) across the membrane. During the coupled synthesis of ATP, protons flow in the reverse direction (down their electrochemical gradient) through ATP synthase (F_0F_1 complex), which protrudes from the cytosolic face in all cases.

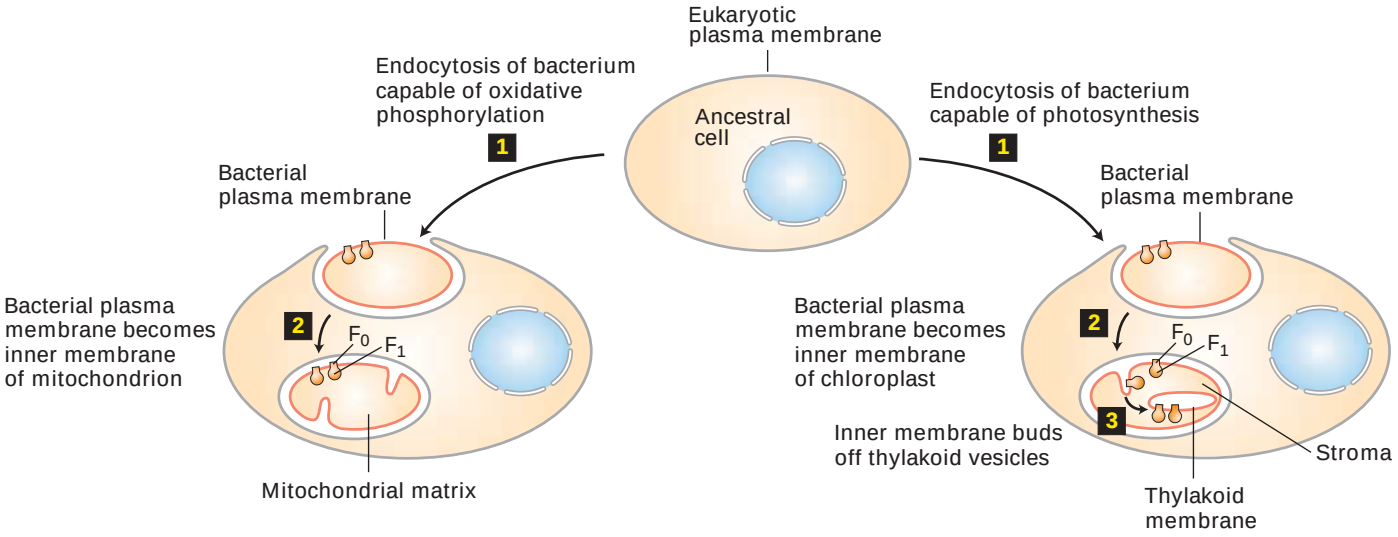

▲ FIGURE 8-3 **Evolutionary origin of mitochondria and chloroplasts according to endosymbiont hypothesis.** Membrane surfaces facing a shaded area are cytosolic faces; surfaces facing an unshaded area are exoplasmic faces. Endocytosis of a bacterium by an ancestral eukaryotic cell would generate an organelle with two membranes, the outer membrane derived from the eukaryotic plasma membrane and the inner one from the bacterial membrane. The F_1 subunit of ATP synthase, localized to the cytosolic face of the bacterial membrane, would then face the matrix of the evolving mitochondrion *(left)* or chloroplast *(right)*. Budding of vesicles from the inner chloroplast membrane, such as occurs during development of chloroplasts in contemporary plants, would generate the thylakoid vesicles with the F_1 subunit remaining on the cytosolic face, facing the chloroplast stroma.

hypothesis, the inner mitochondrial membrane would be derived from the bacterial plasma membrane with the globular F_1 domain still on its cytosolic face pointing toward the matrix space of the mitochondrion. Similarly, the globular F_1 domain would be on the cytosolic face of the thylakoid membrane facing the stromal space of the chloroplast.

In addition to powering ATP synthesis, the proton-motive force can supply energy for the transport of small molecules across a membrane against a concentration gradient (see Figure 8-1). For example, a H^+/sugar symport protein catalyzes the uptake of lactose by certain bacteria, and proton-driven antiporters catalyze the accumulation of ions and sucrose by plant vacuoles (Chapter 7). The proton-motive force also powers the rotation of bacterial flagella. (The beating of eukaryotic cilia, however, is powered by ATP hydrolysis.) Conversely, hydrolysis of ATP by V-class ATP-powered proton pumps, which are similar in structure to F-class pumps (see Figure 7-6), provides the energy for transporting protons against a concentration gradient. Chemiosmotic coupling thus illustrates an important principle introduced in our discussion of active transport in Chapter 7: *the membrane potential, the concentration gradients of protons (and other ions) across a membrane, and the phosphoanhydride bonds in ATP are equivalent and interconvertible forms of chemical potential energy.*

In this brief overview, we've seen that oxygen and carbohydrates are produced during photosynthesis, whereas they are consumed during aerobic oxidation. In both processes, the flow of electrons creates a H^+ electrochemical gradient, or proton-motive force, that can power ATP synthesis. As we examine these two processes at the molecular level, focusing first on aerobic oxidation and then on photosynthesis, the striking parallels between them will become evident.

8.1 Oxidation of Glucose and Fatty Acids to CO_2

The complete aerobic oxidation of each molecule of glucose yields 6 molecules of CO_2 and is coupled to the synthesis of as many as 30 molecules of ATP:

$$C_6H_{12}O_6 + 6\ O_2 + 30\ P_i^{2-} + 30\ ADP^{3-} + 30\ H^+ \longrightarrow 6\ CO_2 + 30\ ATP^{4-} + 36\ H_2O$$

Glycolysis, the initial stage of glucose metabolism, takes place in the cytosol and does not involve molecular O_2. It produces a small amount of ATP and the three-carbon compound *pyruvate*. In aerobic cells, pyruvate formed in glycolysis is transported into the mitochondria, where it is oxidized by O_2 to CO_2. Via chemiosmotic coupling, the oxidation of pyruvate in the mitochondria generates the bulk of the ATP produced during the conversion of glucose to CO_2. In this section, we discuss the biochemical pathways that oxidize glucose and fatty acids to CO_2 and H_2O; the fate of the released electrons is described in the next section.

Cytosolic Enzymes Convert Glucose to Pyruvate During Glycolysis

A set of 10 water-soluble cytosolic enzymes catalyze the reactions constituting the *glycolytic pathway*, in which one molecule of glucose is converted to two molecules of pyruvate (Figure 8-4). All the metabolic intermediates between glucose and pyruvate are water-soluble phosphorylated compounds.

Four molecules of ATP are formed from ADP during glycolysis via **substrate-level phosphorylation,** which is catalyzed by enzymes in the cytosol (reactions 7 and 10). Unlike ATP formation in mitochondria and chloroplasts, a proton-motive force is not involved in substrate-level phosphorylation. Early in the glycolytic pathway, two ATP molecules are consumed: one by the addition of a phosphate residue to glucose in the reaction catalyzed by *hexokinase* (reaction 1), and another by the addition of a second phosphate to fructose 6-phosphate in the reaction catalyzed by *phosphofructokinase-1* (reaction 3). Thus glycolysis yields a net of only two ATP molecules per glucose molecule.

The balanced chemical equation for the conversion of glucose to pyruvate shows that four hydrogen atoms (four protons and four electrons) are also formed:

$$\underset{\text{Glucose}}{C_6H_{12}O_6} \longrightarrow 2\ \underset{\text{Pyruvate}}{CH_3-\overset{\overset{O}{\|}}{C}-\overset{\overset{O}{\|}}{C}-OH} + 4\ H^+ + 4\ e^-$$

(For convenience, we show pyruvate here in its un-ionized form, pyruvic acid, although at physiological pH it would be largely dissociated.) All four electrons and two of the four protons are transferred to two molecules of the oxidized form of the electron carrier **nicotinamide adenine dinucleotide** (**NAD^+**) to produce the reduced form, **NADH** (see Figure 2-26):

$$2\ H^+ + 4\ e^- + 2\ NAD^+ \longrightarrow 2\ NADH$$

The reaction that generates these hydrogen atoms and transfers them to NAD^+ is catalyzed by *glyceraldehyde 3-phosphate dehydrogenase* (see Figure 8-4, reaction 6). The overall chemical equation for this first stage of glucose metabolism is

$$C_6H_{12}O_6 + 2\ NAD^+ + 2\ ADP^{3-} + 2\ P_i^{2-} \longrightarrow 2\ C_3H_4O_3 + 2\ NADH + 2\ ATP^{4-}$$

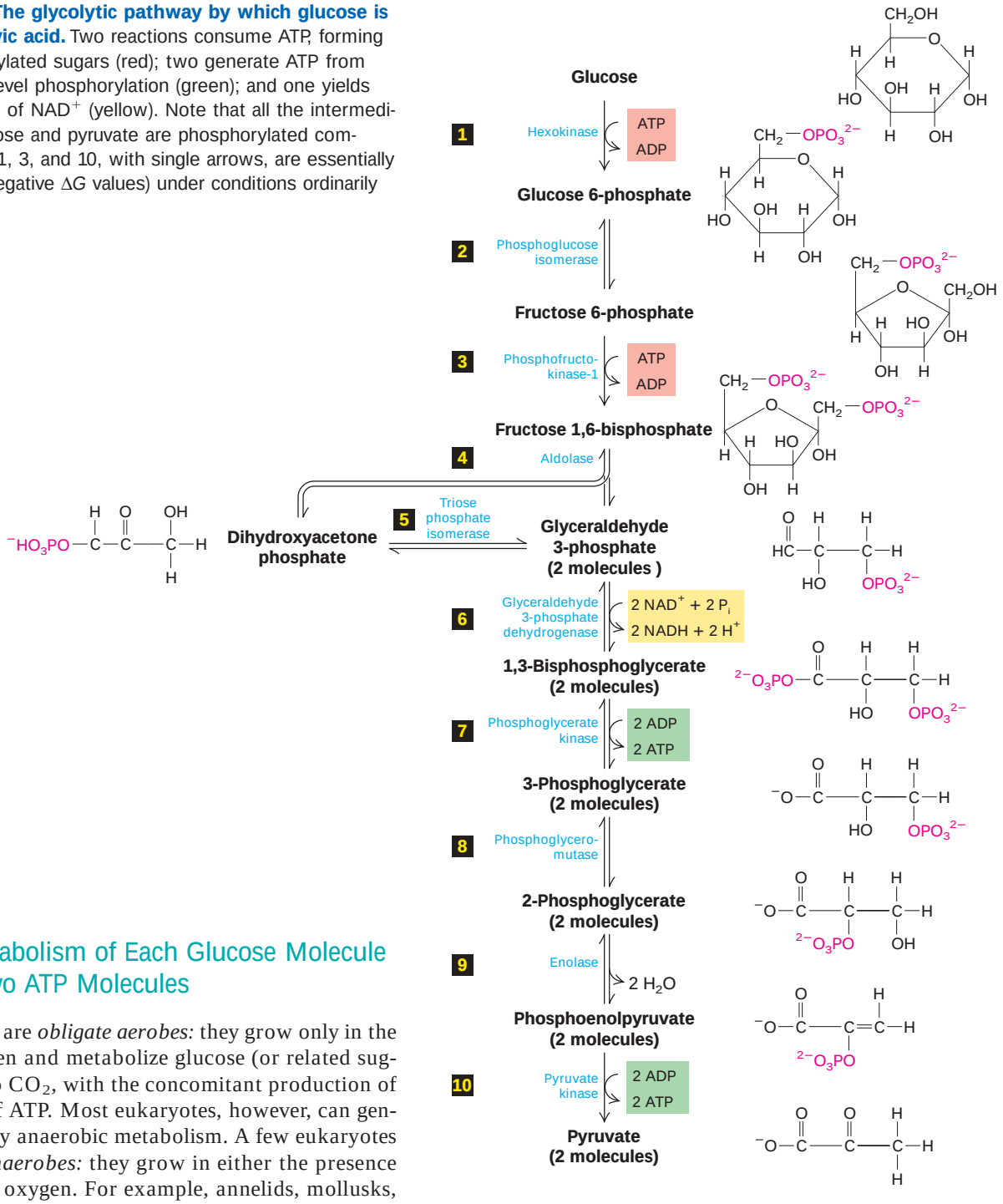

▶ FIGURE 8-4 **The glycolytic pathway by which glucose is degraded to pyruvic acid.** Two reactions consume ATP, forming ADP and phosphorylated sugars (red); two generate ATP from ADP by substrate-level phosphorylation (green); and one yields NADH by reduction of NAD^+ (yellow). Note that all the intermediates between glucose and pyruvate are phosphorylated compounds. Reactions 1, 3, and 10, with single arrows, are essentially irreversible (large negative ΔG values) under conditions ordinarily obtaining in cells.

Anaerobic Metabolism of Each Glucose Molecule Yields Only Two ATP Molecules

Many eukaryotes are *obligate aerobes:* they grow only in the presence of oxygen and metabolize glucose (or related sugars) completely to CO_2, with the concomitant production of a large amount of ATP. Most eukaryotes, however, can generate some ATP by anaerobic metabolism. A few eukaryotes are *facultative anaerobes:* they grow in either the presence or the absence of oxygen. For example, annelids, mollusks, and some yeasts can live and grow for days without oxygen.

In the absence of oxygen, facultative anaerobes convert glucose to one or more two- or three-carbon compounds, which are generally released into the surrounding medium. For instance, yeasts degrade glucose to two pyruvate molecules via glycolysis, generating a net of two ATP. In this process two NADH molecules are formed from NAD^+ per glucose molecule. In the absence of oxygen, yeasts convert pyruvate to one molecule each of ethanol and CO_2; in these reactions two NADH molecules are oxidized to NAD^+ for each two pyruvates converted to ethanol, thereby regenerating the supply of NAD^+ (Figure 8-5a, *left*). This anaerobic degradation of glucose, called *fermentation,* is the basis of beer and wine production.

During the prolonged contraction of mammalian skeletal muscle cells, when oxygen becomes limited, muscle cells

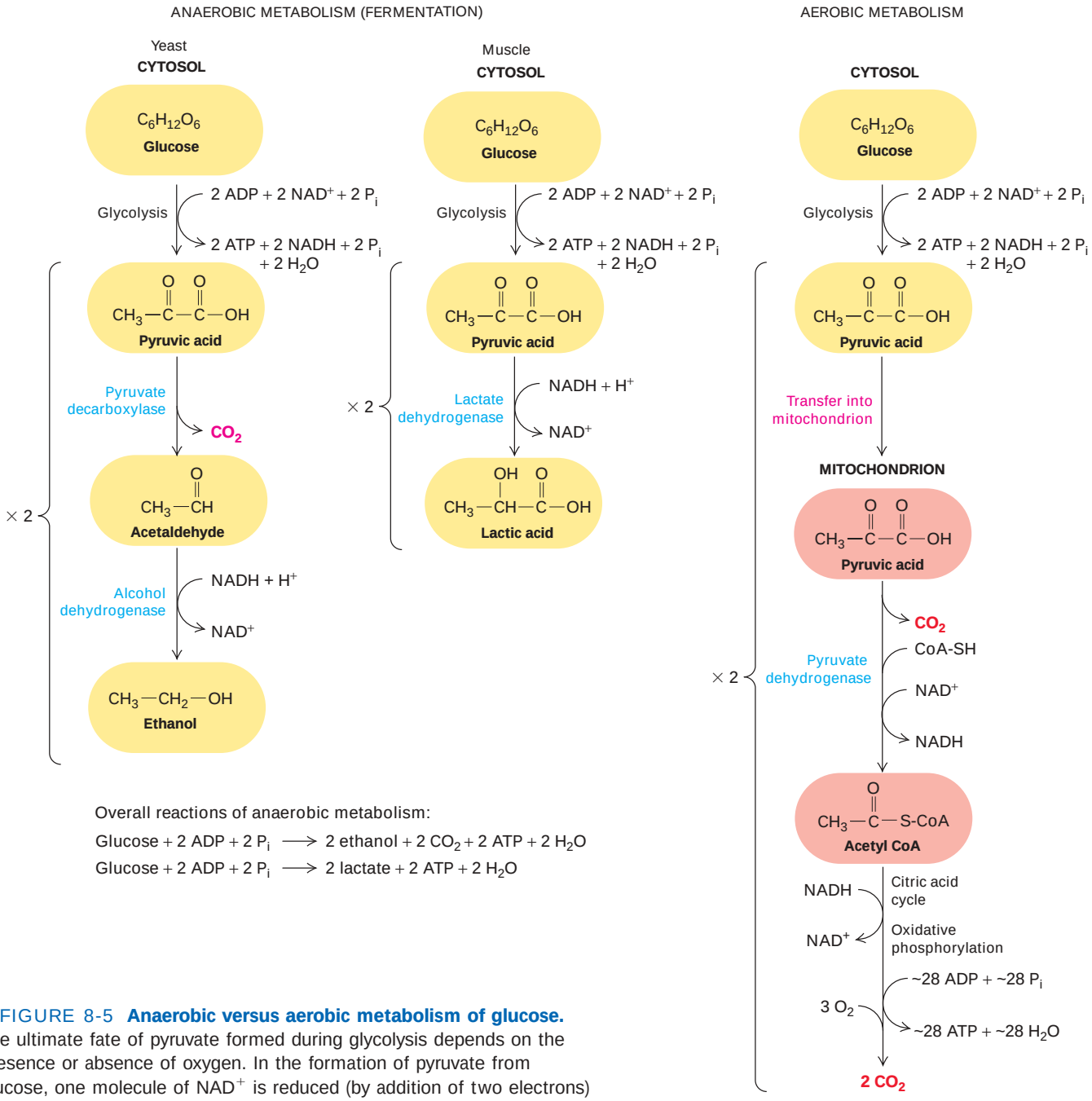

Overall reactions of anaerobic metabolism:

$$\text{Glucose} + 2\ \text{ADP} + 2\ P_i \longrightarrow 2\ \text{ethanol} + 2\ CO_2 + 2\ \text{ATP} + 2\ H_2O$$

$$\text{Glucose} + 2\ \text{ADP} + 2\ P_i \longrightarrow 2\ \text{lactate} + 2\ \text{ATP} + 2\ H_2O$$

Overall reaction of aerobic metabolism:

$$\text{Glucose} + 6\ O_2 + \sim 30\ \text{ADP} + \sim 30\ P_i \longrightarrow 6\ CO_2 + 36\ H_2O + \sim 30\ \text{ATP}$$

▲ FIGURE 8-5 **Anaerobic versus aerobic metabolism of glucose.** The ultimate fate of pyruvate formed during glycolysis depends on the presence or absence of oxygen. In the formation of pyruvate from glucose, one molecule of NAD^+ is reduced (by addition of two electrons) to NADH for each molecule of pyruvate formed (see Figure 8-4, reaction 6). (*Left*) In the absence of oxygen, two electrons are transferred from each NADH molecule to an acceptor molecule to regenerate NAD^+, which is required for continued glycolysis. In yeasts, acetaldehyde is the acceptor and ethanol is the product. This process is called *alcoholic fermentation.* When oxygen is limiting in muscle cells, NADH reduces pyruvate to form lactic acid, regenerating NAD^+. (*Right*) In the presence of oxygen, pyruvate is transported into mitochondria. First it is converted by pyruvate dehydrogenase into one molecule of CO_2 and one of acetic acid, the latter linked to coenzyme A (CoA-SH) to form acetyl CoA, concomitant with reduction of one molecule of NAD^+ to NADH. Further metabolism of acetyl CoA and NADH generates approximately an additional 28 molecules of ATP per glucose molecule oxidized.

ferment glucose to two molecules of lactic acid—again, with the net production of only two molecules of ATP per glucose molecule (Figure 8-5a, *right*). The lactic acid causes muscle and joint aches. It is largely secreted into the blood; some passes into the liver, where it is reoxidized to pyruvate and either further metabolized to CO_2 aerobically or converted to glucose. Much lactate is metabolized to CO_2 by the heart, which is highly perfused by blood and can continue aerobic metabolism at times when exercising skeletal muscles secrete lactate. Lactic acid bacteria (the organisms that "spoil" milk) and other prokaryotes also generate ATP by the fermentation of glucose to lactate.

In the presence of oxygen, however, pyruvate formed in glycolysis is transported into mitochondria, where it is oxidized by O_2 to CO_2 in a series of oxidation reactions collectively termed **cellular respiration** (Figure 8-5b). These reactions generate an estimated 28 additional ATP molecules per glucose molecule, far outstripping the ATP yield from anaerobic glucose metabolism. To understand how mitochondria operate as ATP-generating factories, we first describe their structure and then the reactions they employ to degrade pyruvate.

Mitochondria Possess Two Structurally and Functionally Distinct Membranes

Mitochondria are among the larger organelles in the cell, each one being about the size of an *E. coli* bacterium. Most eukaryotic cells contain many mitochondria, which collectively can occupy as much as 25 percent of the volume of the cytoplasm. They are large enough to be seen under a light microscope, but the details of their structure can be viewed only with the electron microscope (see Figure 5-26). The outer membrane defines the smooth outer perimeter of the mitochondrion. In contrast, the inner membrane has numerous invaginations called *cristae*. These membranes define two submitochondrial compartments: the *intermembrane space* between the outer membrane and the inner membrane with its cristae, and the *matrix*, or central compartment (Figure 8-6). The fractionation and purification of these membranes and compartments have made it possible to determine their protein and phospholipid compositions and to localize each enzyme-catalyzed reaction to a specific membrane or space.

The outer membrane contains mitochondrial *porin*, a transmembrane channel protein similar in structure to

(a)

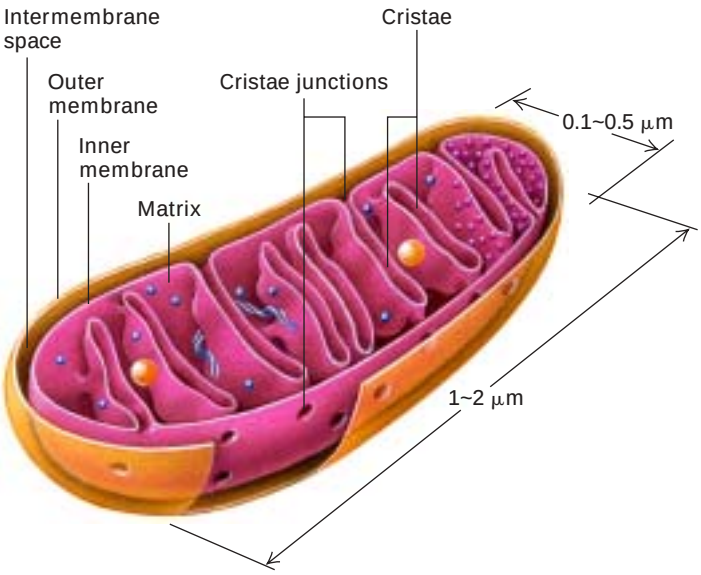

(b)

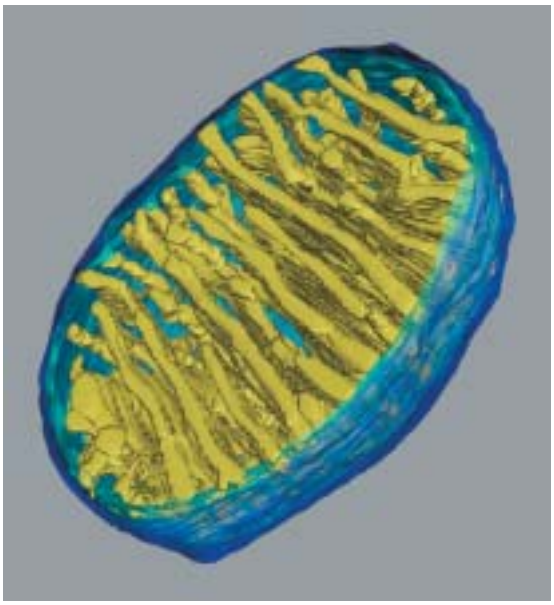

▲ FIGURE 8-6 **Internal structure of a mitochondrion.** (a) Schematic diagram showing the principal membranes and compartments. The cristae form sheets and tubes by invagination of the inner membrane and connect to the inner membrane through relatively small uniform tubular structures called *crista junctions.* The intermembrane space appears continuous with the lumen of each crista. The F_0F_1 complexes (small red spheres), which synthesize ATP, are intramembrane particles that protrude from the cristae and inner membrane into the matrix. The matrix contains the mitochondrial DNA (blue strand), ribosomes (small blue spheres), and granules (large yellow spheres). (b) Computer-generated model of a section of a mitochondrion from chicken brain. This model is based on a three-dimensional electron tomogram calculated from a series of two-dimensional electron micrographs recorded at regular angular intervals. This technique is analogous to a three-dimensional X-ray tomogram or CAT scan. Note the tightly packed cristae (yellow-green), the inner membrane (light blue), and the outer membrane (dark blue). [Part (a) courtesy of T. Frey; part (b) from T. Frey and C. Mannella, 2000, *Trends Biochem. Sci.* **25**:319.]

MEDIA CONNECTIONS
Video: Mitochondrion Reconstructed by Electron Tomography

bacterial porins (see Figure 5-14). Ions and most small molecules (up to about 5000 Da) can readily pass through these channel proteins. Although the flow of metabolites across the outer membrane may limit their rate of mitochondrial oxidation, the inner membrane and cristae are the major permeability barriers between the cytosol and the mitochondrial matrix.

Freeze-fracture studies indicate that mitochondrial cristae contain many protein-rich intramembrane particles. Some are the F_0F_1 complexes that synthesize ATP; others function in transporting electrons to O_2 from NADH or other electron carriers. Various transport proteins located in the inner membrane and cristae allow otherwise impermeable molecules, such as ADP and P_i, to pass from the cytosol to the matrix, and other molecules, such as ATP, to move from the matrix into the cytosol. Protein constitutes 76 percent of the total weight of the inner membrane—a higher fraction than in any other cellular membrane. Cardiolipin (diphosphatidyl glycerol), a lipid concentrated in the inner membrane, sufficiently reduces the membrane's permeability to protons that a proton-motive force can be established across it.

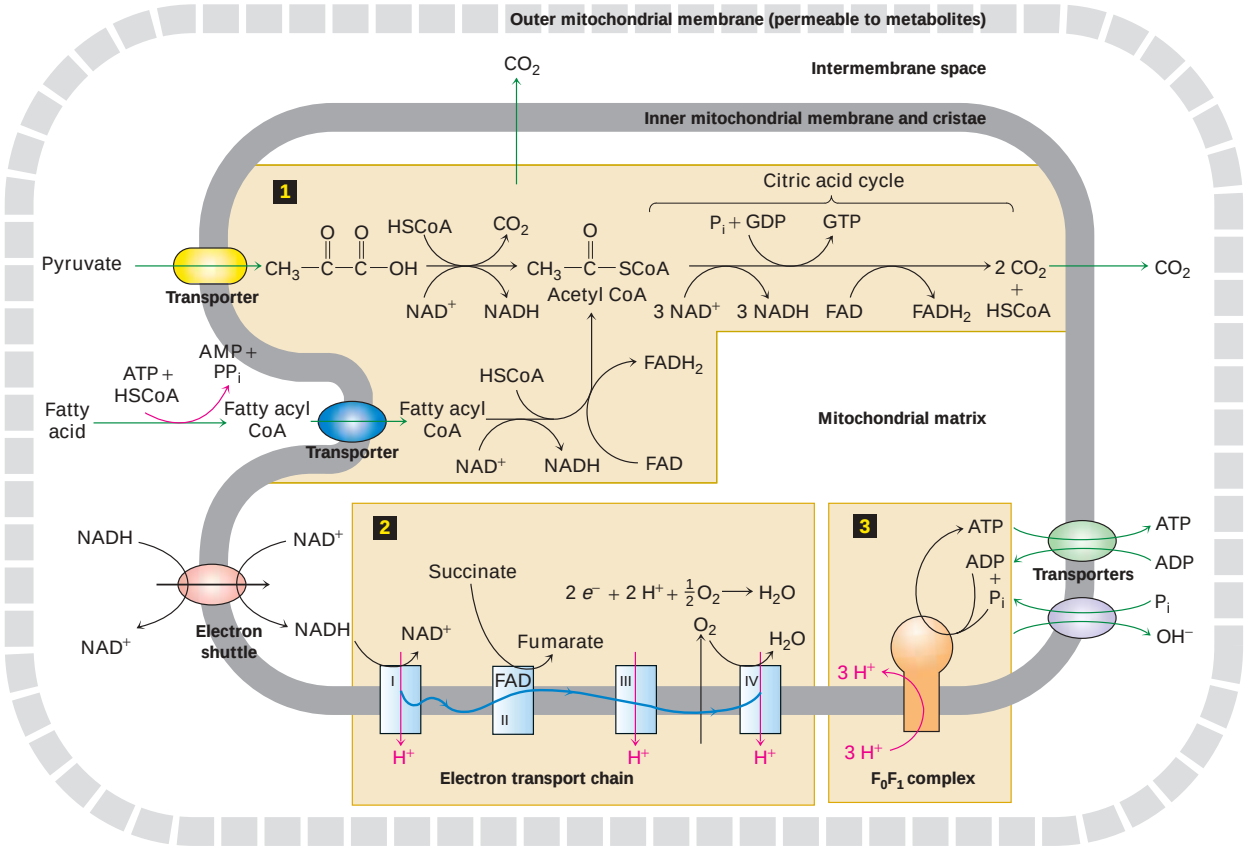

1 Pyruvate dehydrogenase, citric acid cycle, and fatty acid metabolism

2 Electron transport from NADH and $FADH_2$ to oxygen; generation of proton-motive force

3 ATP synthesis by F_0F_1 using proton-motive force

▲ FIGURE 8-7 **Summary of the aerobic oxidation of pyruvate and fatty acids in mitochondria.** The outer membrane is freely permeable to all metabolites, but specific transport proteins (colored ovals) in the inner membrane are required to import pyruvate (yellow), ADP (green), and P_i (purple) into the matrix and to export ATP (green). NADH generated in the cytosol is not transported directly to the matrix because the inner membrane is impermeable to NAD^+ and NADH; instead, a shuttle system (red) transports electrons from cytosolic NADH to NAD^+ in the matrix. O_2 diffuses into the matrix and CO_2 diffuses out. Stage 1: Fatty acyl groups are transferred from fatty acyl CoA and transported across the inner membrane via a special carrier (blue oval) and then reattached to CoA on the matrix side. Pyruvate is converted to acetyl CoA with the formation of NADH, and fatty acids (attached to CoA) are also converted to acetyl CoA with formation of NADH and FADH. Oxidation of acetyl CoA in the citric acid cycle generates NADH and $FADH_2$. Stage 2: Electrons from these reduced coenzymes are transferred via electron-transport complexes (blue boxes) to O_2 concomitant with transport of H^+ ions from the matrix to the intermembrane space, generating the proton-motive force. Electrons from NADH flow directly from complex I to complex III, bypassing complex II. Stage 3: ATP synthase, the F_0F_1 complex (orange), harnesses the proton-motive force to synthesize ATP. Blue arrows indicate electron flow; red arrows transmembrane movement of protons; and green arrows transport of metabolites.

The mitochondrial inner membrane, cristae, and matrix are the sites of most reactions involving the oxidation of pyruvate and fatty acids to CO_2 and H_2O and the coupled synthesis of ATP from ADP and P_i. These processes involve many steps but can be subdivided into three groups of reactions, each of which occurs in a discrete membrane or space in the mitochondrion (Figure 8-7):

1. Oxidation of pyruvate and fatty acids to CO_2 coupled to reduction of NAD^+ to NADH and of **flavin adenine dinucleotide (FAD),** another oxidized electron carrier, to its reduced form, $FADH_2$ (see Figure 2-26). These electron carriers are often referred to as *coenzymes.* NAD^+, NADH, FAD, and $FADH_2$ are diffusible and not permanently bound to proteins. Most of the reactions occur in the matrix; two are catalyzed by inner-membrane enzymes that face the matrix.

2. Electron transfer from NADH and $FADH_2$ to O_2, regenerating the oxidized electron carriers NAD^+ and FAD. These reactions occur in the inner membrane and are coupled to the generation of a proton-motive force across it.

3. Harnessing of the energy stored in the electrochemical proton gradient for ATP synthesis by the F_0F_1 complex in the inner membrane.

The cristae greatly expand the surface area of the inner mitochondrial membrane, enhancing its ability to generate ATP (see Figure 8-6). In typical liver mitochondria, for example, the area of the inner membrane including cristae is about five times that of the outer membrane. In fact, the total area of all inner mitochondrial membranes in liver cells is about 17 times that of the plasma membrane. The mitochondria in heart and skeletal muscles contain three times as many cristae as are found in typical liver mitochondria—presumably reflecting the greater demand for ATP by muscle cells.

In plants, stored carbohydrates, mostly in the form of starch, are hydrolyzed to glucose. Glycolysis then produces pyruvate, which is transported into mitochondria, as in animal cells. Mitochondrial oxidation of pyruvate and concomitant formation of ATP occur in photosynthetic cells during dark periods when photosynthesis is not possible, and in roots and other nonphotosynthetic tissues all the time. ▮

Acetyl CoA Derived from Pyruvate Is Oxidized to Yield CO_2 and Reduced Coenzymes in Mitochondria

Immediately after pyruvate is transported from the cytosol across the mitochondrial membranes to the matrix, it reacts with coenzyme A, forming CO_2 and the intermediate **acetyl CoA** (Figure 8-8). This reaction, catalyzed by *pyruvate dehydrogenase,* is highly exergonic ($\Delta G^{\circ\prime} = -8.0$ kcal/mol) and essentially irreversible. Note that during the pyruvate dehydrogenase reaction, NAD^+ is reduced, forming NADH; in contrast, during the reactions catalyzed by lactate dehydrogenase and alcohol dehydrogenase, NADH is oxidized, forming NAD^+ (see Figure 8-5).

As discussed later, acetyl CoA plays a central role in the oxidation of fatty acids and many amino acids. In addition, it is an intermediate in numerous biosynthetic reactions, such as the transfer of an acetyl group to lysine residues in histone proteins and to the N-termini of many mammalian proteins. Acetyl CoA also is a biosynthetic precursor of cholesterol and other steroids and of the farnesyl and related groups that form the lipid anchors used to attach some proteins (e.g., Ras) to membranes (see Figure 5-15). In respiring mitochondria, however, the acetyl group of acetyl CoA is almost always oxidized to CO_2.

The final stage in the oxidation of glucose entails a set of nine reactions in which the acetyl group of acetyl CoA is oxidized to CO_2. These reactions operate in a cycle that is referred to by several names: the **citric acid cycle,** the **tricarboxylic acid cycle,** and the **Krebs cycle.** The net result is that for each acetyl group entering the cycle as acetyl CoA, two molecules of CO_2 are produced.

As shown in Figure 8-9, the cycle begins with condensation of the two-carbon acetyl group from acetyl CoA with the four-carbon molecule *oxaloacetate* to yield the six-carbon *citric acid*. The two-step conversion of citrate to iso-citrate (reactions 2 and 3) is carried out by a single multifunctional enzyme. In both reactions 4 and 5, a CO_2 molecule is released. Reaction 5, catalyzed by the enzyme α-ketoglutarate dehydrogenase, also results in reduction of NAD^+ to NADH. This reaction is chemically similar to that catalyzed by pyruvate dehydrogenase, and indeed these two large enzyme complexes are similar in structure and mechanism. Reduction of NAD^+ to NADH also occurs during reactions 4 and 9; thus three molecules of NADH are generated per turn of the cycle. In reaction 7, two electrons and two protons are transferred

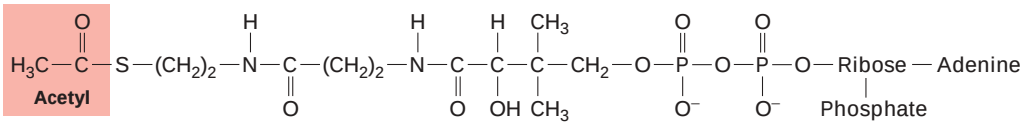

Coenzyme A (CoA)

▲ FIGURE 8-8 **The structure of acetyl CoA.** This compound is an important intermediate in the aerobic oxidation of pyruvate, fatty acids, and many amino acids. It also contributes acetyl groups in many biosynthetic pathways.

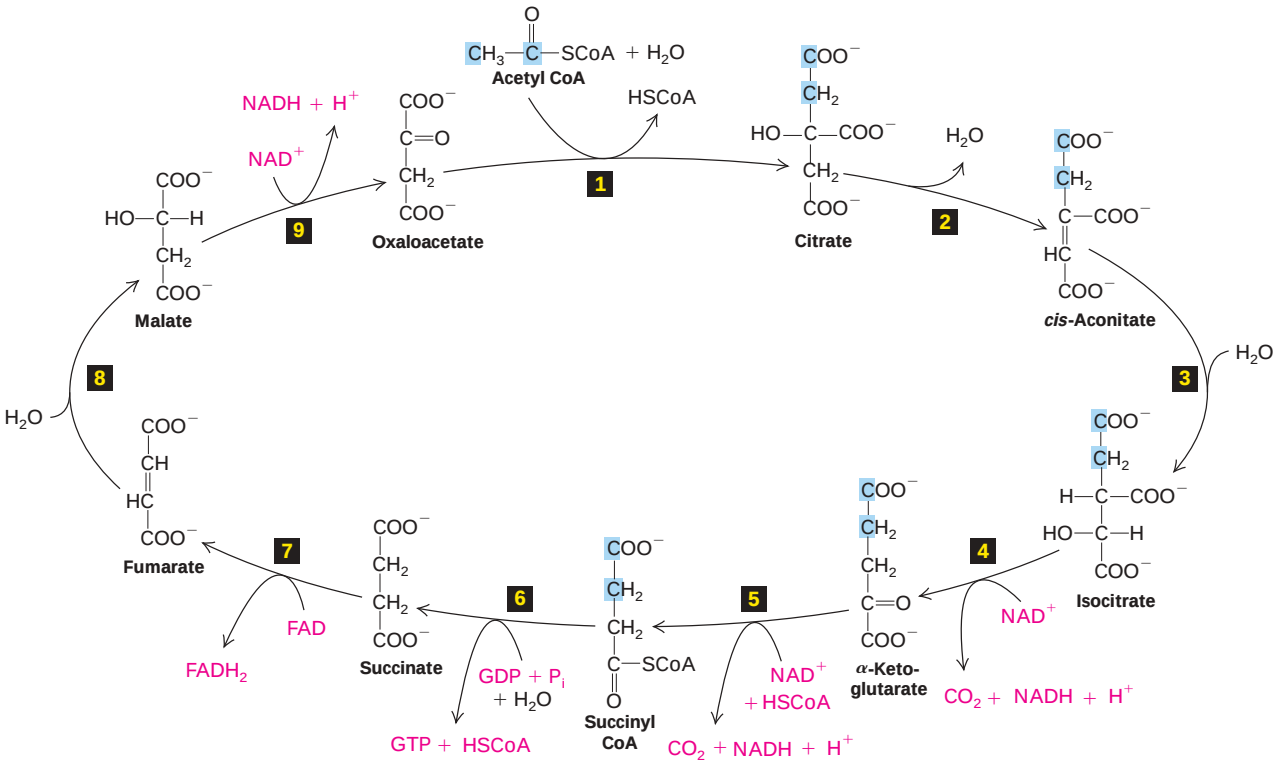

▲ FIGURE 8-9 **The citric acid cycle, in which acetyl groups transferred from acetyl CoA are oxidized to CO_2.** In reaction 1, a two-carbon acetyl residue from acetyl CoA condenses with the four-carbon molecule oxaloacetate to form the six-carbon molecule citrate. In the remaining reactions (2–9) each molecule of citrate is eventually converted back to oxaloacetate, losing two CO_2 molecules in the process. In each turn of the cycle, four pairs of electrons are removed from carbon atoms, forming three molecules of NADH and one molecule of $FADH_2$. The two carbon atoms that enter the cycle with acetyl CoA are highlighted in blue through succinyl CoA. In succinate and fumarate, which are symmetric molecules, they can no longer be specifically denoted. Isotope labeling studies have shown that these carbon atoms are *not* lost in the turn of the cycle in which they enter; on average one will be lost as CO_2 during the next turn of the cycle and the other in subsequent turns.

to FAD, yielding the reduced form of this coenzyme, $FADH_2$. In reaction 6, hydrolysis of the high-energy thioester bond in succinyl CoA is coupled to synthesis of one GTP by substrate-level phosphorylation (GTP and ATP are interconvertible). Reaction 9, the final one, also regenerates oxaloacetate, so the cycle can begin again. Note that molecular O_2 does not participate in the citric acid cycle.

Most enzymes and small molecules involved in the citric acid cycle are soluble in aqueous solution and are localized to the mitochondrial matrix. These include CoA, acetyl CoA, succinyl CoA, NAD^+, and NADH, as well as six of the eight cycle enzymes. *Succinate dehydrogenase*, (reaction 7) and *α-ketoglutarate dehydrogenase* (reaction 5) are integral proteins in the inner membrane, with their active sites facing the matrix. When mitochondria are disrupted by gentle ultrasonic vibration or osmotic lysis, the six non-membrane-bound enzymes in the citric acid cycle are released as a very large multiprotein complex. The reaction product of one enzyme is thought to pass directly to the next enzyme without diffusing through the solution. However, much work is needed to determine the structure of this enzyme complex as it exists in the cell.

Since glycolysis of one glucose molecule generates two acetyl CoA molecules, the reactions in the glycolytic pathway and citric acid cycle produce six CO_2 molecules, ten NADH molecules, and two $FADH_2$ molecules per glucose molecule (Table 8-1). Although these reactions also generate four high-energy phosphoanhydride bonds in the form of two ATP and two GTP molecules, this represents only a small fraction of the available energy released in the complete aerobic oxidation of glucose. The remaining energy is stored in the reduced coenzymes NADH and $FADH_2$.

Synthesis of most of the ATP generated in aerobic oxidation is coupled to the reoxidation of NADH and $FADH_2$ by O_2 in a stepwise process involving the **respiratory chain,** also called the *electron transport chain*. Even though molecular O_2 is not involved in any reaction of the citric acid cycle, in the absence of O_2 the cycle soon stops operating as the supply of NAD^+ and FAD dwindles. Before considering electron transport and the coupled formation of ATP in detail, we discuss first how the supply of NAD^+ in the cytosol is regenerated and then the oxidation of fatty acids to CO_2.

TABLE 8-1 Net Result of the Glycolytic Pathway and the Citric Acid Cycle

Reaction	CO_2 Molecules Produced	NAD^+ Molecules Reduced to NADH	FAD Molecules Reduced to $FADH_2$
1 glucose molecule to 2 pyruvate molecules	0	2	0
2 pyruvates to 2 acetyl CoA molecules	2	2	0
2 acetyl CoA to 4 CO_2 molecules	4	6	2
Total	6	10	2

Transporters in the Inner Mitochondrial Membrane Allow the Uptake of Electrons from Cytosolic NADH

For aerobic oxidation to continue, the NADH produced during glycolysis in the cytosol must be oxidized to NAD^+. As with NADH generated in the mitochondrial matrix, electrons from cytosolic NADH are ultimately transferred to O_2 via the respiratory chain, concomitant with the generation of a proton-motive force. Although the inner mitochondrial membrane is impermeable to NADH itself, several *electron shuttles* can transfer electrons from cytosolic NADH to the matrix.

Operation of the most widespread shuttle—the *malate-aspartate shuttle*—is depicted in Figure 8-10. Critical to the shuttle are two antiport proteins in the inner mitochondrial membrane, a malate/α-ketoglutarate antiporter and a glutamate/aspartate antiporter, that permit transport of their

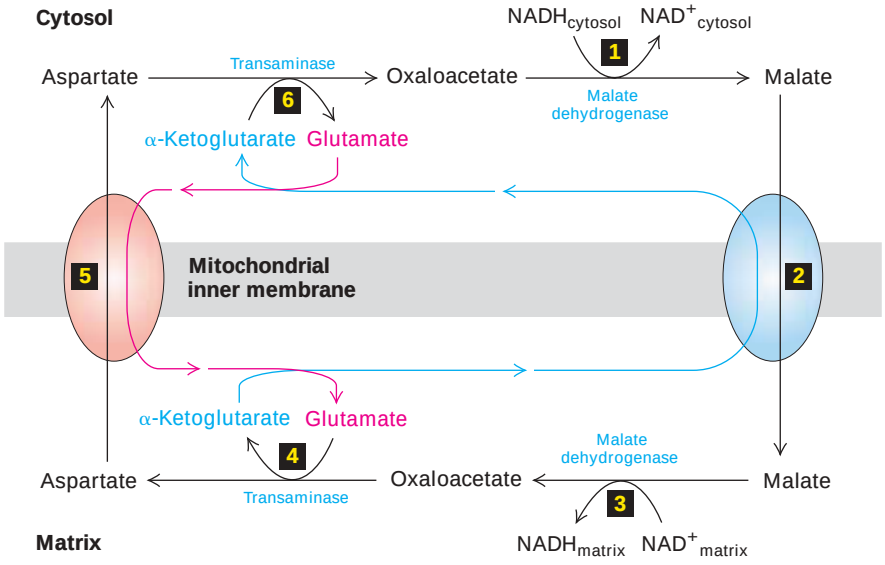

▲ FIGURE 8-10 **The malate shuttle.** This cyclical series of reactions transfers electrons from NADH in the cytosol (intermembrane space) across the inner mitochondrial membrane, which is impermeable to NADH itself. Step 1: Cytosolic malate dehydrogenase transfers electrons from cytosolic NADH to oxaloacetate, forming malate. Step 2: An antiporter (blue oval) in the inner mitochondrial membrane transports malate into the matrix in exchange for α-ketoglutarate. Step 3: Mitochondrial malate dehydrogenase converts malate back to oxaloacetate, reducing NAD^+ in the matrix to NADH in the process. Step 4: Oxaloacetate, which cannot directly cross the inner membrane, is converted to aspartate by addition of an amino group from glutamate. In this transaminase-catalyzed reaction in the matrix, glutamate is converted to α-ketoglutarate. Step 5: A second antiporter (red oval) exports aspartate to the cytosol in exchange for glutamate. Step 6: A cytosolic transaminase converts aspartate to oxaloacetate, completing the cycle. The blue and red arrows reflect the movement of the α-ketoglutarate and glutamate, respectively. In step 4 glutamate is deaminated to α-ketoglutarate, which is transported to the cytosol by an antiporter (step 2; in step 6, the α-ketoglutarate is aminated, converting it back to glutamate, which is transported to the matrix by the antiporter in step 5.

substrates into and out of the matrix. Because oxaloacetate, one component of the shuttle, cannot directly cross the inner membrane, it is converted to the amino acid aspartate in the matrix and to malate in the cytosol. The net effect of the reactions constituting the malate-aspartate shuttle is oxidation of cytosolic NADH to NAD^+ and reduction of matrix NAD^+ to NADH:

$$NADH_{cytosol} + NAD^+_{matrix} \longrightarrow NAD^+_{cytosol} + NADH_{matrix}$$

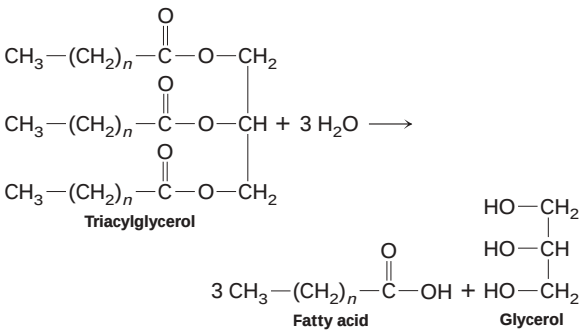

Mitochondrial Oxidation of Fatty Acids Is Coupled to ATP Formation

Fatty acids are stored as **triacylglycerols,** primarily as droplets in adipose (fat-storing) cells. In response to hormones such as adrenaline, triacylglycerols are hydrolyzed in the cytosol to free fatty acids and glycerol:

Fatty acids released into the blood are taken up and oxidized by most other cells, constituting the major energy source for many tissues, particularly heart muscle. In humans, the oxidation of fats is quantitatively more important than the oxidation of glucose as a source of ATP. The oxidation of

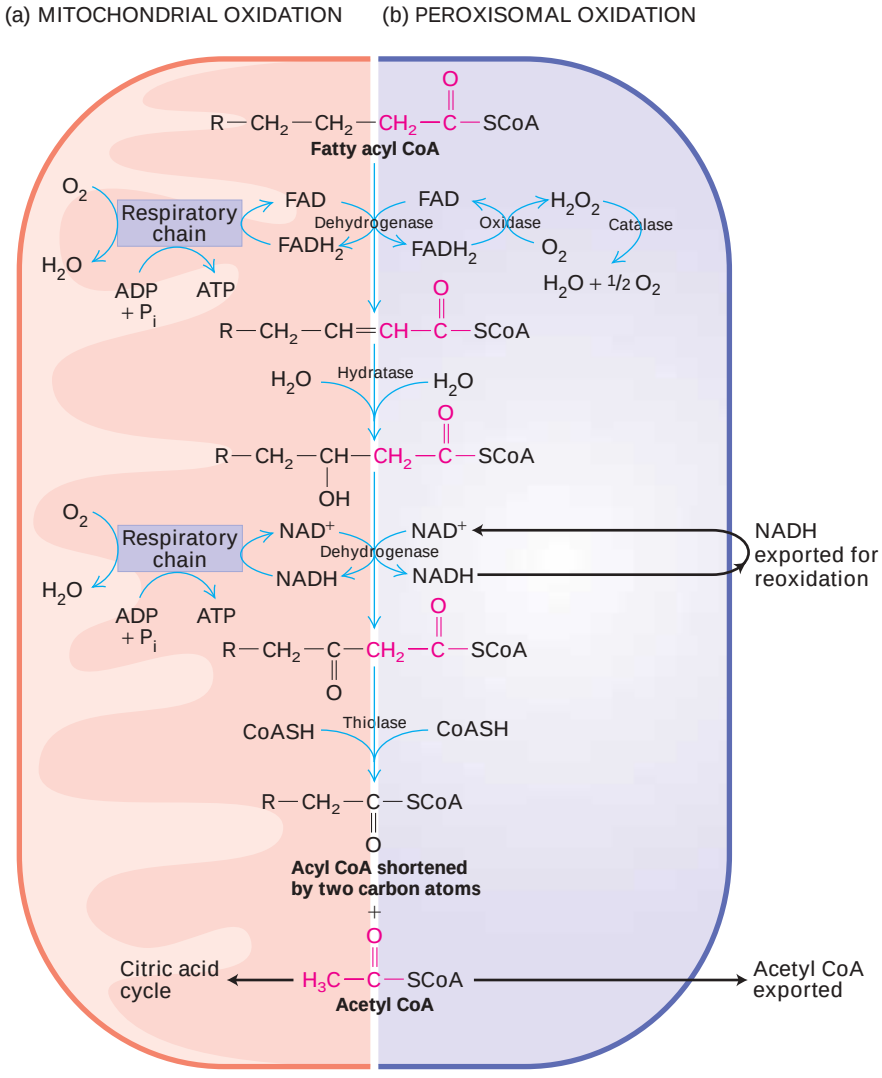

▶ FIGURE 8-11 **Oxidation of fatty acids in mitochondria and peroxisomes.** In both mitochondrial oxidation (a) and peroxisomal oxidation (b), four identical enzyme-catalyzed reactions (shown down the center of the figure) convert a fatty acyl CoA molecule to acetyl CoA and a fatty acyl CoA shortened by two carbon atoms. Concomitantly (in reactions moving to the left of center for mitochondria and to the right of center for peroxisomes), one FAD molecule is reduced to $FADH_2$, and one NAD^+ molecule is reduced to NADH. The cycle is repeated on the shortened acyl CoA until fatty acids with an even number of carbon atoms are completely converted to acetyl CoA. In mitochondria, electrons from $FADH_2$ and NADH enter the respiratory chain and ultimately are used to generate ATP; the acetyl CoA generated is oxidized in the citric acid cycle, resulting in synthesis of additional ATP. Because peroxisomes lack the electron-transport complexes composing the respiratory chain and the enzymes of the citric acid cycle, oxidation of fatty acids in these organelles yields no ATP. [Adapted from D. L. Nelson and M. M. Cox, *Lehninger Principles of Biochemistry,* 3d ed., 2000, Worth Publishers.]

1 g of triacylglycerol to CO_2 generates about six times as much ATP as does the oxidation of 1 g of hydrated glycogen, the polymeric storage form of glucose in muscle and liver. Triglycerides are more efficient for storage of energy because they are stored in anhydrous form and are much more reduced (have more hydrogens) than carbohydrates and therefore yield more energy when oxidized.

In the cytosol, free fatty acids are esterified to coenzyme A to form a fatty acyl CoA in an exergonic reaction coupled to the hydrolysis of ATP to AMP and PP_i (inorganic pyrophosphate):

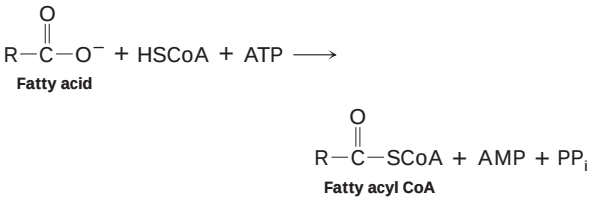

Subsequent hydrolysis of PP_i to two molecules of phosphate (P_i) drives this reaction to completion. Then the fatty acyl group is transferred to carnitine and moved across the inner mitochondrial membrane by an acylcarnitine transporter protein (see Figure 8-7, blue oval); on the matrix side, the fatty acyl group is released from carnitine and reattached to another CoA molecule.

Each molecule of a fatty acyl CoA in the mitochondrion is oxidized in a cyclical sequence of four reactions in which all the carbon atoms are converted to acetyl CoA with generation of NADH and $FADH_2$ (Figure 8-11a). For example, mitochondrial oxidation of each molecule of the 18-carbon stearic acid, $CH_3(CH_2)_{16}COOH$, yields nine molecules of acetyl CoA and eight molecules each of NADH and $FADH_2$. As with acetyl CoA generated from pyruvate, these acetyl groups enter the citric acid cycle and are oxidized to CO_2. Electrons from the reduced coenzymes produced in the oxidation of fatty acyl CoA to acetyl CoA and in the subsequent oxidation of acetyl CoA in the citric acid cycle move via the respiratory chain to O_2. This electron movement is coupled to generation of a proton-motive force that is used to power ATP synthesis as described previously for the oxidation of pyruvate (see Figure 8-7).

Peroxisomal Oxidation of Fatty Acids Generates No ATP

Mitochondrial oxidation of fatty acids is the major source of ATP in mammalian liver cells, and biochemists at one time believed this was true in all cell types. However, rats treated with clofibrate, a drug used to reduce the level of blood lipoproteins, were found to exhibit an increased rate of fatty acid oxidation and a large increase in the number of peroxisomes in their liver cells. This finding suggested that peroxisomes, as well as mitochondria, can oxidize fatty acids. These small organelles, ≈0.2–1 μm in diameter, are lined by a single membrane (see Figure 5-21). They are present in all mammalian cells except erythrocytes and are also found in plant cells, yeasts, and probably most other eukaryotic cells.

The peroxisome is now recognized as the principal organelle in which fatty acids are oxidized in most cell types. Indeed, very long chain fatty acids containing more than about 20 CH_2 groups are degraded only in peroxisomes; in mammalian cells, mid-length fatty acids containing 10–20 CH_2 groups can be degraded in both peroxisomes and mitochondria. In contrast to mitochondrial oxidation of fatty acids, which is coupled to generation of ATP, peroxisomal oxidation of fatty acids is not linked to ATP formation, and the released energy is converted to heat.

The reaction pathway by which fatty acids are degraded to acetyl CoA in peroxisomes is similar to that used in liver mitochondria (Figure 8-11b). However, peroxisomes lack a respiratory chain, and electrons from the $FADH_2$ produced during the oxidation of fatty acids are immediately transferred to O_2 by *oxidases*, regenerating FAD and forming hydrogen peroxide (H_2O_2). In addition to oxidases, peroxisomes contain abundant *catalase*, which quickly decomposes the H_2O_2, a highly cytotoxic metabolite. NADH produced during oxidation of fatty acids is exported and reoxidized in the cytosol. Peroxisomes also lack the citric acid cycle, so acetyl CoA generated during peroxisomal degradation of fatty acids cannot be oxidized further; instead it is transported into the cytosol for use in the synthesis of cholesterol and other metabolites.

Before fatty acids can be degraded in the peroxisome, they must first be transported into the organelle from the cytosol. Mid-length fatty acids are esterified to coenzyme A in the cytosol; the resulting fatty acyl CoAs are then transported into the peroxisome by a specific transporter. However, very long chain fatty acids enter the peroxisome by another transporter and then are esterified to CoA once inside. In the human genetic disease X-linked adrenoleukodystrophy (ALD), peroxisomal oxidation of very long chain fatty acids is specifically defective, while the oxidation of mid-length fatty acids is normal. The most common peroxisomal disorder, ALD is marked by elevated levels of very long chain fatty acids in the plasma and tissues. Patients with the most severe form of ALD are unaffected until mid-childhood, when severe neurological disorders appear, followed by death within a few years. In recent years, the gene that is defective in ALD patients has been identified and cloned by techniques described in Chapter 9. Sequence analysis shows that the gene encodes an ABC transport protein (ABCD1) that is localized to peroxisomal membranes and is thought to mediate the import of very long chain fatty acids into the organelle. ▮

The Rate of Glucose Oxidation Is Adjusted to Meet the Cell's Need for ATP

All enzyme-catalyzed reactions and metabolic pathways are regulated by cells so as to produce the needed amounts of

metabolites but not an excess. The primary function of the oxidation of glucose to CO_2 via the glycolytic pathway, the pyruvate dehydrogenase reaction, and the citric acid cycle is to produce NADH and $FADH_2$, whose oxidation in mitochondria generates ATP. Operation of the glycolytic pathway and citric acid cycle is continuously regulated, primarily by **allosteric** mechanisms, to meet the cell's need for ATP (see Chapter 3 for general principles of allosteric control).

Three allosterically controlled glycolytic enzymes play a key role in regulating the entire glycolytic pathway (see Figure 8-4). *Hexokinase* (step 1) is inhibited by its reaction product, glucose 6-phosphate. *Pyruvate kinase* (step 10) is inhibited by ATP, so glycolysis slows down if too much ATP is present. The third enzyme, *phosphofructokinase-1*, which converts fructose 6-phosphate to fructose 1,6-bisphosphate (step 3), is the principal rate-limiting enzyme of the glycolytic pathway. Emblematic of its critical role in regulating the rate of glycolysis, this enzyme is allosterically controlled by several molecules (Figure 8-12).

Phosphofructokinase-1 is allosterically *inhibited* by ATP and allosterically *activated* by AMP. As a result, the rate of glycolysis is very sensitive to the cell's energy charge, reflected in the ATP:AMP ratio. The allosteric inhibition of phosphofructokinase-1 by ATP may seem unusual, since ATP is also a substrate of this enzyme. But the affinity of the substrate-binding site for ATP is much higher (has a lower K_m) than that of the allosteric site. Thus at low concentrations, ATP binds to the catalytic but not to the inhibitory allosteric site, and enzymatic catalysis proceeds at near maximal rates. At high concentrations, ATP also binds to the allosteric site, inducing a conformational change that reduces the affinity of the enzyme for the other substrate, fructose 6-phosphate, and thus inhibits the rate of this reaction and the overall rate of glycolysis.

Another important allosteric activator of phosphofructokinase-1 is *fructose 2,6-bisphosphate*. This metabolite is formed from fructose 6-phosphate by *phosphofructokinase-2*, an enzyme different from phosphofructokinase-1. Fructose 6-phosphate accelerates the formation of fructose 2,6-bisphosphate, which, in turn, activates phosphofructokinase-1. This type of control, by analogy with feedback control, is known as *feed-forward activation*, in which the abundance of a metabolite (here, fructose 6-phosphate) induces an acceleration in its metabolism. Fructose 2,6-bisphosphate allosterically activates phosphofructokinase-1 in liver cells by decreasing the inhibitory effect of high ATP and by increasing the affinity of phosphofructokinase-1 for one of its substrates, fructose 6-phosphate.

The three glycolytic enzymes that are regulated by allosteric molecules catalyze reactions with large negative $\Delta G^{\circ\prime}$ values—reactions that are essentially irreversible under ordinary conditions. These enzymes thus are particularly suitable for regulating the entire glycolytic pathway. Additional control is exerted by glyceraldehyde 3-phosphate dehydrogenase, which catalyzes the reduction of NAD^+ to NADH (see Figure 8-4, step 6). If cytosolic NADH builds up owing to a slowdown in mitochondrial oxidation, this reaction will be slowed by mass action. As we discuss later, mitochondrial oxidation of NADH and $FADH_2$, produced in the glycolytic pathway and citric acid cycle, also is tightly controlled to produce the appropriate amount of ATP required by the cell.

Glucose metabolism is controlled differently in various mammalian tissues to meet the metabolic needs of the organism as a whole. During periods of carbohydrate starvation, for instance, glycogen in the liver is converted directly to glucose 6-phosphate (without involvement of hexokinase). Under these conditions, there is a reduction in fructose 2,6-bisphos-

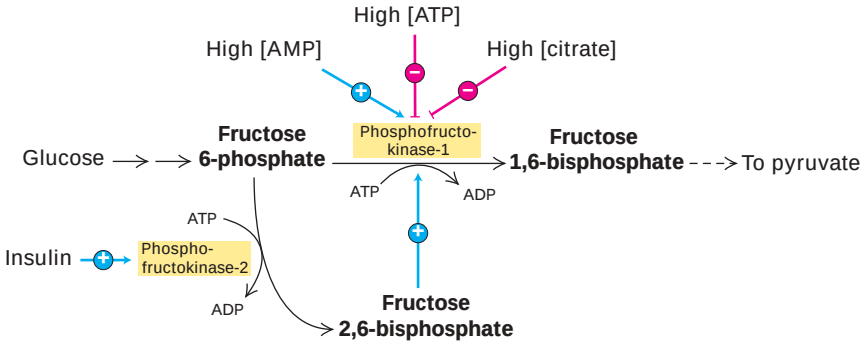

▲ FIGURE 8-12 **Allosteric control of glucose metabolism in the cytosol at the level of fructose 6-phosphate.** The key regulatory enzyme in glycolysis, phosphofructokinase-1, is allosterically activated by AMP and fructose 2,6-bisphosphate, which are elevated when the cell's energy stores are low. The enzyme is inhibited by ATP and citrate, which are elevated when the cell is actively oxidizing glucose to CO_2. Phosphofructokinase-2 (PFK2) is a bifunctional enzyme: its kinase activity forms fructose 2,6-bisphosphate from fructose 6-phosphate, and its phosphatase activity catalyzes the reverse reaction. Insulin, which is released by the pancreas when blood glucose levels are high, promotes PFK2 kinase activity and thus stimulates glycolysis. At low blood glucose, glucagon is released by the pancreas and promotes PFK2 phosphatase activity in the liver, indirectly slowing down glycolysis. We describe the role of insulin and glucagon in the integrated control of blood glucose levels in Chapter 15.

phate levels and decreased phosphofructokinase-1 activity (see Figure 8-12). As a result, glucose 6-phosphate derived from glycogen is not metabolized to pyruvate; rather, it is converted to glucose by a phosphatase and released into the blood to nourish the brain and red blood cells, which depend primarily on glucose as an energy fuel. (Chapter 13 contains a more detailed discussion of hormonal control of glucose metabolism in liver and muscle.) In all cases, the activity of these regulated enzymes is controlled by the level of small-molecule metabolites, generally by allosteric interactions or by hormone-mediated phosphorylation and dephosphorylation.

KEY CONCEPTS OF SECTION 8.1

Oxidation of Glucose and Fatty Acids to CO_2

- In the cytosol of eukaryotic cells, glucose is converted to pyruvate via the glycolytic pathway, with the net formation of two ATPs and the net reduction of two NAD^+ molecules to NADH (see Figure 8-4). ATP is formed by two substrate-level phosphorylation reactions in the conversion of glyceraldehyde 3-phosphate to pyruvate.
- In anaerobic conditions, cells can metabolize pyruvate to lactate or to ethanol plus CO_2 (in the case of yeast), with the reoxidation of NADH. In aerobic conditions, pyruvate is transported into the mitochondrion, where pyruvate dehydrogenase converts it into acetyl CoA and CO_2 (see Figure 8-5).
- Mitochondria have a permeable outer membrane and an inner membrane, which is the site of electron transport and ATP synthesis.
- In each turn of the citric acid cycle, acetyl CoA condenses with the four-carbon molecule oxaloacetate to form the six-carbon citrate, which is converted back to oxaloacetate by a series of reactions that release two molecules of CO_2 and generate three NADH molecules, one $FADH_2$ molecule and one GTP (see Figure 8-9).
- Although cytosolic NADH generated during glycolysis cannot enter mitochondria directly, the malate-aspartate shuttle indirectly transfers electrons from the cytosol to the mitochondrial matrix, thereby regenerating cytosolic NAD^+ for continued glycolysis.
- The flow of electrons from NADH and $FADH_2$ to O_2, via a series of electron carriers in the inner mitochondrial membrane, is coupled to pumping of protons across the inner membrane (see Figure 8-7). The resulting proton-motive force powers ATP synthesis and generates most of the ATP resulting from aerobic oxidation of glucose.
- Oxidation of fatty acids in mitochondria yields acetyl CoA, which enters the citric acid cycle, and the reduced coenzymes NADH and $FADH_2$. Subsequent oxidation of these metabolites is coupled to formation of ATP.
- In most eukaryotic cells, oxidation of fatty acids, especially very long chain fatty acids, occurs primarily in peroxisomes and is not linked to ATP production; the released energy is converted to heat.
- The rate of glucose oxidation via glycolysis and the citric acid cycle is controlled by the inhibition or stimulation of several enzymes, depending on the cell's need for ATP. This complex regulation coordinates the activities of the glycolytic pathway and the citric acid cycle and results in the storage of glucose (as glycogen) or fat when ATP is abundant.

8.2 Electron Transport and Generation of the Proton-Motive Force

As noted in the previous section, most of the free energy released during the oxidation of glucose to CO_2 is retained in the reduced coenzymes NADH and $FADH_2$ generated during glycolysis and the citric acid cycle. During respiration, electrons are released from NADH and $FADH_2$ and eventually are transferred to O_2, forming H_2O according to the following overall reactions:

$$NADH + H^+ + \tfrac{1}{2}\,O_2 \longrightarrow NAD^+ + H_2O$$

$$FADH_2 + \tfrac{1}{2}\,O_2 \longrightarrow FAD + H_2O$$

The $\Delta G^{\circ\prime}$ values for these strongly exergonic reactions are -52.6 kcal/mol (NADH) and -43.4 kcal/mol ($FADH_2$). Recall that the conversion of 1 glucose molecule to CO_2 via the glycolytic pathway and citric acid cycle yields 10 NADH and 2 $FADH_2$ molecules (see Table 8-1). Oxidation of these reduced coenzymes has a total $\Delta G^{\circ\prime}$ of -613 kcal/mol [10 (-52.6) + 2 (-43.4)]. Thus, of the potential free energy present in the chemical bonds of glucose (-680 kcal/mol), about 90 percent is conserved in the reduced coenzymes.

The free energy released during oxidation of a single NADH or $FADH_2$ molecule by O_2 is sufficient to drive the synthesis of several molecules of ATP from ADP and P_i, a reaction with a $\Delta G^{\circ\prime}$ of +7.3 kcal/mol. The mitochondrion maximizes the production of ATP by transferring electrons from NADH and $FADH_2$ through a series of electron carriers, all but one of which are integral components of the inner membrane. This step-by-step transfer of electrons via the respiratory (electron-transport) chain allows the free energy in NADH and $FADH_2$ to be released in small increments and stored as the proton-motive force.

At several sites during electron transport from NADH to O_2, protons from the mitochondrial matrix are pumped across the inner mitochondrial membrane; this "uphill" transport generates a proton concentration gradient across the inner membrane (Figure 8-13). Because the outer membrane is freely permeable to protons, whereas the inner membrane is not, this pumping causes the pH of the mitochondrial matrix to become higher (i.e., the H^+ concentration is lower) than that of the cytosol and intermembrane space. An electric potential across the inner membrane also

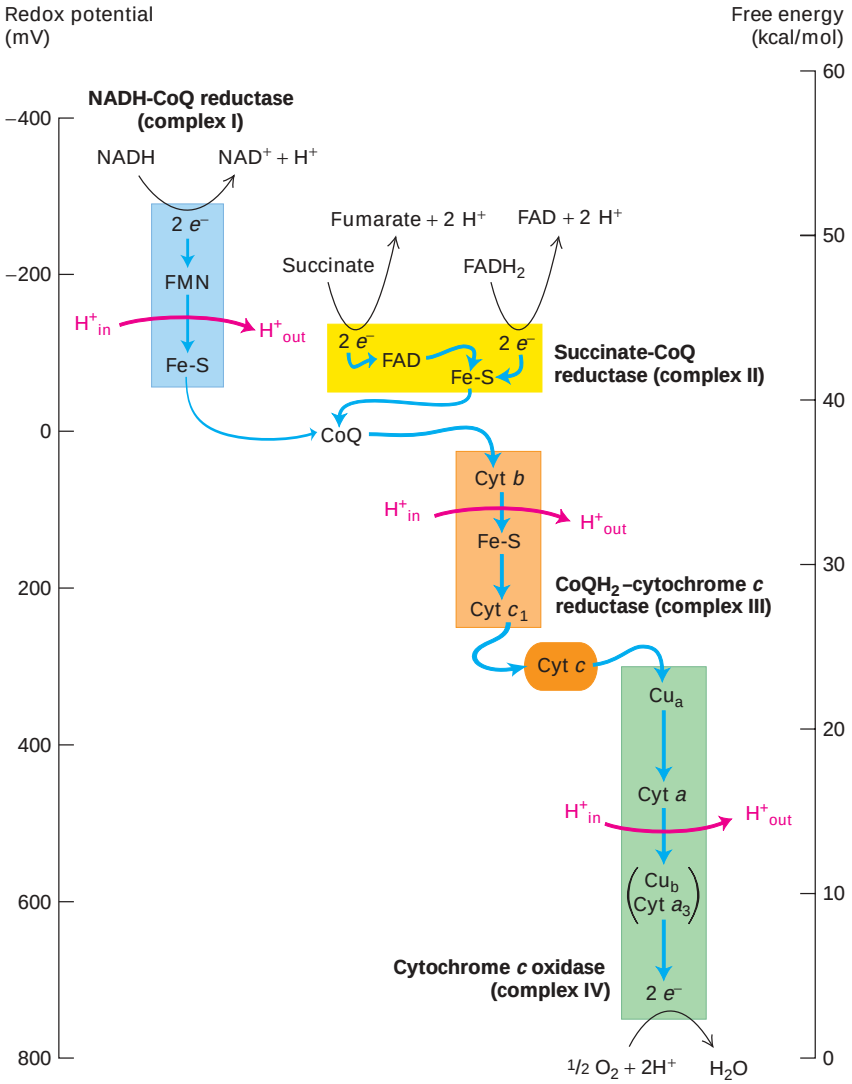

▲ FIGURE 8-13 **Changes in redox potential and free energy during stepwise flow of electrons through the respiratory chain.** Blue arrows indicate electron flow; red arrows, translocation of protons across the inner mitochondrial membrane. Four large multiprotein complexes located in the inner membrane contain several electron-carrying prosthetic groups. Coenzyme Q (CoQ) and cytochrome *c* transport electrons between the complexes. Electrons pass through the multiprotein complexes from those at a lower reduction potential to those with a higher (more positive) potential (left scale), with a corresponding reduction in free energy (right scale). The energy released as electrons flow through three of the complexes is sufficient to power the pumping of H^+ ions across the membrane, establishing a proton-motive force.

results from the uphill pumping of H^+ outward from the matrix, which becomes negative with respect to the intermembrane space. Thus free energy released during the oxidation of NADH or $FADH_2$ is stored both as an electric potential and a proton concentration gradient—collectively, the proton-motive force—across the inner membrane. The movement of protons back across the inner membrane, driven by this force, is coupled to the synthesis of ATP from ADP and P_i by ATP synthase (see Figure 8-7).

The synthesis of ATP from ADP and P_i, driven by the transfer of electrons from NADH or $FADH_2$ to O_2, is the major source of ATP in aerobic nonphotosynthetic cells. Much evidence shows that in mitochondria and bacteria this process, called **oxidative phosphorylation,** depends on generation of a proton-motive force across the inner membrane, with electron transport, proton pumping, and ATP formation occurring simultaneously. In the laboratory, for instance, addition of O_2 and an oxidizable substrate such as pyruvate or succinate to isolated intact mitochondria results in a net synthesis of ATP if the inner mitochondrial membrane is intact. In the presence of minute amounts of detergents that make the membrane leaky, electron transport and the oxidation of these metabolites by O_2 still occurs, but no ATP is made. Under these conditions, no transmembrane proton concentration gradient or membrane electric potential can be maintained.

In this section we first discuss the magnitude of the proton-motive force, then the components of the respiratory chain and the pumping of protons across the inner membrane. In the following section we describe the structure of the ATP synthase and how it uses the proton-motive force to synthesize ATP. We also consider how mitochondrial oxidation of NADH and $FADH_2$ is controlled to meet the cell's need for ATP.

The Proton-Motive Force in Mitochondria Is Due Largely to a Voltage Gradient Across the Inner Membrane

As we've seen, the proton-motive force (pmf) is the sum of a transmembrane proton concentration (pH) gradient and electric potential, or voltage gradient. The relative contribution of the two components to the total pmf depends on the permeability of the membrane to ions other than H^+. A significant voltage gradient can develop only if the membrane is poorly permeable to other cations and to anions, as is the inner mitochondrial membrane. In this case, the developing voltage gradient (i.e., excess H^+ ions on the intermembrane face and excess anions on the matrix face) soon prevents further proton movement, so only a small pH gradient is generated. In contrast, a significant pH gradient can develop only if the membrane is also permeable to a major anion (e.g., Cl^-) or if the H^+ ions are exchanged for another cation (e.g., K^+). In either case, proton movement does not lead to a voltage gradient across the membrane because there is always an equal concentration of positive and negative ions on each side of the membrane. This is the situation in the chloroplast thylakoid membrane during photosynthesis, as we discuss later. Compared with chloroplasts, then, a greater portion of the pmf in mitochondria is due to the membrane electric potential, and the actual pH gradient is smaller.

Since a difference of one pH unit represents a tenfold difference in H^+ concentration, a pH gradient of one unit across a membrane is equivalent to an electric potential of 59 mV at 20 °C according to the Nernst equation (Chapter 7). Thus we can define the proton-motive force, pmf, as

$$\text{pmf} = \Psi - \left(\frac{RT}{F} \times \Delta\text{pH}\right) = \Psi - 59\ \Delta\text{pH}$$

where R is the gas constant of 1.987 cal/(degree·mol), T is the temperature (in degrees Kelvin), F is the Faraday constant [23,062 cal/(V·mol)], and Ψ is the transmembrane electric potential; Ψ and pmf are measured in millivolts. Measurements on respiring mitochondria have shown that the electric potential Ψ across the inner membrane is −160 mV (negative inside matrix) and that ΔpH is ≈1.0 (equivalent to ≈60 mV). Thus the total pmf is −220 mV, with the transmembrane electric potential responsible for about 73 percent.

Because mitochondria are much too small to be impaled with electrodes, the electric potential and pH gradient across the inner mitochondrial membrane cannot be determined by direct measurement. However, researchers can measure the inside pH by trapping fluorescent pH-sensitive dyes inside vesicles formed from the inner mitochondrial membrane. They also can determine the electric potential by adding radioactive $^{42}K^+$ ions and a trace amount of valinomycin to a suspension of respiring mitochondria. Although the inner membrane is normally impermeable to K^+, valinomycin is an **ionophore**, a small lipid-soluble molecule that selectively binds a specific ion (in this case, K^+) in its hydrophilic interior and carries it across otherwise impermeable membranes. In the presence of valinomycin, $^{42}K^+$ equilibrates across the inner membrane of isolated mitochondria in accordance with the electric potential; the more negative the matrix side of the membrane, the more $^{42}K^+$ will accumulate in the matrix.

Addition of small amounts of valinomycin and radioactive K^+ has little effect on oxidative phosphorylation by a suspension of respiring mitochondria. At equilibrium, the measured concentration of radioactive K^+ ions in the matrix, $[K_{in}]$, is about 500 times greater than that in the surrounding medium, $[K_{out}]$. Substitution of this value into the Nernst equation shows that the electric potential E (in mV) across the inner membrane in respiring mitochondria is −160 mV, with the inside negative:

$$E = -59 \log \frac{[K_{in}]}{[K_{out}]} = -59 \log 500 = -160 \text{ mV}$$

Electron Transport in Mitochondria Is Coupled to Proton Translocation

The coupling between electron transport from NADH (or $FADH_2$) to O_2 and proton transport across the inner mitochondrial membrane, which generates the proton-motive force, also can be demonstrated experimentally with isolated mitochondria (Figure 8-14). As soon as O_2 is added to a suspension of mitochondria, the medium outside the mitochondria becomes acidic. During electron transport from NADH to O_2, protons translocate from the matrix to the intermembrane space; since the outer membrane is freely permeable to protons, the pH of the outside medium is lowered briefly. The measured change in pH indicates that about 10 protons are transported out of the matrix for every electron pair transferred from NADH to O_2.

When this experiment is repeated with succinate rather than NADH as the reduced substrate, the medium outside the mitochondria again becomes acidic, but less so. Recall that oxidation of succinate to fumarate in the citric acid cycle generates $FADH_2$ (see Figure 8-9). Because electrons in $FADH_2$ have less potential energy (43.4 kcal/mol) than electrons in NADH (52.6 kcal/mole), $FADH_2$ transfers electrons to the respiratory chain at a later point than NADH does. As a result, electron transport from $FADH_2$ (or succinate) results in translocation of fewer protons from the matrix, and thus a smaller change in pH (see Figure 8-13).

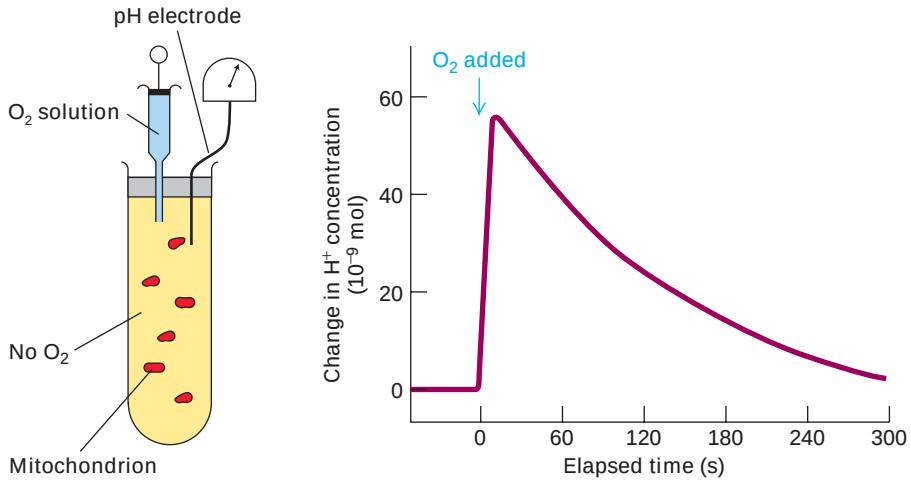

▲ EXPERIMENTAL FIGURE 8-14 **Electron transfer from NADH or $FADH_2$ to O_2 is coupled to proton transport across the mitochondrial membrane.** If NADH is added to a suspension of mitochondria depleted of O_2, no NADH is oxidized. When a small amount of O_2 is added to the system (arrow), the pH of the surrounding medium drops sharply—a change that corresponds to an *increase* in protons outside the mitochondria. (The presence of a large amount of valinomycin and K^+ in the reaction dissipates the voltage gradient generated by H^+ translocation, so that all pumped H^+ ions contribute to the pH change.) Thus the oxidation of NADH by O_2 is coupled to the movement of protons out of the matrix. Once the O_2 is depleted, the excess protons slowly move back into the mitochondria (powering the synthesis of ATP) and the pH of the extracellular medium returns to its initial value.

Electrons Flow from $FADH_2$ and NADH to O_2 Through a Series of Four Multiprotein Complexes

We now examine more closely the energetically favored movement of electrons from NADH and $FADH_2$ to the final electron acceptor, O_2. In respiring mitochondria, each NADH molecule releases two electrons to the respiratory chain; these electrons ultimately reduce one oxygen atom (half of an O_2 molecule), forming one molecule of water:

$$NADH \longrightarrow NAD^+ + H^+ + 2\,e^-$$

$$2\,e^- + 2\,H^+ + \tfrac{1}{2}\,O_2 \longrightarrow H_2O$$

As electrons move from NADH to O_2, their potential declines by 1.14 V, which corresponds to 26.2 kcal/mol of electrons transferred, or ≈ 53 kcal/mol for a pair of electrons. As noted earlier, much of this energy is conserved in the proton-motive force generated across the inner mitochondrial membrane.

Each of the four large multiprotein complexes in the respiratory chain spans the inner mitochondrial membrane and contains several *prosthetic groups* that participate in moving electrons. These small nonpeptide organic molecules or metal ions are tightly and specifically associated with the multiprotein complexes (Table 8-2). Before considering the function of each complex, we examine several of these electron carriers.

Several types of *heme*, an iron-containing prosthetic group similar to that in hemoglobin and myoglobin, are tightly bound or covalently linked to mitochondrial proteins, forming the **cytochromes** (Figure 8-15a). Electron flow through the cytochromes occurs by oxidation and reduction of the Fe atom in the center of the heme molecule:

$$Fe^{3+} + e^- \rightleftharpoons Fe^{2+}$$

TABLE 8-2 Electron-Carrying Prosthetic Groups in the Respiratory Chain

Protein Component	Prosthetic Groups*
NADH-CoQ reductase (complex I)	FMN Fe-S
Succinate-CoQ reductase (complex II)	FAD Fe-S
$CoQH_2$–cytochrome *c* reductase (complex III)	Heme b_L Heme b_H Fe-S Heme c_1
Cytochrome *c*	Heme *c*
Cytochrome *c* oxidase (complex IV)	Cu_a^{2+} Heme *a* Cu_b^{2+} Heme a_3

*Not included is coenzyme Q, an electron carrier that is not permanently bound to a protein complex.
SOURCE: J. W. De Pierre and L. Ernster, 1977, *Ann. Rev. Biochem.* **46**:201.

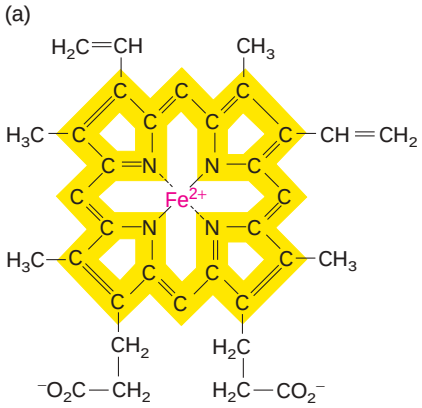

▲ FIGURE 8-15 **Heme and iron-sulfur prosthetic groups in the respiratory (electron-transport) chain.** (a) Heme portion of cytochromes b_L and b_H, which are components of the $CoQH_2$–cytochrome *c* reductase complex. The same porphyrin ring (yellow) is present in all hemes. The chemical substituents attached to the porphyrin ring differ in the other cytochromes in the respiratory chain. All hemes accept and release one electron at a time. (b) Dimeric iron-sulfur cluster (2Fe-2S). Each Fe atom is bonded to four S atoms: two are inorganic sulfur and two are in cysteine side chains of the associated protein. (Note that only the two inorganic S atoms are counted in the chemical formula.) All Fe-S clusters accept and release one electron at a time.

In the respiratory chain, electrons move through the cytochromes in the following order: *b*, c_1, *c*, *a*, and a_3 (see Figure 8-13). The various cytochromes have slightly different heme groups and axial ligands, which generate different environments for the Fe ion. Therefore, each cytochrome has a different reduction potential, or tendency to accept an electron—an important property dictating the unidirectional electron flow along the chain. Because the heme ring in cytochromes consists of alternating double- and single-bonded atoms, a large number of resonance forms exist, and the extra electron is delocalized to the heme carbon and nitrogen atoms as well as to the Fe ion. All the cytochromes, except cytochrome *c*, are components of multiprotein complexes in the inner mitochondrial membrane. Although cytochrome *c* comprises a heme-protein complex, it moves freely by diffusion in the intermembrane space.

Iron-sulfur clusters are nonheme, iron-containing prosthetic groups consisting of Fe atoms bonded both to inorganic S atoms and to S atoms on cysteine residues on a protein (Figure 8-15b). Some Fe atoms in the cluster bear a +2 charge; others have a +3 charge. However, the net charge of each Fe atom is actually between +2 and +3 because electrons in the outermost orbits are dispersed among the Fe atoms and move rapidly from one atom to another. Iron-sulfur clusters accept and release electrons one at a time; the additional electron is also dispersed over all the Fe atoms in the cluster.

Coenzyme Q (CoQ), also called *ubiquinone*, is the only electron carrier in the respiratory chain that is not a protein-bound prosthetic group. It is a carrier of hydrogen atoms, that is, protons plus electrons. The oxidized quinone form of CoQ can accept a single electron to form a semiquinone, a charged free radical denoted by $CoQ^{-}\cdot$. Addition of a second electron and two protons to $CoQ^{-}\cdot$ forms dihydroubiquinone ($CoQH_2$), the fully reduced form (Figure 8-16). Both CoQ and $CoQH_2$ are soluble in phospholipids and diffuse freely in the inner mitochondrial membrane.

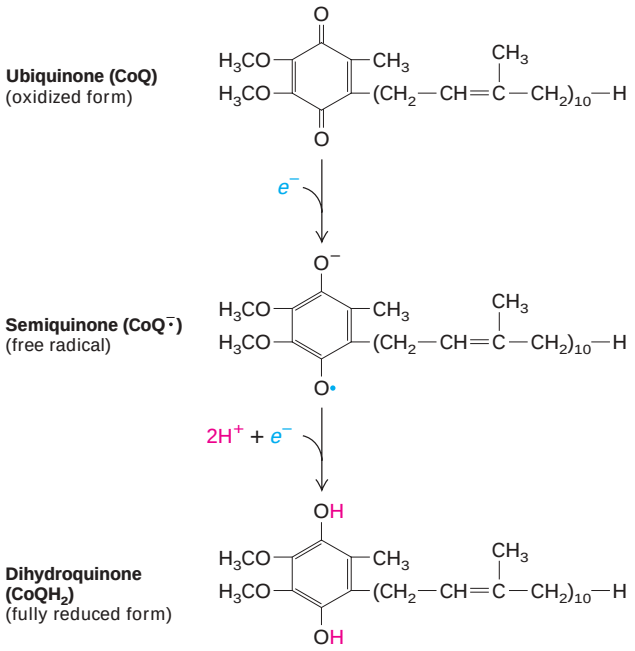

▲ FIGURE 8-16 **Oxidized and reduced forms of coenzyme Q (CoQ), which carries two protons and two electrons.** Because of its long hydrocarbon "tail" of isoprene units, CoQ is soluble in the hydrophobic core of phospholipid bilayers and is very mobile. Reduction of CoQ to the fully reduced form, QH_2, occurs in two steps with a half-reduced free-radical intermediate, called *semiquinone*.

MEDIA CONNECTIONS
Focus Animation: Electron Transport

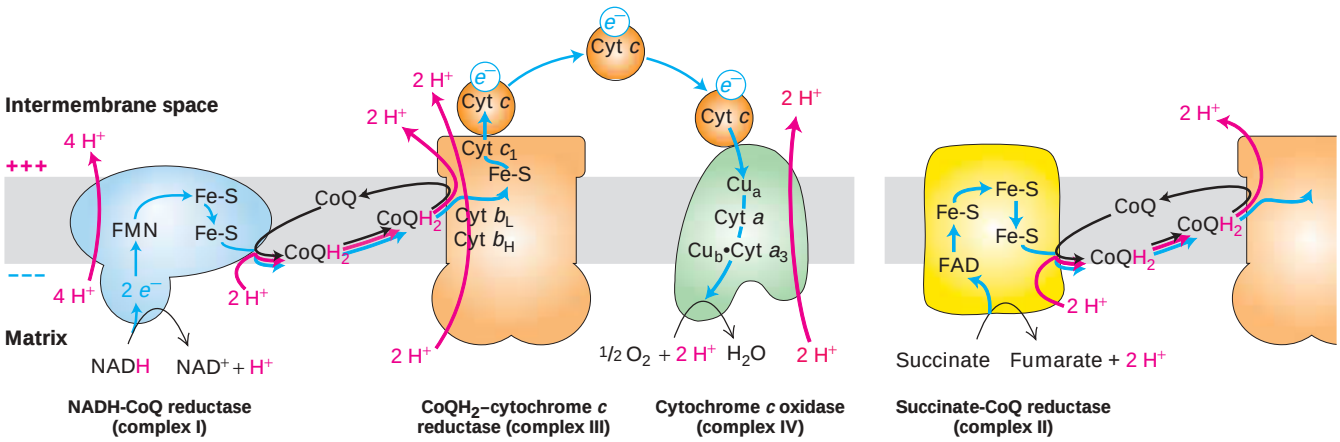

▲ FIGURE 8-17 **Overview of multiprotein complexes, bound prosthetic groups, and associated mobile carriers in the respiratory chain.** Blue arrows indicate electron flow; red arrows indicate proton translocation. (*Left*) Pathway from NADH. A total of 10 protons are translocated per pair of electrons that flow from NADH to O_2. The protons released into the matrix space during oxidation of NADH by NADH-CoQ reductase are consumed in the formation of water from O_2 by cytochrome c oxidase, resulting in no net proton translocation from these reactions. (*Right*) Pathway from succinate. During oxidation of succinate to fumarate and reduction of CoQ by the succinate-CoQ reductase complex, no protons are translocated across the membrane. The remainder of electron transport from $CoQH_2$ proceeds by the same pathway as in the left diagram. Thus for every pair of electrons transported from succinate to O_2, six protons are translocated from the matrix into the intermembrane space. Coenzyme Q and cytochrome *c* function as mobile carriers in electron transport from both NADH and succinate. See the text for details.

As shown in Figure 8-17, CoQ accepts electrons released from the NADH-CoQ reductase complex (I) and the succinate-CoQ reductase complex (II) and donates them to the $CoQH_2$–cytochrome *c* reductase complex (III). Importantly, reduction and oxidation of CoQ are coupled to pumping of protons. Whenever CoQ accepts electrons, it does so at a binding site on the cytosolic (matrix) face of the protein complex, always picking up protons from the medium facing the cytosolic face. Whenever $CoQH_2$ releases its electrons, it does so at a binding site on the exoplasmic face of the protein complex, releasing protons into the exoplasmic medium (intermembrane space). Thus transport of each pair of electrons by CoQ is obligatorily coupled to movement of two protons from the cytosolic to the exoplasmic medium.

NADH-CoQ Reductase (Complex I) Electrons are carried from NADH to CoQ by the NADH-CoQ reductase complex. NAD^+ is exclusively a two-electron carrier: it accepts or releases a pair of electrons at a time. In the NADH-CoQ reductase complex, electrons first flow from NADH to FMN (flavin mononucleotide), a cofactor related to FAD, then to an iron-sulfur cluster, and finally to CoQ (see Figure 8-17). FMN, like FAD, can accept two electrons, but does so one electron at a time.

The overall reaction catalyzed by this complex is

$$\underset{\text{(Reduced)}}{\text{NADH}} + \underset{\text{(Oxidized)}}{\text{CoQ}} + 2\,\text{H}^+ \longrightarrow \underset{\text{(Oxidized)}}{\text{NAD}^+} + \text{H}^+ + \underset{\text{(Reduced)}}{\text{CoQH}_2}$$

Each transported electron undergoes a drop in potential of ≈360 mV, equivalent to a $\Delta G^{\circ\prime}$ of −16.6 kcal/mol for the two electrons transported (see Figure 8-13). Much of this released energy is used to transport four protons across the inner membrane per molecule of NADH oxidized by the NADH-CoQ reductase complex.

Succinate-CoQ Reductase (Complex II) Succinate dehydrogenase, the enzyme that oxidizes a molecule of succinate to fumarate in the citric acid cycle, is an integral component of the succinate-CoQ reductase complex. The two electrons released in conversion of succinate to fumarate are transferred first to FAD, then to an iron-sulfur cluster, and finally to CoQ (see Figure 8-17). The overall reaction catalyzed by this complex is

$$\underset{\text{(Reduced)}}{\text{Succinate}} + \underset{\text{(Oxidized)}}{\text{CoQ}} \longrightarrow \underset{\text{(Oxidized)}}{\text{fumarate}} + \underset{\text{(Reduced)}}{\text{CoQH}_2}$$

Although the $\Delta G^{\circ\prime}$ for this reaction is negative, the released energy is insufficient for proton pumping. Thus no protons are translocated across the membrane by the succinate-CoQ reductase complex, and no proton-motive force is generated in this part of the respiratory chain.

$CoQH_2$–Cytochrome *c* Reductase (Complex III) A $CoQH_2$ generated either by complex I or complex II donates two electrons to the $CoQH_2$–cytochrome *c* reductase complex, regenerating oxidized CoQ. Concomitantly it releases two protons picked up on the cytosolic face into the intermembrane space, generating part of the proton-motive force. Within complex III, the released electrons first are transferred to an iron-sulfur cluster within complex III and then to

two *b*-type cytochromes (b_L and b_H) or cytochrome c_1. Finally, the two electrons are transferred to two molecules of the oxidized form of cytochrome *c*, a water-soluble peripheral protein that diffuses in the intermembrane space (see Figure 8-17). For each pair of electrons transferred, the overall reaction catalyzed by the $CoQH_2$–cytochrome *c* reductase complex is

$$\underset{\text{(Reduced)}}{CoQH_2} + 2\ \underset{\text{(Oxidized)}}{\text{Cyt } c^{3+}} \longrightarrow \underset{\text{(Oxidized)}}{CoQ} + 2\ H^+ + 2\ \underset{\text{(Reduced)}}{\text{Cyt } c^{2+}}$$

The $\Delta G^{\circ\prime}$ for this reaction is sufficiently negative that two additional protons are translocated from the mitochondrial matrix across the inner membrane for each pair of electrons transferred; this involves the proton-motive Q cycle discussed later.

Cytochrome *c* Oxidase (Complex IV) Cytochrome *c*, after being reduced by the $CoQH_2$–cytochrome *c* reductase complex, transports electrons, one at a time, to the cytochrome *c* oxidase complex (Figure 8-18). Within this complex, electrons are transferred, again one at a time, first to a pair of copper ions called Cu_a^{2+}, then to cytochrome *a*, next to a complex of another copper ion (Cu_b^{2+}) and cytochrome a_3, and finally to O_2, the ultimate electron acceptor, yielding H_2O. For each pair of electrons transferred, the overall reaction catalyzed by the cytochrome *c* oxidase complex is

$$2\ \underset{\text{(Reduced)}}{\text{Cyt } c^{2+}} + 2\ H^+ + \tfrac{1}{2}\ O_2 \longrightarrow 2\ \underset{\text{(Oxidized)}}{\text{Cyt } c^{3+}} + H_2O$$

During transport of each pair of electrons through the cytochrome *c* oxidase complex, two protons are translocated across the membrane.

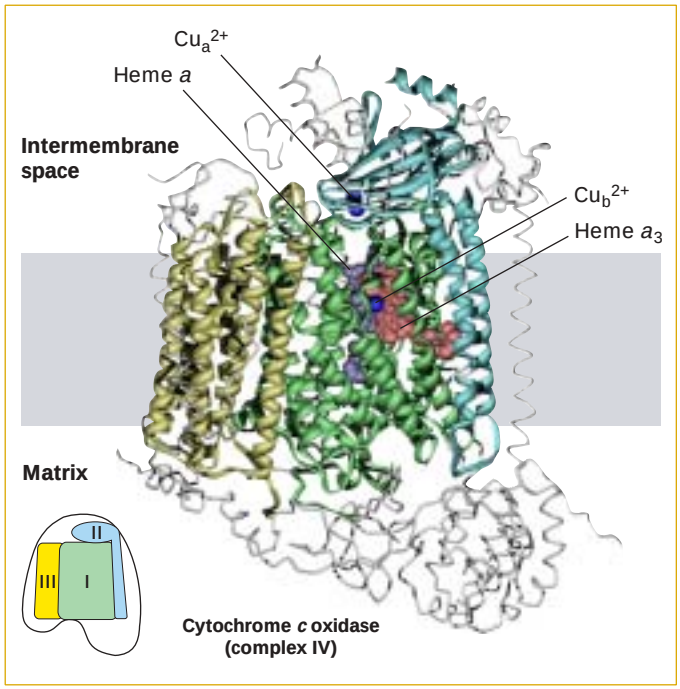

▲ FIGURE 8-18 **Molecular structure of the core of the cytochrome *c* oxidase complex in the inner mitochondrial membrane.** Mitochondrial cytochrome *c* oxidases contain 13 different subunits, but the catalytic core of the enzyme consists of only three subunits: I (green), II (blue), and III (yellow). The function of the remaining subunits (white) is not known. Bacterial cytochrome *c* oxidases contain only the three catalytic subunits. Hemes *a* and a_3 are shown as purple and orange space-filling models, respectively; the three copper atoms are dark blue spheres. [Adapted from T. Tsukihara et al., 1996, *Science* **272:**1136.]

CoQ and Cytochrome *c* as Mobile Electron Shuttles The four electron-transport complexes just described are laterally mobile in the inner mitochondrial membrane; moreover, they are present in unequal amounts and do not form stable contacts with one another. These properties preclude the direct transfer of electrons from one complex to the next. Instead, electrons are transported from one complex to another by diffusion of CoQ in the membrane and by cytochrome *c* in the intermembrane space, as depicted in Figure 8-17.

Reduction Potentials of Electron Carriers Favor Electron Flow from NADH to O_2

As we saw in Chapter 2, the **reduction potential** *E* for a partial reduction reaction

$$\text{Oxidized molecule} + e^- \rightleftharpoons \text{reduced molecule}$$

is a measure of the equilibrium constant of that partial reaction. With the exception of the *b* cytochromes in the $CoQH_2$–cytochrome *c* reductase complex, the standard reduction potential $E^{\circ\prime}$ of the carriers in the mitochondrial respiratory chain increases steadily from NADH to O_2. For instance, for the partial reaction

$$NAD^+ + H^+ + 2\ e^- \rightleftharpoons NADH$$

the value of the standard reduction potential is −320 mV, which is equivalent to a $\Delta G^{\circ\prime}$ of +14.8 kcal/mol for transfer of two electrons. Thus this partial reaction tends to proceed toward the left, that is, toward the oxidation of NADH to NAD^+.

By contrast, the standard reduction potential for the partial reaction

$$\text{Cytochrome } c_{ox}\ (Fe^{3+}) + e^- \rightleftharpoons \text{cytochrome } c_{red}\ (Fe^{2+})$$

is +220 mV ($\Delta G^{\circ\prime} = -5.1$ kcal/mol) for transfer of one electron. Thus this partial reaction tends to proceed toward the right, that is, toward the reduction of cytochrome *c* (Fe^{3+}) to cytochrome *c* (Fe^{2+}).

The final reaction in the respiratory chain, the reduction of O_2 to H_2O

$$2\ H^+ + \tfrac{1}{2}\ O_2 + 2\ e^- \longrightarrow H_2O$$

has a standard reduction potential of +816 mV ($\Delta G^{\circ\prime} = -37.8$ kcal/mol for transfer of two electrons), the most

positive in the whole series; thus this reaction also tends to proceed toward the right.

As illustrated in Figure 8-13, the steady increase in $E^{\circ\prime}$ values, and the corresponding decrease in $\Delta G^{\circ\prime}$ values, of the carriers in the respiratory chain favors the flow of electrons from NADH and succinate to oxygen.

CoQ and Three Electron-Transport Complexes Pump Protons Out of the Mitochondrial Matrix

The multiprotein complexes responsible for proton pumping coupled to electron transport have been identified by selectively extracting mitochondrial membranes with detergents, isolating each of the complexes in near purity, and then preparing artificial phospholipid vesicles (liposomes) containing each complex (see Figure 7-5). When an appropriate electron donor and electron acceptor are added to such liposomes, a change in pH of the medium will occur if the embedded complex transports protons (Figure 8-19). Studies of this type indicate that the NADH-CoQ reductase complex translocates four protons per pair of electrons transported, whereas the cytochrome *c* oxidase complex translocates two protons per electron pair transported (or, equivalently, for every two molecules of cytochrome *c* oxidized).

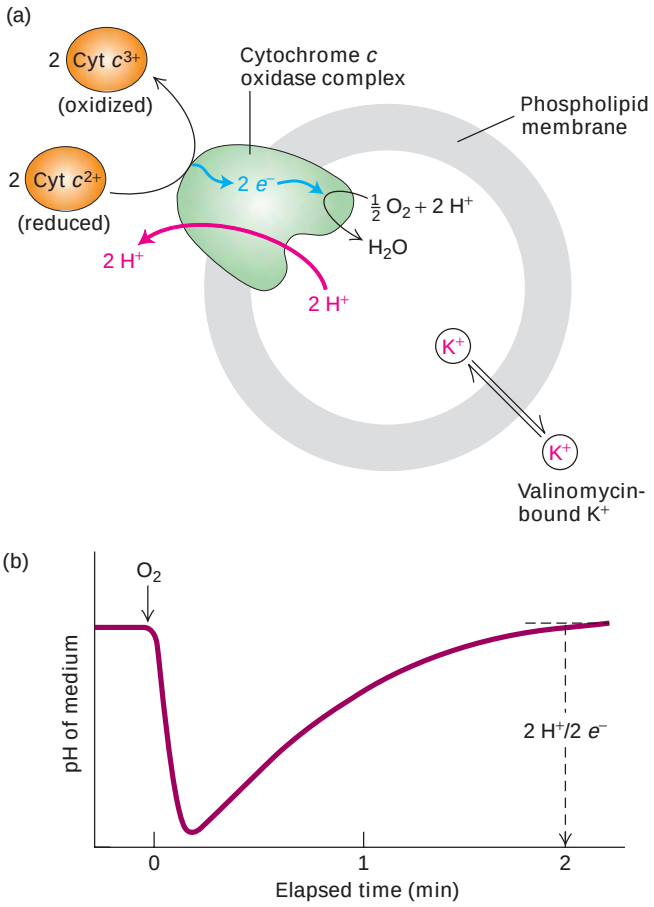

Current evidence suggests that a total of 10 protons are transported from the matrix space across the inner mitochondrial membrane for every electron pair that is transferred from NADH to O_2 (see Figure 8-17). Since the succinate-CoQ reductase complex does not transport protons, only six protons are transported across the membrane for every electron pair that is transferred from succinate (or $FADH_2$) to O_2. Relatively little is known about the coupling of electron flow and proton translocation by the NADH-CoQ reductase complex. More is known about operation of the cytochrome *c* oxidase complex, which we discuss here. The coupled electron and proton movements mediated by the $CoQH_2$–cytochrome *c* reductase complex, which involves a unique mechanism, are described separately.

After cytochrome *c* is reduced by the QH_2–cytochrome *c* reductase complex, it is reoxidized by the cytochrome *c* oxidase complex, which transfers electrons to oxygen. As noted earlier, cytochrome *c* oxidase contains three copper ions and two heme groups (see Figure 8-18). The flow of electrons through these carriers is depicted in Figure 8-20. Four molecules of reduced cytochrome *c* bind, one at a time, to a site on subunit II of the oxidase. An electron is transferred from the heme of each cytochrome *c*, first to Cu_a^{2+} bound to subunit II, then to the heme *a* bound to subunit I, and finally to the Cu_b^{2+} and heme a_3 that make up the oxygen reduction center.

The cyclic oxidation and reduction of the iron and copper in the oxygen reduction center of cytochrome *c* oxidase, together with the uptake of four protons from the matrix space, are coupled to the transfer of the four electrons to oxygen and the formation of water. Proposed intermediates in oxygen reduction include the peroxide anion (O_2^{2-}) and probably the hydroxyl radical (OH·) as well as unusual complexes of iron and oxygen atoms. These intermediates would be harmful to the cell if they escaped from the reaction center, but they do so only rarely.

◀ EXPERIMENTAL FIGURE 8-19 **Electron transfer from reduced cytochrome *c* (Cyt c^{2+}) to O_2 via the cytochrome *c* oxidase complex is coupled to proton transport.** The oxidase complex is incorporated into liposomes with the binding site for cytochrome *c* positioned on the outer surface. (a) When O_2 and reduced cytochrome *c* are added, electrons are transferred to O_2 to form H_2O and protons are transported from the inside to the outside of the vesicles. Valinomycin and K^+ are added to the medium to dissipate the voltage gradient generated by the translocation of H^+, which would otherwise reduce the number of protons moved across the membrane. (b) Monitoring of the medium pH reveals a sharp drop in pH following addition of O_2. As the reduced cytochrome *c* becomes fully oxidized, protons leak back into the vesicles, and the pH of the medium returns to its initial value. Measurements show that two protons are transported per O atom reduced. Two electrons are needed to reduce one O atom, but cytochrome *c* transfers only one electron; thus two molecules of Cyt c^{2+} are oxidized for each O reduced. [Adapted from B. Reynafarje et al., 1986, *J. Biol. Chem.* **261**:8254.]

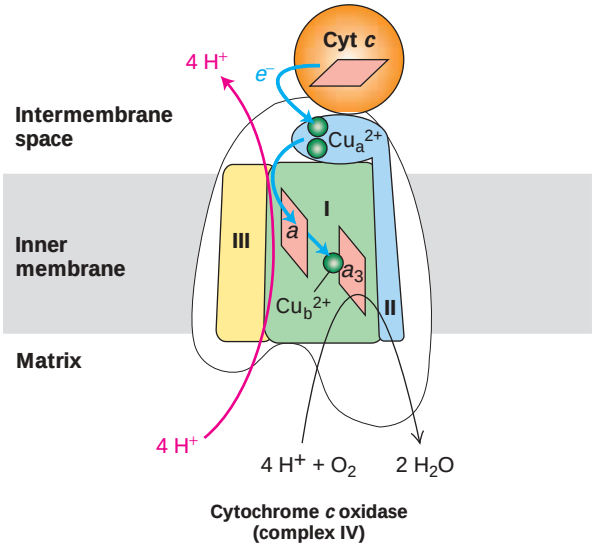

Cytochrome *c* oxidase (complex IV)

▲ FIGURE 8-20 **Schematic depiction of the cytochrome *c* oxidase complex showing the pathway of electron flow from reduced cytochrome *c* to O_2.** Heme groups are denoted by red diamonds. Blue arrows indicate electron flow. Four electrons, sequentially released from four molecules of reduced cytochrome *c*, together with four protons from the matrix, combine with one O_2 molecule to form two water molecules. Additionally, for each electron transferred from cytochrome *c* to oxygen, one proton is transported from the matrix to the intermembrane space, or a total of four for each O_2 molecule reduced to two H_2O molecules.

For every four electrons transferred from reduced cytochrome *c* through cytochrome *c* oxidase (i.e., for every molecule of O_2 reduced to two H_2O molecules), four protons are translocated from the matrix space to the intermembrane space (two protons per electron pair). However, the mechanism by which these protons are translocated is not known.

The Q Cycle Increases the Number of Protons Translocated as Electrons Flow Through the $CoQH_2$–Cytochrome *c* Reductase Complex

Experiments like the one depicted in Figure 8-19 have shown that four protons are translocated across the membrane per electron pair transported from $CoQH_2$ through the $CoQH_2$–cytochrome *c* reductase complex. Thus this complex transports two protons per electron transferred, whereas the cytochrome *c* oxidase complex transports only one proton per electron transferred. An evolutionarily conserved mechanism, called the *Q cycle*, accounts for the two-for-one transport of protons and electrons by the $CoQH_2$–cytochrome *c* reductase complex.

$CoQH_2$ is generated both by the NADH-CoQ reductase and succinate-CoQ reductase complexes and, as we shall see, by the $CoQH_2$–cytochrome *c* reductase complex itself. In all cases, a molecule from the pool of reduced $CoQH_2$ in the membrane binds to the Q_o site on the *intermembrane space (outer) side* of the $CoQH_2$–cytochrome *c* reductase complex (Figure 8-21, step 1). Once bound to this site, $CoQH_2$ releases two protons into the intermembrane space (step 2a); these represent two of the four protons pumped per pair of electrons transferred. Operation of the Q cycle results in pumping of the other two protons. To understand this cycle, we first need to focus on the fates of the two electrons released by $CoQH_2$ at the Q_o site. One of the two

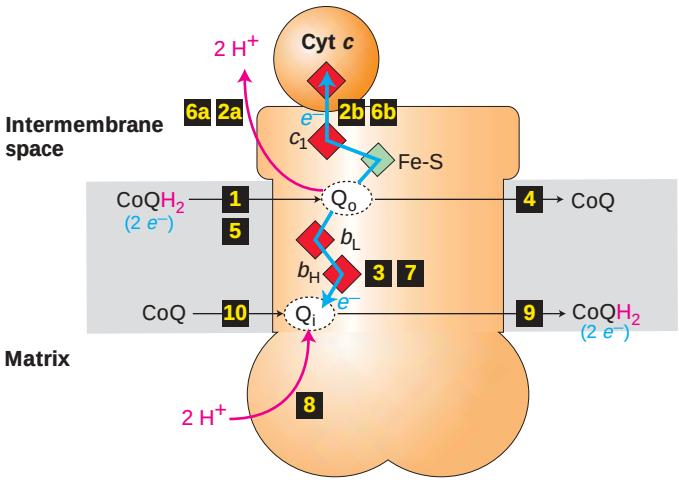

$CoQH_2$–cytochrome *c* reductase (complex III)

At Q_o site: $2\ CoQH_2 + 2\ Cyt\ c^{3+} \longrightarrow 2\ CoQ + 2\ Cyt\ c^{2+} + 2\ e^- + 4\ H^+_{(outside)}$
($4\ H^+$, $4\ e^-$) ($2\ e^-$)

At Q_i site: $CoQ + 2\ e^- + 2\ H^+_{(matrix\ side)} \longrightarrow CoQH_2$
($2\ H^+$, $2\ e^-$)

Net Q cycle (sum of reactions at Q_o and Q_i):

$CoQH_2 + 2\ Cyt\ c^{3+} + 2\ H^+_{(matrix\ side)} \longrightarrow CoQ + 2\ Cyt\ c^{2+} + 4\ H^+_{(outside)}$
($2\ H^+$, $2\ e^-$) ($2\ e^-$)

Per $2\ e^-$ transferred through complex III to cytochrome *c*, $4\ H^+$ released to the intermembrane space

▲ FIGURE 8-21 **The Q cycle.** $CoQH_2$ binds to the Q_o site on the intermembrane space (outer) side of CoQ–cytochrome *c* reductase complex and CoQ binds to the Q_i site on the matrix (inner) side. One electron from the $CoQH_2$ bound to Q_o travels directly to cytochrome *c* via an Fe-S cluster and cytochrome c_1. The other electron moves through the *b* cytochromes to CoQ at the Q_i site, forming the partially reduced semiquinone ($Q^-\cdot$). Simultaneously, $CoQH_2$ releases its two protons into the intermembrane space. The CoQ now at the Q_o site dissociates and a second $CoQH_2$ binds there. As before, one electron moves directly to cytochrome c_1 and the other to the $Q^-\cdot$ at the Q_i site forming, together with two protons picked up from the matrix space, $CoQH_2$, which then dissociates. The net result is that four protons are translocated from the matrix to the intermembrane space for each pair of electrons transported through the $CoQH_2$–cytochrome *c* reductase complex *(bottom)*. See the text for details. [Adapted from B. Trumpower, 1990, *J. Biol. Chem.* **265:**11409, and E. Darrouzet et al., 2001, *Trends Biochem. Sci.* **26:**445.]

electrons from $CoQH_2$ is transported, via an iron-sulfur protein and cytochrome c_1, directly to cytochrome *c* (step 2b). The other electron released from the $CoQH_2$ moves through cytochromes b_L and b_H and partially reduces an oxidized CoQ molecule bound to the Q_i site on the *matrix (inner) side* of the complex, forming a CoQ semiquinone anion $Q^{-}\cdot$ (step 3).

After the loss of two protons and two electrons, the now oxidized CoQ at the Q_o site dissociates (step 4), and a second $CoQH_2$ binds to the site (step 5). As before, the bound $CoQH_2$ releases two protons into the intermembrane space (step 6a), while simultaneously one electron from $CoQH_2$ moves directly to cytochrome *c* (step 6b), and the other electron moves through the *b* cytochromes to the $Q^{-}\cdot$ bound at the Q_i site (step 7). There the addition of two protons from the matrix yields a fully reduced $CoQH_2$ molecule at the Q_i site (step 8). This $CoQH_2$ molecule then dissociates from the $CoQH_2$–cytochrome *c* reductase complex (step 9), freeing the Q_i to bind a new molecule of CoQ (step 10) and begin the Q cycle over again.

In the Q cycle, two molecules of $CoQH_2$ are oxidized to CoQ at the Q_o site and release a total of four protons into the intermembrane space, but one molecule of $CoQH_2$ is regenerated from CoQ at the Q_i site (see Figure 8-21, *bottom*). Thus the *net* result of the Q cycle is that four protons are translocated to the intermembrane space for every two electrons transported through the $CoQH_2$–cytochrome *c* reductase complex and accepted by two molecules of cytochrome *c*. The translocated protons are all derived from the matrix, taken up either by the NADH-CoQ reductase complex or by the $CoQH_2$–cytochrome c reductase complex during reduction of CoQ. While seemingly cumbersome, the Q cycle increases the numbers of protons pumped per pair of electrons moving through the $CoQH_2$–cytochrome *c* reductase complex. The Q cycle is found in all plants and animals as well as in bacteria. Its formation at a very early stage of cellular evolution was likely essential for the success of all life-forms as a way of converting the potential energy in reduced coenzyme Q into the maximum proton-motive force across a membrane.

Although the model presented in Figure 8-21 is consistent with a great deal of mutagenesis and spectroscopic studies on the $CoQH_2$–cytochrome *c* reductase complex, it raises a number of questions. For instance, how are the two electrons released from $CoQH_2$ at the Q_o site directed to different acceptors (cytochromes c_1 and b_L)? Previous studies implicated an iron-sulfur (2Fe-2S) cluster in the transfer of electrons, one at a time, from $CoQH_2$ at the Q_o site to cytochrome c_1. Yet the recently determined three-dimensional structure of the $CoQH_2$–cytochrome *c* reductase complex, which is a dimeric protein, initially suggested that the 2Fe-2S cluster is positioned too far away from the Q_o site for an electron to "jump" to it. Subsequently, researchers discovered that the subunit containing the 2Fe-2S cluster has a flexible hinge that permits it to exist in two conformational states (Figure 8-22). In one conformation, the 2Fe-2S cluster is close enough to the Q_o site to pick up an electron from $CoQH_2$ bound there. Movement of the hinge then positions the 2Fe-2S cluster near enough to the heme on cytochrome c_1 for electron transfer to occur. With the Fe-S subunit in this alternative conformation, the second electron released from $CoQH_2$ bound to the Q_o site cannot move to the 2Fe-2S cluster and has to take the less thermodynamically favored route to cytochrome b_L.

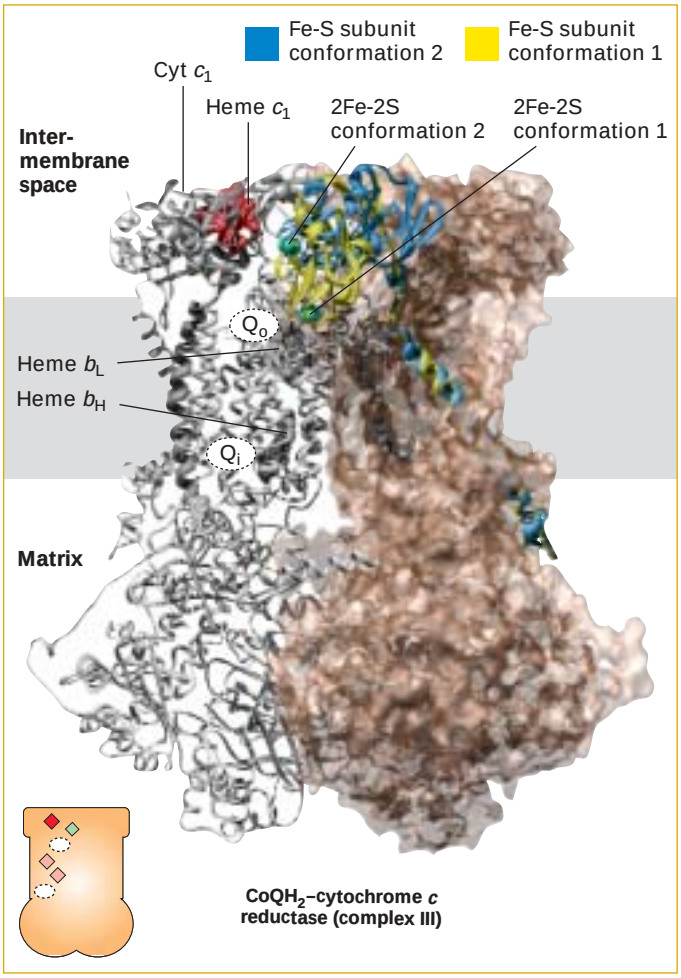

▲ FIGURE 8-22 **Alternative three-dimensional conformations of the Fe-S subunit of the CoQ–cytochrome *c* reductase complex.** In the dimeric complex, cytochromes b_L and b_H are associated with one subunit and the 2Fe-2S cluster with the other subunit. The subunit containing the 2Fe-2S cluster is shown in its two alternative conformational states, which differ primarily in the portion of the protein toward the intermembrane space. In one conformation (yellow), the 2Fe-2S cluster (green) is positioned near the Q_o site on the intermembrane side of the protein, able to pick up an electron from $CoQH_2$. In the alternative conformation (blue), the 2Fe-2S cluster is located adjacent to the c_1 heme on cytochrome c_1 and able to transfer an electron to it. [Adapted from Z. Zhang et al., 1998, *Nature* **392**:678; see also E. Darrouzet et al., 2001, *Trends Biochem. Sci.* **26**:445.]

KEY CONCEPTS OF SECTION 8.2

Electron Transport and Generation of the Proton-Motive Force

- The proton-motive force is a combination of a proton concentration (pH) gradient (exoplasmic face > cytosolic face) and an electric potential (negative cytosolic face) across a membrane.
- In the mitochondrion, the proton-motive force is generated by coupling electron flow from NADH and $FADH_2$ to O_2 to the uphill transport of protons from the matrix across the inner membrane to the intermembrane space.
- The major components of the mitochondrial respiratory chain are four inner membrane multiprotein complexes: NADH-CoQ reductase (I), succinate-CoQ reductase (II), $CoQH_2$–cytochrome *c* reductase (III), and cytochrome *c* oxidase (IV). The last complex transfers electrons to O_2 to form H_2O.
- Each complex contains one or more electron-carrying prosthetic groups: iron-sulfur clusters, flavins, heme groups, and copper ions (see Table 8-2). Cytochrome *c*, which contains heme, and coenzyme Q (CoQ) are mobile electron carriers.
- Each electron carrier accepts an electron or electron pair from a carrier with a less positive reduction potential and transfers the electron to a carrier with a more positive reduction potential. Thus the reduction potentials of electron carriers favor unidirectional electron flow from NADH and $FADH_2$ to O_2 (see Figure 8-13).
- A total of 10 H^+ ions are translocated from the matrix across the inner membrane per electron pair flowing from NADH to O_2 (see Figure 8-17).
- The Q cycle allows four protons (rather than two) to be translocated per pair of electrons moving through the $CoQH_2$–cytochrome *c* reductase complex (see Figure 8-21).

8.3 Harnessing the Proton-Motive Force for Energy-Requiring Processes

The hypothesis that a proton-motive force across the inner mitochondrial membrane is the immediate source of energy for ATP synthesis was proposed in 1961 by Peter Mitchell. Virtually all researchers working in oxidative phosphorylation and photosynthesis initially opposed this chemiosmotic mechanism. They favored a mechanism similar to the well-elucidated substrate-level phosphorylation in glycolysis, in which oxidation of a substrate molecule is directly coupled to ATP synthesis. By analogy, electron transport through the membranes of chloroplasts or mitochondria was believed to generate an intermediate containing a high-energy chemical bond (e.g., a phosphate linked to an enzyme by an ester bond), which was then used to convert P_i and ADP to ATP. Despite intense efforts by a large number of investigators, however, no such intermediate was ever identified.

Definitive evidence supporting the role of the proton-motive force in ATP synthesis awaited development of techniques to purify and reconstitute organelle membranes and membrane proteins. The experiment with chloroplast thylakoid vesicles containing F_0F_1 particles, outlined in Figure 8-23, was one of several demonstrating that the F_0F_1 complex is an ATP-generating enzyme and that ATP generation is

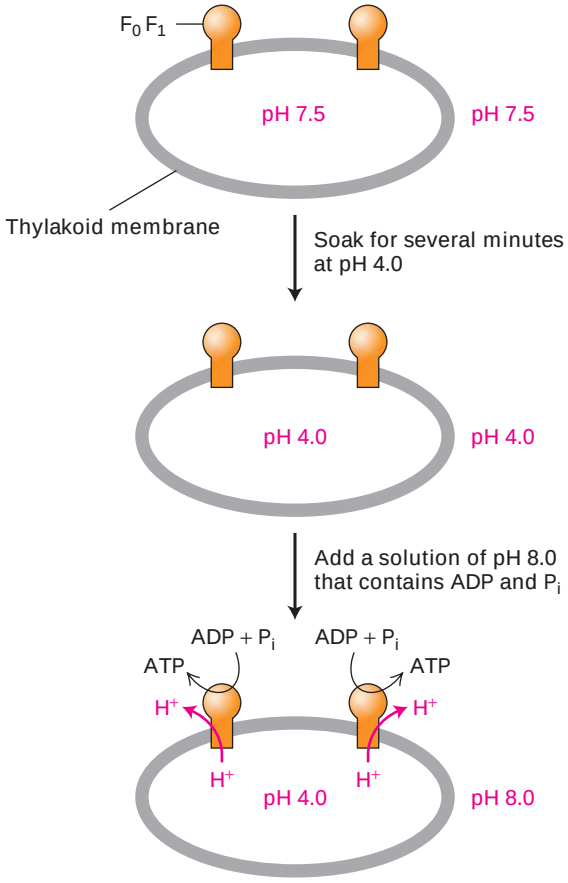

▲ EXPERIMENTAL FIGURE 8-23 **Synthesis of ATP by F_0F_1 depends on a pH gradient across the membrane.** Isolated chloroplast thylakoid vesicles containing F_0F_1 particles were equilibrated in the dark with a buffered solution at pH 4.0. When the pH in the thylakoid lumen became 4.0, the vesicles were rapidly mixed with a solution at pH 8.0 containing ADP and P_i. A burst of ATP synthesis accompanied the transmembrane movement of protons driven by the 10,000-fold H^+ concentration gradient (10^{-4} M versus 10^{-8} M). In similar experiments using "inside-out" preparations of submitochondrial vesicles, an artificially generated membrane electric potential also resulted in ATP synthesis.

dependent on proton movement down an electrochemical gradient. With general acceptance of Mitchell's chemiosmotic mechanism, researchers turned their attention to the structure and operation of the F_0F_1 complex.

Bacterial Plasma-Membrane Proteins Catalyze Electron Transport and Coupled ATP Synthesis

Although bacteria lack any internal membranes, aerobic bacteria nonetheless carry out oxidative phosphorylation by the same processes that occur in eukaryotic mitochondria. Enzymes that catalyze the reactions of both the glycolytic pathway and the citric acid cycle are present in the cytosol of bacteria; enzymes that oxidize NADH to NAD^+ and transfer the electrons to the ultimate acceptor O_2 are localized to the bacterial plasma membrane.

The movement of electrons through these membrane carriers is coupled to the pumping of protons out of the cell (see Figure 8-2). The movement of protons back into the cell, down their concentration gradient, is coupled to the synthesis of ATP. Bacterial F_0F_1 complexes are essentially identical in structure and function with the mitochondrial F_0F_1 complex, but are simpler to purify and study. The protonmotive force across the bacterial plasma membrane is also used to power the uptake of nutrients such as sugars, using proton/sugar symporters, and the rotation of bacterial flagella (see Figure 8-1). As we noted earlier, a primitive aerobic bacterium was probably the progenitor of mitochondria in eukaryotic cells (see Figure 8-3).

ATP Synthase Comprises Two Multiprotein Complexes Termed F_0 and F_1

The F_0F_1 complex, or ATP synthase, has two principal components, F_0 and F_1, both of which are multimeric proteins (Figure 8-24). The F_0 component contains three types of integral membrane proteins, designated **a**, **b**, and **c**. In bacteria and in yeast mitochondria the most common subunit composition is $\mathbf{a}_1\mathbf{b}_2\mathbf{c}_{10}$, but F_0 complexes in animal mitochondria have 12 **c** subunits and those in chloroplasts have 14. In all cases the **c** subunits form a donut-shaped ring in the plane of the membrane. The **a** and two **b** subunits are rigidly linked to one another but not to the ring of **c** subunits.

The F_1 portion is a water-soluble complex of five distinct polypeptides with the composition $\alpha_3\beta_3\gamma\delta\varepsilon$. The lower part of the F_1 γ subunit is a coiled coil that fits into the center of the **c**-subunit ring of F_0 and appears rigidly attached to it. The F_1 ε subunit is rigidly attached to γ and also forms rigid contacts with several of the **c** subunits of F_0. The F_1 α and β subunits associate in alternating order to form a hexamer, $\alpha\beta\alpha\beta\alpha\beta$, or $(\alpha\beta)_3$, which rests atop the single long γ subunit. The F_1 δ subunit is permanently linked to one of the F_1 α subunits and also to the **b** subunit of F_0. Thus the F_0 **a** and **b** subunits and the δ subunit and $(\alpha\beta)_3$ hexamer of the F_1 complex form a rigid structure anchored in the membrane. The rodlike **b** subunits form a "stator" that prevents the $(\alpha\beta)_3$ hexamer from moving while it rests on the γ subunit (see Figure 8-24).

When ATP synthase is embedded in a membrane, the F_1 component forms a knob that protrudes from the cytosolic

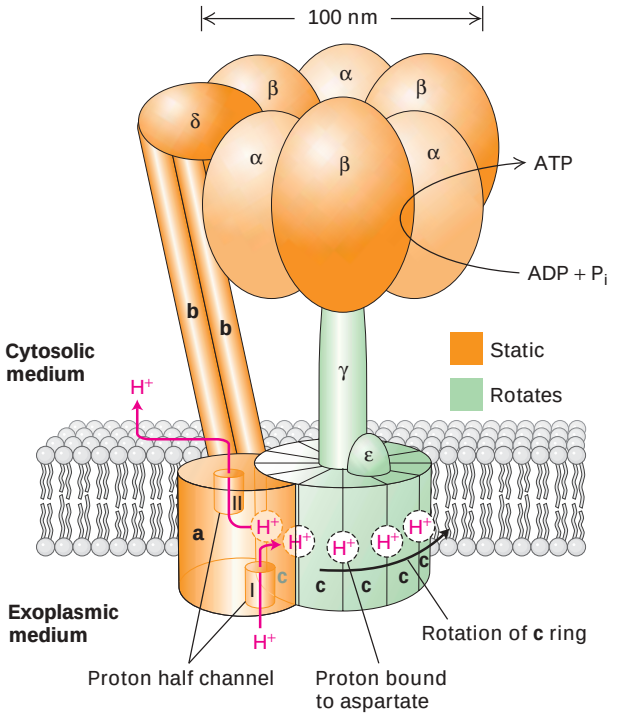

▶ FIGURE 8-24 **Model of the structure and function of ATP synthase (the F_0F_1 complex) in the bacterial plasma membrane.** The F_0 portion is built of three integral membrane proteins: one copy of **a**, two copies of **b**, and on average 10 copies of **c** arranged in a ring in the plane of the membrane. Two proton half-channels lie at the interface between the **a** subunit and the **c** ring. Half-channel I allows protons to move one at a time from the exoplasmic medium and bind to aspartate-61 in the center of a **c** subunit near the middle of the membrane. Half-channel II (after rotation of the **c** ring) permits protons to dissociate from the aspartate and move into the cytosolic medium. The F_1 portion contains three copies each of subunits α and β that form a hexamer resting atop the single rod-shaped γ subunit, which is inserted into the **c** ring of F_0. The ε subunit is rigidly attached to the γ subunit and also to several of the **c** subunits. The δ subunit permanently links one of the α subunits in the F_1 complex to the **b** subunit of F_0. Thus the F_0 **a** and **b** subunits and the F_1 δ subunit and $(\alpha\beta)_3$ hexamer form a rigid structure anchored in the membrane (orange). During proton flow, the **c** ring and the attached F_1 ε and γ subunits rotate as a unit (green), causing conformation changes in the F_1 β subunits leading to ATP synthesis. [Adapted from M. J. Schnitzer, 2001, *Nature* **410**:878, and P. D. Boyer, 1999, *Nature* **402**:247.]

MEDIA CONNECTIONS
Focus Animation: ATP Synthesis

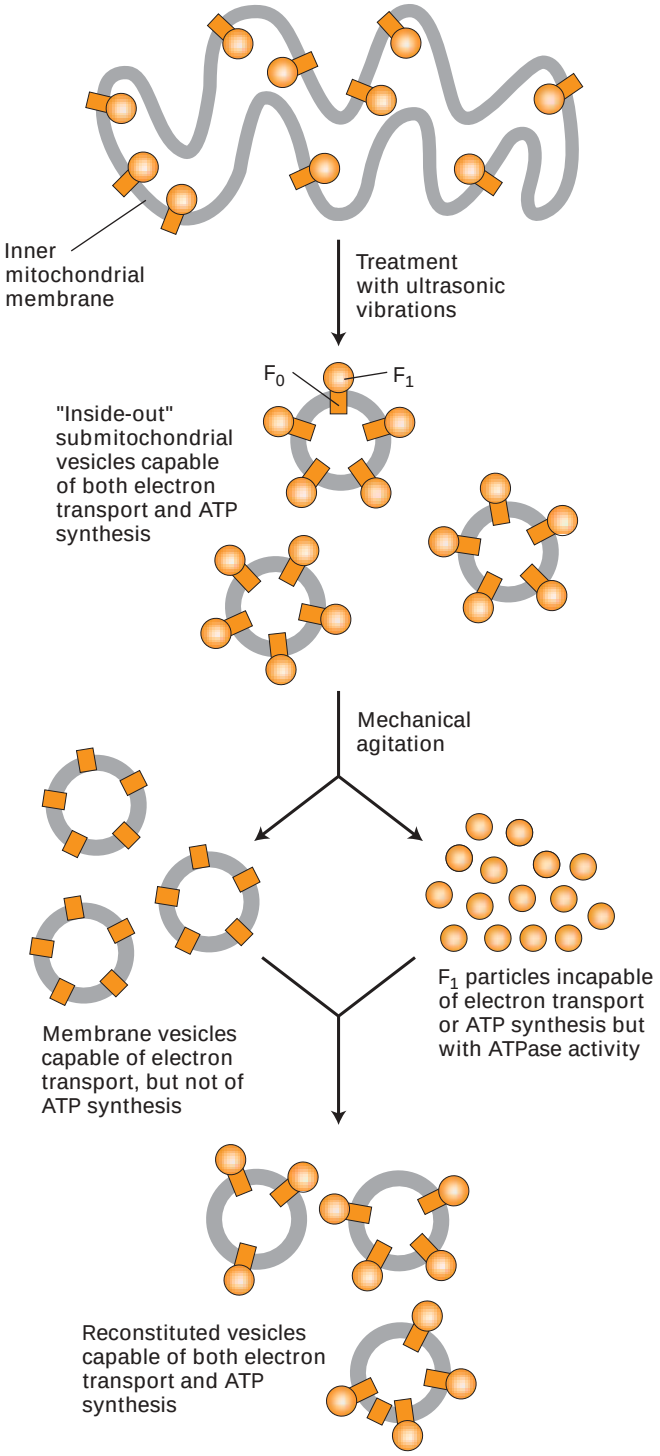

▲ EXPERIMENTAL FIGURE 8-25 **Mitochondrial F_1 particles are required for ATP synthesis, but not for electron transport.** "Inside-out" membrane vesicles that lack F_1 and retain the electron transport complexes are prepared as indicated. Although these can transfer electrons from NADH to O_2, they cannot synthesize ATP. The subsequent addition of F_1 particles reconstitutes the native membrane structure, restoring the capacity for ATP synthesis. When detached from the membrane, F_1 particles exhibit ATPase activity.

face. As demonstrated in the experiment depicted in Figure 8-25, submitochondrial vesicles from which F_1 is removed by mechanical agitation cannot catalyze ATP synthesis; when F_1 particles reassociate with these vesicles, they once again become fully active in ATP synthesis. Because F_1 separated from membranes is capable of catalyzing ATP hydrolysis, it has been called the F_1 ATPase; however, its function in the cells is to synthesize ATP. We examine how it does so in the next section.

Rotation of the F_1 γ Subunit, Driven by Proton Movement Through F_0, Powers ATP Synthesis

Each of the three β subunits in the complete F_0F_1 complex can bind ADP and P_i and catalyze ATP synthesis. However, the coupling between proton flow and ATP synthesis must be indirect, since the nucleotide-binding sites on the β subunits of F_1, where ATP synthesis occurs, are 9–10 nm from the surface of the mitochondrial membrane. The most widely accepted model for ATP synthesis by the F_0F_1 complex—the *binding-change mechanism*—posits just such an indirect coupling (Figure 8-26).

According to this mechanism, energy released by the "downhill" movement of protons through F_0 directly powers rotation of the **c**-subunit ring together with its attached γ and ε subunits (see Figure 8-24). The γ subunit acts as a cam, or rotating shaft, whose movement within F_1 causes cyclical changes in the conformations of the β subunits. As schematically depicted in Figure 8-26, rotation of the γ subunit relative to the fixed $(\alpha\beta)_3$ hexamer causes the nucleotide-binding site of each β subunit to cycle through three conformational states in the following order:

1. An O state that binds ATP very poorly and ADP and P_i weakly

2. An L state that binds ADP and P_i more strongly

3. A T state that binds ADP and P_i so tightly that they spontaneously form ATP and that binds ATP very strongly

A final rotation of γ returns the β subunit to the O state, thereby releasing ATP and beginning the cycle again. ATP or ADP also binds to regulatory or allosteric sites on the three α subunits; this binding modifies the rate of ATP synthesis according to the level of ATP and ADP in the matrix, but is not directly involved in synthesis of ATP from ADP and P_i.

Several types of evidence support the binding-change mechanism, which is now generally accepted. First, biochemical studies showed that one of the three β subunits on isolated F_1 particles can tightly bind ADP and P_i and then form ATP, which remains tightly bound. The measured ΔG for this reaction is near zero, indicating that once ADP and P_i are bound to what is now called the T state of a β subunit, they spontaneously form ATP. Importantly, dissociation of the bound ATP from the β subunit on isolated F_1 particles occurs extremely slowly. This finding suggested that dissociation of ATP would have to be powered by a conformational change in the β subunit, which, in turn, would be caused by proton movement.

MEDIA CONNECTIONS
Focus Animation: ATP Synthesis

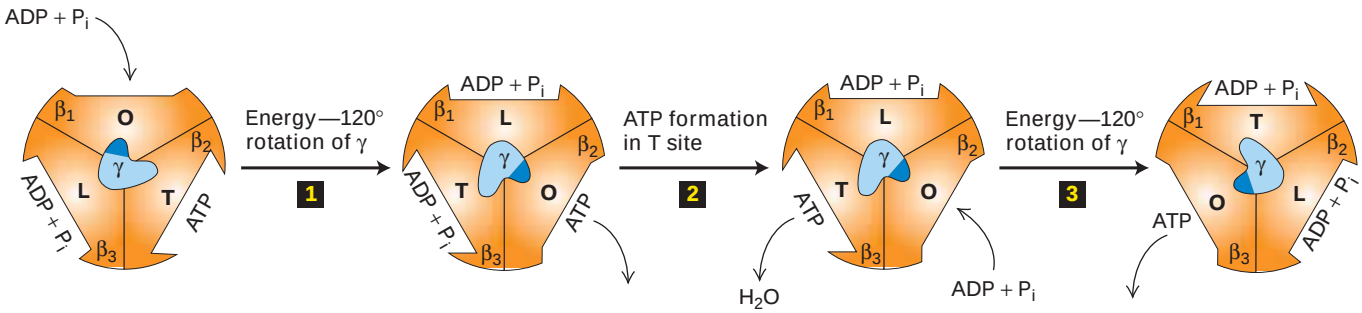

▲ FIGURE 8-26 **The binding-change mechanism of ATP synthesis from ADP and P_i by the F_0F_1 complex.** This view is looking up at F_1 from the membrane surface (see Figure 8-24). Each of the F_1 β subunits alternate between three conformational states that differ in their binding affinities for ATP, ADP, and P_i. Step **1**: After ADP and P_i bind to one of the three β subunits (here, arbitrarily designated β_1) whose nucleotide-binding site is in the O (open) conformation, proton flux powers a 120° rotation of the γ subunit (relative to the fixed β subunits). This causes an increase in the binding affinity of the β_1 subunit for ADP and P_i to L (low), an increase in the binding affinity of the β_3 subunit for ADP and P_i from L to T (tight), and a decrease in the binding affinity of the β_2 subunit for ATP from T to O, causing release of the bound ATP. Step **2**: The ADP and P_i in the T site (here the β_3 subunit) form ATP, a reaction that does not require an input of energy, and ADP and P_i bind to the β_2 subunit, which is in the O state. This generates an F_1 complex identical with that which started the process (*left*) except that it is rotated 120°. Step **3**: Another 120° rotation of γ again causes the O → L → T → O conformational changes in the β subunits described above. Repetition of steps **1** and **2** leads to formation of three ATP molecules for every 360° rotation of γ. [Adapted from P. Boyer, 1989, *FASEB J.* **3**:2164, and Y. Zhou et al., 1997, *Proc. Nat'l. Acad. Sci. USA* **94**:10583.]

MEDIA CONNECTIONS
Video: Rotation of Actin Filament Bound to ATP Synthase

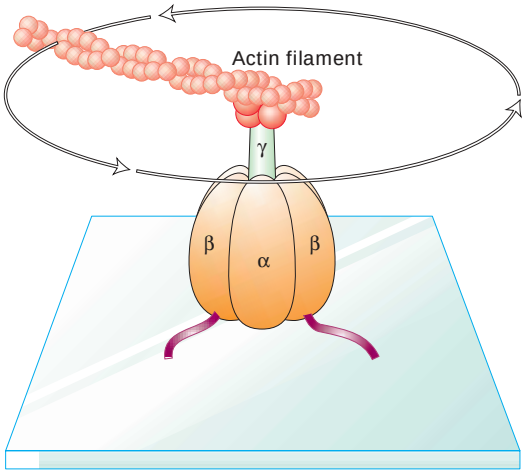

▲ EXPERIMENTAL FIGURE 8-27 **Rotation of the γ subunit of the F_1 complex relative to the $(\alpha\beta)_3$ hexamer can be observed microscopically.** F_1 complexes were engineered that contained β subunits with an additional His_6 sequence, which causes them to adhere to a glass plate coated with a metal reagent that binds histidine. The γ subunit in the engineered F_1 complexes was linked covalently to a fluorescently labeled actin filament. When viewed in a fluorescence microscope, the actin filaments were seen to rotate counterclockwise in discrete 120° steps in the presence of ATP, powered by ATP hydrolysis by the β subunits. [Adapted from H. Noji et al., 1997, *Nature* **386**:299, and R. Yasuda et al., 1998, *Cell* **93**:1117.] See also K. Nishio et al., 2002, *Proc. Nat'l. Acad. Sci.* **97**:13448, for another way to demonstrate α and β subunit rotation relative to the **c** subunit ring.]

Later x-ray crystallographic analysis of the $(\alpha\beta)_3$ hexamer yielded a striking conclusion: although the three β subunits are identical in sequence and overall structure, the ADP/ATP-binding sites have different conformations in each subunit. The most reasonable conclusion was that the three β subunits cycle between three conformational states, with different nucleotide-binding sites, in an energy-dependent reaction.

In other studies, intact F_0F_1 complexes were treated with chemical cross-linking agents that covalently linked the γ and ε subunits and the **c**-subunit ring. The observation that such treated complexes could synthesize ATP or use ATP to power proton pumping indicates that the cross-linked proteins normally rotate together.

Finally, rotation of the γ subunit relative to the fixed $(\alpha\beta)_3$ hexamer, as proposed in the binding-change mechanism, was observed directly in the clever experiment depicted in Figure 8-27. In one modification of this experiment in which tiny gold particles were attached to the γ subunit, rotation rates of 134 revolutions per second were observed. Recalling that hydrolysis of 3 ATPs is thought to power one revolution (see Figure 8-26), this result is close to the experimentally determined rate of ATP hydrolysis by F_0F_1 complexes: about 400 ATPs per second. In a related experiment, a γ subunit linked to an ε subunit and a ring of **c** subunits was seen to rotate relative to the fixed $(\alpha\beta)_3$ hexamer. Rotation of the γ subunit in these experiments was powered by ATP hydrolysis, the reverse of the normal process in which proton movement through the F_0 complex drives rotation of the γ subunit. Nonetheless, these observations established that the γ subunit, along with the attached **c** ring and ε subunit, does indeed rotate, thereby driving the conformational changes in

the β subunits that are required for binding of ADP and P_i, followed by synthesis and subsequent release of ATP.

Number of Translocated Protons Required for ATP Synthesis A simple calculation indicates that the passage of more than one proton is required to synthesize one molecule of ATP from ADP and P_i. Although the ΔG for this reaction under standard conditions is +7.3 kcal/mol, at the concentrations of reactants in the mitochondrion, ΔG is probably higher (+10 to +12 kcal/mol). We can calculate the amount of free energy released by the passage of 1 mol of protons down an electrochemical gradient of 220 mV (0.22 V) from the Nernst equation, setting $n = 1$ and measuring ΔE in volts:

$$\begin{aligned}\Delta G \text{ (cal/mol)} &= -nF\Delta E = -(23{,}062 \text{ cal}\cdot\text{V}^{-1}\cdot\text{mol}^{-1})\,\Delta E \\ &= (23{,}062 \text{ cal}\cdot\text{V}^{-1}\cdot\text{mol}^{-1})(0.22 \text{ V}) \\ &= -5074 \text{ cal/mol, or } -5.1 \text{ kcal/mol}\end{aligned}$$

Since the downhill movement of 1 mol of protons releases just over 5 kcal of free energy, the passage of at least two protons is required for synthesis of each molecule of ATP from ADP and P_i.

Proton Movement Through F_0 and Rotation of the c Ring Each copy of subunit **c** contains two membrane-spanning α helices that form a hairpin. An aspartate residue, Asp61, in the center of one of these helices is thought to participate in proton movement. Chemical modification of this aspartate by the poison dicyclohexylcarbodiimide or its mutation to alanine specifically blocks proton movement through F_0. According to one current model, two proton half-channels lie at the interface between the **a** subunit and **c** ring (see Figure 8-24). Protons are thought to move one at a time through half-channel I from the exoplasmic medium and bind to the carboxylate side chain on Asp61 of one **c** subunit. Binding of a proton to this aspartate would result in a conformational change in the **c** subunit, causing it to move relative to the fixed **a** subunit, or equivalently to rotate in the membrane plane. This rotation would bring the adjacent **c** subunit, with its ionized aspartyl side chain, into channel I, thereby allowing it to receive a proton and subsequently move relative to the **a** subunit. Continued rotation of the **c** ring, due to binding of protons to additional **c** subunits, eventually would align the first **c** subunit containing a protonated Asp61 with the second half-channel (II), which is connected to the cytosol. Once this occurs, the proton on the aspartyl residue could dissociate (forming ionized aspartate) and move into the cytosolic medium.

Since the γ subunit of F_1 is tightly attached to the **c** ring of F_0, rotation of the **c** ring associated with proton movement causes rotation of the γ subunit. According to the binding-change mechanism, a 120° rotation of γ powers synthesis of one ATP (see Figure 8-26). Thus complete rotation of the **c** ring by 360° would generate three ATPs. In *E. coli*, where the F_0 composition is $\mathbf{a}_1\mathbf{b}_2\mathbf{c}_{10}$, movement of 10 protons drives one complete rotation and thus synthesis of three ATPs. This value is consistent with experimental data on proton flux during ATP synthesis, providing indirect support for the model coupling proton movement to **c**-ring rotation depicted in Figure 8-24. The F_0 from chloroplasts contains 14 **c** subunits per ring, and movement of 14 protons would be needed for synthesis of three ATPs. Why these otherwise similar F_0F_1 complexes have evolved to have different H^+:ATP ratios in not clear.

ATP-ADP Exchange Across the Inner Mitochondrial Membrane Is Powered by the Proton-Motive Force

In addition to powering ATP synthesis, the proton-motive force across the inner mitochondrial membrane also powers the exchange of ATP formed by oxidative phosphorylation inside the mitochondrion for ADP and P_i in the cytosol. This exchange, which is required for oxidative phosphorylation to continue, is mediated by two proteins in the inner membrane: a *phosphate transporter* (HPO_4^{2-}/OH^- antiporter) and an *ATP/ADP antiporter* (Figure 8-28).

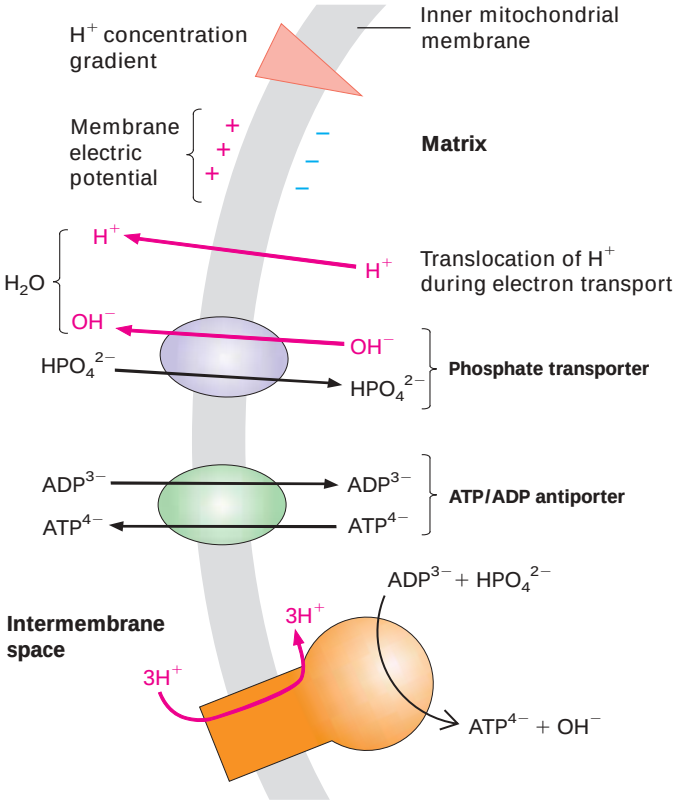

▲ FIGURE 8-28 **The phosphate and ATP/ADP transport system in the inner mitochondrial membrane.** The coordinated action of two antiporters (purple and green) results in the uptake of one ADP^{3-} and one HPO_4^{2-} in exchange for one ATP^{4-}, powered by the outward translocation of one proton during electron transport. The outer membrane is not shown here because it is permeable to molecules smaller than 5000 Da.

The phosphate transporter catalyzes the import of one HPO_4^{2-} coupled to the export of one OH^-. Likewise, the ATP/ADP antiporter allows one molecule of ADP to enter only if one molecule of ATP exits simultaneously. The ATP/ADP antiporter, a dimer of two 30,000-Da subunits, makes up 10–15 percent of the protein in the inner membrane, so it is one of the more abundant mitochondrial proteins. Functioning of the two antiporters together produces an influx of one ADP and one P_i and efflux of one ATP together with one OH^-. Each OH^- transported outward combines with a proton, translocated during electron transport to the intermembrane space, to form H_2O. This drives the overall reaction in the direction of ATP export and ADP and P_i import.

Because some of the protons translocated out of the mitochondrion during electron transport provide the power (by combining with the exported OH^-) for the ATP-ADP exchange, fewer protons are available for ATP synthesis. It is estimated that for every four protons translocated out, three are used to synthesize one ATP molecule and one is used to power the export of ATP from the mitochondrion in exchange for ADP and P_i. This expenditure of energy from the proton concentration gradient to export ATP from the mitochondrion in exchange for ADP and P_i ensures a high ratio of ATP to ADP in the cytosol, where hydrolysis of the high-energy phosphoanhydride bond of ATP is utilized to power many energy-requiring reactions.

Rate of Mitochondrial Oxidation Normally Depends on ADP Levels

If intact isolated mitochondria are provided with NADH (or $FADH_2$), O_2, and P_i, but not with ADP, the oxidation of NADH and the reduction of O_2 rapidly cease, as the amount of endogenous ADP is depleted by ATP formation. If ADP then is added, the oxidation of NADH is rapidly restored. Thus mitochondria can oxidize $FADH_2$ and NADH only as long as there is a source of ADP and P_i to generate ATP. This phenomenon, termed *respiratory control,* occurs because oxidation of NADH, succinate, or $FADH_2$ is obligatorily coupled to proton transport across the inner mitochondrial membrane. If the resulting proton-motive force is not dissipated in the synthesis of ATP from ADP and P_i (or for some other purpose), both the transmembrane proton concentration gradient and the membrane electric potential will increase to very high levels. At this point, pumping of additional protons across the inner membrane requires so much energy that it eventually ceases, thus blocking the coupled oxidation of NADH and other substrates.

Certain poisons, called **uncouplers,** render the inner mitochondrial membrane permeable to protons. One example is the lipid-soluble chemical 2,4-dinitrophenol (DNP), which can reversibly bind and release protons and shuttle protons across the inner membrane from the intermembrane space into the matrix. As a result, DNP dissipates the proton-motive force by short-circuiting both the transmembrane proton concentration gradient and the membrane electric potential. Uncouplers such as DNP abolish ATP synthesis and overcome respiratory control, allowing NADH oxidation to occur regardless of the ADP level. The energy released by the oxidation of NADH in the presence of DNP is converted to heat.

Brown-Fat Mitochondria Contain an Uncoupler of Oxidative Phosphorylation

Brown-fat tissue, whose color is due to the presence of abundant mitochondria, is specialized for the generation of heat. In contrast, *white-fat tissue* is specialized for the storage of fat and contains relatively few mitochondria.

The inner membrane of brown-fat mitochondria contains *thermogenin,* a protein that functions as a natural uncoupler of oxidative phosphorylation. Like synthetic uncouplers, thermogenin dissipates the proton-motive force across the inner mitochondrial membrane, converting energy released by NADH oxidation to heat. Thermogenin is a proton transporter, not a proton channel, and shuttles protons across the membrane at a rate that is a millionfold slower than that of typical ion channels. Its amino acid sequence is similar to that of the mitochondrial ATP/ADP antiporter, and it functions at a rate that is characteristic of other transporters (see Figure 7-2).

Environmental conditions regulate the amount of thermogenin in brown-fat mitochondria. For instance, during the adaptation of rats to cold, the ability of their tissues to generate heat is increased by the induction of thermogenin synthesis. In cold-adapted animals, thermogenin may constitute up to 15 percent of the total protein in the inner mitochondrial membrane.

Adult humans have little brown fat, but human infants have a great deal. In the newborn, thermogenesis by brown-fat mitochondria is vital to survival, as it also is in hibernating mammals. In fur seals and other animals naturally acclimated to the cold, muscle-cell mitochondria contain thermogenin; as a result, much of the proton-motive force is used for generating heat, thereby maintaining body temperature.

KEY CONCEPTS OF SECTION 8.3

Harnessing the Proton-Motive Force for Energy-Requiring Processes

- The multiprotein F_0F_1 complex catalyzes ATP synthesis as protons flow back through the inner mitochondrial membrane (plasma membrane in bacteria) down their electrochemical proton gradient.
- F_0 contains a ring of 10–14 **c** subunits that is rigidly linked to the rod-shaped γ subunit and ε subunit of F_1. Resting atop the γ subunit is the hexameric knob of F_1 $[(\alpha\beta)_3]$, which protrudes into the mitochondrial matrix

(cytosol in bacteria). The three β subunits are the sites of ATP synthesis (see Figure 8-24).

- Movement of protons across the membrane via two half-channels at the interface of the F_0 **a** subunit and the **c** ring powers rotation of the **c** ring with its attached F_1 ε and γ subunits.
- Rotation of the F_1 γ subunit leads to changes in the conformation of the nucleotide-binding sites in the F_1 β subunits (see Figure 8-26). By means of this binding-change mechanism, the β subunits bind ADP and P_i, condense them to form ATP, and then release the ATP.
- The proton-motive force also powers the uptake of P_i and ADP from the cytosol in exchange for mitochondrial ATP and OH^-, thus reducing some of the energy available for ATP synthesis.
- Continued mitochondrial oxidation of NADH and the reduction of O_2 are dependent on sufficient ADP being present. This phenomenon, termed *respiratory control*, is an important mechanism for coordinating oxidation and ATP synthesis in mitochondria.
- In brown fat, the inner mitochondrial membrane contains thermogenin, a proton transporter that converts the proton-motive force into heat. Certain chemicals (e.g., DNP) have the same effect, uncoupling oxidative phosphorylation from electron transport.

8.4 Photosynthetic Stages and Light-Absorbing Pigments

We now shift our attention to photosynthesis, the second main process for synthesizing ATP. Photosynthesis in plants occurs in chloroplasts, large organelles found mainly in leaf cells. The principal end products are two carbohydrates that are polymers of hexose (six-carbon) sugars: sucrose, a glucose-fructose disaccharide (see Figure 2-17), and leaf **starch**, a large insoluble glucose polymer that is the primary storage carbohydrate in higher plants (Figure 8-29). Leaf starch is synthesized and stored in the chloroplast. Sucrose is synthesized in the leaf cytosol from three-carbon precursors generated in the chloroplast; it is transported to nonphotosynthetic (nongreen) plant tissues (e.g., roots and seeds), which metabolize sucrose for energy by the pathways described in the previous sections. Photosynthesis in plants, as well as in eukaryotic single-celled algae and in several photosynthetic bacteria (e.g., the cyanobacteria and prochlorophytes), also generates oxygen. The overall reaction of oxygen-generating photosynthesis,

$$6\ CO_2 + 6\ H_2O \longrightarrow 6\ O_2 + C_6H_{12}O_6$$

is the reverse of the overall reaction by which carbohydrates are oxidized to CO_2 and H_2O.

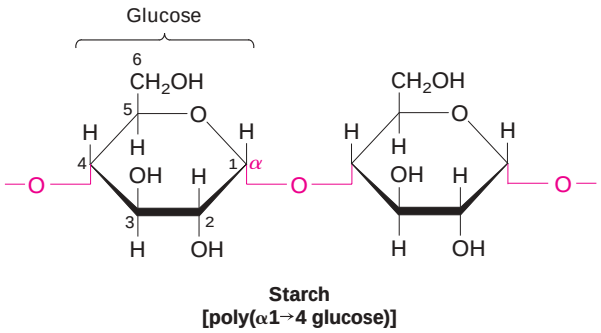

Starch
[poly(α1→4 glucose)]

▲ FIGURE 8-29 **Structure of starch.** This large glucose polymer and the disaccharide sucrose (see Figure 2-17) are the principal end products of photosynthesis. Both are built of six-carbon sugars.

Although green and purple bacteria also carry out photosynthesis, they use a process that does not generate oxygen. As discussed in Section 8.5, detailed analysis of the photosynthetic system in these bacteria has provided insights about the first stages in the more common process of oxygen-generating photosynthesis. In this section, we provide an overview of the stages in oxygen-generating photosynthesis and introduce the main components, including the **chlorophylls,** the principal light-absorbing pigments.

Thylakoid Membranes Are the Sites of Photosynthesis in Plants

Chloroplasts are bounded by two membranes, which do not contain chlorophyll and do not participate directly in photosynthesis (Figure 8-30). As in mitochondria, the outer membrane of chloroplasts contains porins and thus is permeable to metabolites of small molecular weight. The inner membrane forms a permeability barrier that contains transport proteins for regulating the movement of metabolites into and out of the organelle.

Unlike mitochondria, chloroplasts contain a third membrane—the *thylakoid membrane*—on which photosynthesis occurs. The chloroplast thylakoid membrane is believed to constitute a single sheet that forms numerous small, interconnected flattened vesicles, the **thylakoids,** which commonly are arranged in stacks termed *grana* (see Figure 8-30). The spaces within all the thylakoids constitute a single continuous compartment, the *thylakoid lumen*. The thylakoid membrane contains a number of integral membrane proteins to which are bound several important prosthetic groups and light-absorbing pigments, most notably chlorophyll. Carbohydrate synthesis occurs in the *stroma*, the soluble phase between the thylakoid membrane and the inner membrane. In photosynthetic bacteria extensive invaginations of the plasma membrane form a set of internal membranes, also termed *thylakoid membranes*, where photosynthesis occurs.

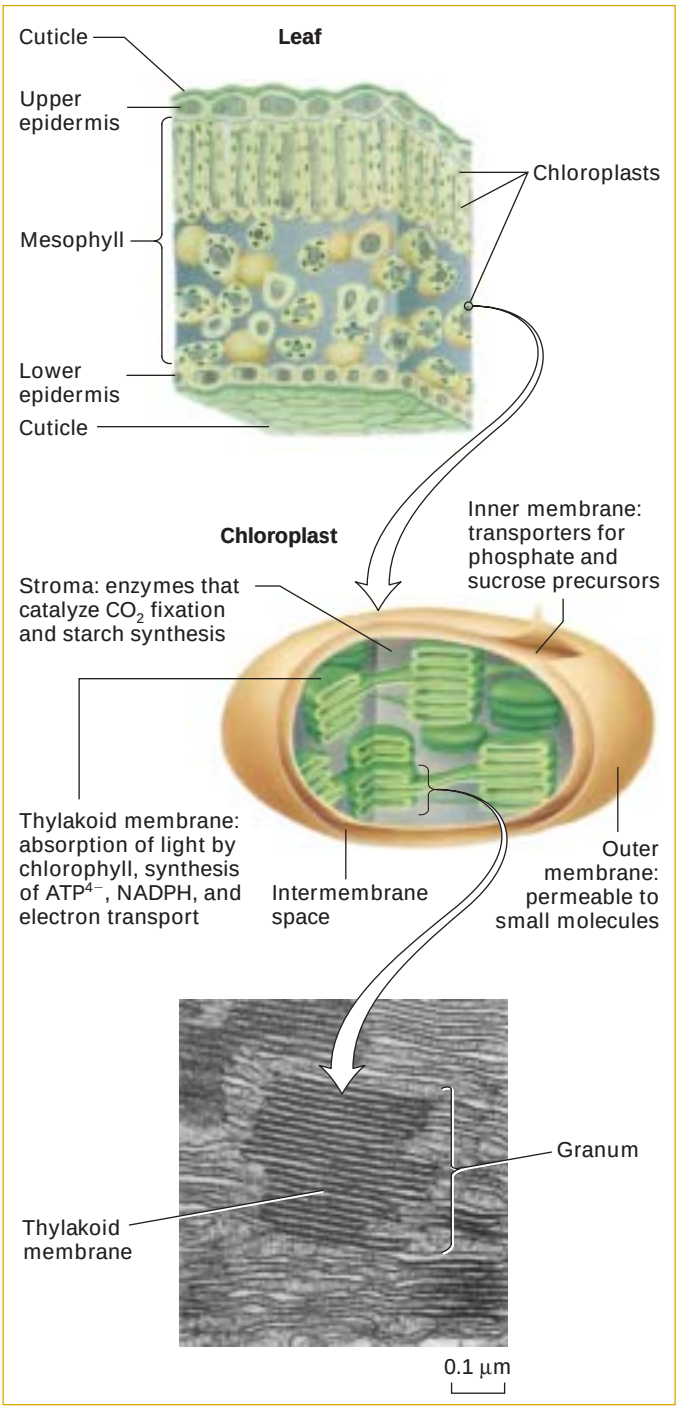

▲ FIGURE 8-30 **Cellular structure of a leaf and chloroplast.** Like mitochondria, plant chloroplasts are bounded by a double membrane separated by an intermembrane space. Photosynthesis occurs on the thylakoid membrane, which forms a series of flattened vesicles (thylakoids) that enclose a single interconnected luminal space. The green color of plants is due to the green color of chlorophyll, all of which is localized to the thylakoid membrane. A granum is a stack of adjacent thylakoids. The stroma is the space enclosed by the inner membrane and surrounding the thylakoids. [Photomicrograph courtesy of Katherine Esau, University of California, Davis.]

Three of the Four Stages in Photosynthesis Occur Only During Illumination

The photosynthetic process in plants can be divided into four stages, each localized to a defined area of the chloroplast: (1) absorption of light, (2) electron transport leading to formation of O_2 from H_2O, reduction of $NADP^+$ to NADPH, and generation of a proton-motive force, (3) synthesis of ATP, and (4) conversion of CO_2 into carbohydrates, commonly referred to as **carbon fixation.** All four stages of photosynthesis are tightly coupled and controlled so as to produce the amount of carbohydrate required by the plant. All the reactions in stages 1–3 are catalyzed by proteins in the thylakoid membrane. The enzymes that incorporate CO_2 into chemical intermediates and then convert them to starch are soluble constituents of the chloroplast stroma. The enzymes that form sucrose from three-carbon intermediates are in the cytosol.

Stage 1: Absorption of Light The initial step in photosynthesis is the absorption of light by chlorophylls attached to proteins in the thylakoid membranes. Like the heme component of cytochromes, chlorophylls consist of a porphyrin ring attached to a long hydrocarbon side chain (Figure 8-31). In contrast to the hemes, chlorophylls contain a central

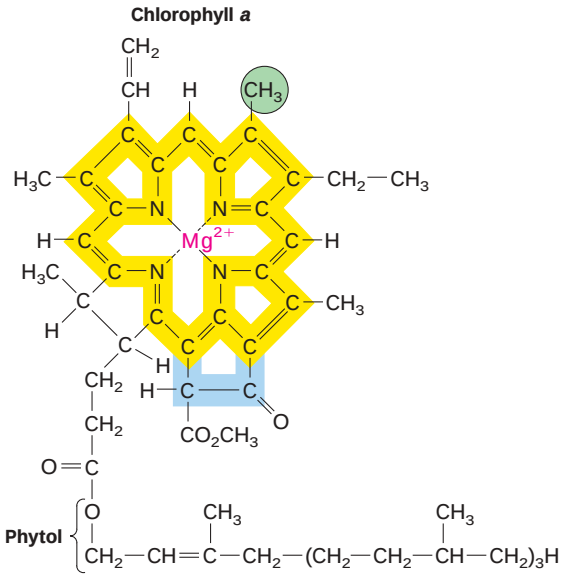

▲ FIGURE 8-31 **Structure of chlorophyll *a*, the principal pigment that traps light energy.** The CH_3 group (green) is replaced by a CHO group in chlorophyll *b*. In the porphyrin ring (yellow), electrons are delocalized among three of the four central rings and the atoms that interconnect them in the molecule. In chlorophyll, an Mg^{2+} ion, rather than an Fe^{3+} ion, is in the center of the porphyrin ring and an additional five-membered ring (blue) is present; otherwise, its structure is similar to that of heme found in molecules such as hemoglobin and cytochromes (see Figure 8-15a). The hydrocarbon phytol "tail" facilitates binding of chlorophyll to hydrophobic regions of chlorophyll-binding proteins.

Mg^{2+} ion (rather than Fe atom) and have an additional five-membered ring. The energy of the absorbed light is used to remove electrons from an unwilling donor (water, in green plants), forming oxygen,

$$2\ H_2O \xrightarrow{\text{light}} O_2 + 4\ H^+ + 4\ e^-$$

and then to transfer the electrons to a *primary electron acceptor,* a quinone designated Q, which is similar to CoQ.

Stage 2: Electron Transport and Generation of a Proton-Motive Force Electrons move from the quinone primary electron acceptor through a series of electron carriers until they reach the ultimate electron acceptor, usually the oxidized form of **nicotinamide adenine dinucleotide phosphate ($NADP^+$),** reducing it to NADPH. (NADP is identical in structure with NAD except for the presence of an additional phosphate group. Both molecules gain and lose electrons in the same way; see Figure 2-26a.) The transport of electrons in the thylakoid membrane is coupled to the movement of protons from the stroma to the thylakoid lumen, forming a pH gradient across the membrane ($pH_{lumen} < pH_{stroma}$). This process is analogous to generation of a proton-motive force across the inner mitochondrial membrane during electron transport (see Figure 8-2).

Thus the overall reaction of stages 1 and 2 can be summarized as

$$2\ H_2O + 2\ NADP^+ \xrightarrow{\text{light}} 2\ H^+ + 2\ NADPH + O_2$$

Stage 3: Synthesis of ATP Protons move down their concentration gradient from the thylakoid lumen to the stroma through the F_0F_1 complex (ATP synthase), which couples proton movement to the synthesis of ATP from ADP and P_i. The mechanism whereby chloroplast F_0F_1 harnesses the proton-motive force to synthesize ATP is identical with that used by ATP synthase in the inner mitochondrial membrane and bacterial plasma membrane (see Figures 8-24 and 8-26).

Stage 4: Carbon Fixation The ATP and NADPH generated by the second and third stages of photosynthesis provide the energy and the electrons to drive the synthesis of polymers of six-carbon sugars from CO_2 and H_2O. The overall balanced chemical equation is written as

$$6\ CO_2 + 18\ ATP^{4-} + 12\ NADPH + 12\ H_2O \longrightarrow$$
$$C_6H_{12}O_6 + 18\ ADP^{3-} + 18\ P_i^{2-} + 12\ NADP^+ + 6\ H^+$$

The reactions that generate the ATP and NADPH used in carbon fixation are directly dependent on light energy; thus stages 1–3 are called the *light reactions* of photosynthesis. The reactions in stage 4 are indirectly dependent on light energy; they are sometimes called the *dark reactions* of photosynthesis because they can occur in the dark, utilizing the supplies of ATP and NADPH generated by light energy. However, the reactions in stage 4 are not confined to the dark; in fact, they occur primarily during illumination.

Each Photon of Light Has a Defined Amount of Energy

Quantum mechanics established that light, a form of electromagnetic radiation, has properties of both waves and particles. When light interacts with matter, it behaves as discrete packets of energy (quanta) called *photons.* The energy of a photon, ε, is proportional to the frequency of the light wave: $\varepsilon = h\gamma$, where h is Planck's constant (1.58×10^{-34} cal·s, or 6.63×10^{-34} J·s) and γ is the frequency of the light wave. It is customary in biology to refer to the wavelength of the light wave, λ, rather than to its frequency γ. The two are related by the simple equation $\gamma = c \div \lambda$, where c is the velocity of light (3×10^{10} cm/s in a vacuum). Note that photons of *shorter* wavelength have *higher* energies.

Also, the energy in 1 mol of photons can be denoted by $E = N\varepsilon$, where N is Avogadro's number (6.02×10^{23} molecules or photons/mol). Thus

$$E = Nh\gamma = \frac{Nhc}{\lambda}$$

The energy of light is considerable, as we can calculate for light with a wavelength of 550 nm (550×10^{-7} cm), typical of sunlight:

$$E = \frac{(6.02 \times 10^{23}\ \text{photons/mol})\,(1.58 \times 10^{-34}\text{cal·s})\,(3 \times 10^{10}\ \text{cm/s})}{550 \times 10^{-7}\text{cm}}$$
$$= 51{,}881\ \text{cal/mol}$$

or about 52 kcal/mol. This is enough energy to synthesize several moles of ATP from ADP and P_i if all the energy were used for this purpose.

Photosystems Comprise a Reaction Center and Associated Light-Harvesting Complexes

The absorption of light energy and its conversion into chemical energy occurs in multiprotein complexes called **photosystems.** Found in all photosynthetic organisms, both eukaryotic and prokaryotic, photosystems consist of two closely linked components: a *reaction center,* where the primary events of photosynthesis occur, and an antenna complex consisting of numerous protein complexes, termed *light-harvesting complexes (LHCs),* which capture light energy and transmit it to the reaction center.

Both reaction centers and antennas contain tightly bound light-absorbing pigment molecules. Chlorophyll *a* is the principal pigment involved in photosynthesis, being present in both reaction centers and antennas. In addition to chlorophyll *a,* antennas contain other light-absorbing pigments: *chlorophyll b* in vascular plants and *carotenoids* in both plants and photosynthetic bacteria. Carotenoids consist of long hydrocarbon chains with alternating single and double bonds; they are similar in structure to the visual pigment retinal, which absorbs light in the eye (Chapter 7). The presence of various antenna pigments, which absorb light at

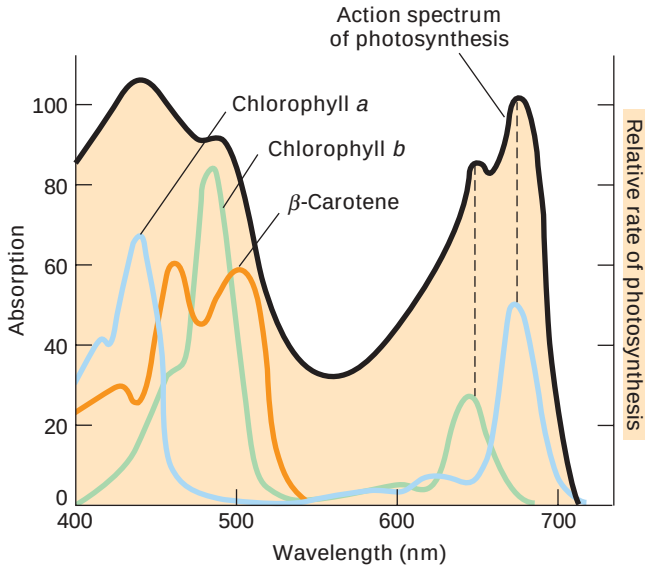

▲ EXPERIMENTAL FIGURE 8-32 **The rate of photosynthesis is greatest at wavelengths of light absorbed by three pigments.** The action spectrum of photosynthesis in plants, that is, the ability of light of different wavelengths to support photosynthesis, is shown in black. Absorption spectra for three photosynthetic pigments present in the antennas of plant photosystems are shown in color. Each absorption spectrum shows how well light of different wavelengths is absorbed by one of the pigments. A comparison of the action spectrum with the individual absorption spectra suggests that photosynthesis at 680 nm is primarily due to light absorbed by chlorophyll *a;* at 650 nm, to light absorbed by chlorophyll *b;* and at shorter wavelengths, to light absorbed by chlorophylls *a* and *b* and by carotenoid pigments, including β-carotene.

different wavelengths, greatly extends the range of light that can be absorbed and used for photosynthesis.

One of the strongest pieces of evidence for the involvement of chlorophylls and carotenoids in photosynthesis is that the absorption spectrum of these pigments is similar to the action spectrum of photosynthesis (Figure 8-32). The latter is a measure of the relative ability of light of different wavelengths to support photosynthesis.

When chlorophyll *a* (or any other molecule) absorbs visible light, the absorbed light energy raises the chlorophyll *a* to a higher energy (excited) state. This differs from the ground (unexcited) state largely in the distribution of electrons around the C and N atoms of the porphyrin ring. Excited states are unstable and return to the ground state by one of several competing processes. For chlorophyll *a* molecules dissolved in organic solvents such as ethanol, the principal reactions that dissipate the excited-state energy are the emission of light (fluorescence and phosphorescence) and thermal emission (heat). When the same chlorophyll *a* is bound to the unique protein environment of the reaction center, dissipation of excited-state energy occurs by a quite different process that is the key to photosynthesis.

Photoelectron Transport from Energized Reaction-Center Chlorophyll *a* Produces a Charge Separation

The absorption of a photon of light of wavelength ≈680 nm by chlorophyll *a* increases its energy by 42 kcal/mol (the first excited state). Such an energized chlorophyll *a* molecule in a plant reaction center rapidly donates an electron to an intermediate acceptor, and the electron is rapidly passed on to the primary electron acceptor, quinone Q, on the stromal surface of the thylakoid membrane. This light-driven electron transfer, called **photoelectron transport,** depends on the unique environment of both the chlorophylls and the acceptor within the reaction center. Photoelectron transport, which occurs nearly every time a photon is absorbed, leaves a positive charge on the chlorophyll *a* close to the luminal surface and generates a reduced, negatively charged acceptor (Q^-) near the stromal surface (Figure 8-33).

The Q^- produced by photoelectron transport is a powerful reducing agent with a strong tendency to transfer an electron to another molecule, ultimately to $NADP^+$. The positively charged chlorophyll a^+, a strong oxidizing agent, attracts an electron from an electron donor on the luminal surface to regenerate the original chlorophyll *a*. In plants, the oxidizing power of four chlorophyll a^+ molecules is used, by way of intermediates, to remove four electrons from 2 H_2O molecules bound to a site on the luminal surface to form O_2:

$$2\ H_2O + 4\ \text{chlorophyll}\ a^+ \longrightarrow 4\ H^+ + O_2 + 4\ \text{chlorophyll}\ a$$

These potent biological reductants and oxidants provide all the energy needed to drive all subsequent reactions of photosynthesis: electron transport, ATP synthesis, and CO_2 fixation.

Chlorophyll *a* also absorbs light at discrete wavelengths shorter than 680 nm (see Figure 8-32). Such absorption raises

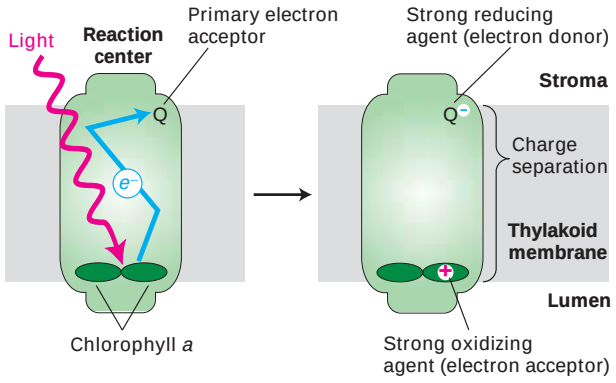

▲ FIGURE 8-33 **Photoelectron transport, the primary event in photosynthesis.** After absorption of a photon of light, one of the excited special pair of chlorophyll *a* molecules in the reaction center (*left*) donates an electron to a loosely bound acceptor molecule, the quinone Q, on the stromal surface of the thylakoid membrane, creating an essentially irreversible charge separation across the membrane (*right*). The electron cannot easily return through the reaction center to neutralize the positively charged chlorophyll *a*.

MEDIA CONNECTIONS
Focus Animation: Photosynthesis

the molecule into one of several higher excited states, which decay within 10^{-12} seconds (1 picosecond, ps) to the first excited state with loss of the extra energy as heat. Because photoelectron transport and the resulting charge separation occur only from the first excited state of the reaction-center chlorophyll *a*, the quantum yield—the amount of photosynthesis per absorbed photon—is the same for all wavelengths of visible light shorter (and, therefore, of higher energy) than 680 nm.

Light-Harvesting Complexes Increase the Efficiency of Photosynthesis

Although chlorophyll *a* molecules within a reaction center are capable of directly absorbing light and initiating photosynthesis, they most commonly are energized indirectly by energy transferred from light-harvesting complexes (LHCs) in an associated antenna. Even at the maximum light intensity encountered by photosynthetic organisms (tropical noontime sunlight), each reaction-center chlorophyll *a* molecule absorbs only about one photon per second, which is not enough to support photosynthesis sufficient for the needs of the plant. The involvement of LHCs greatly increases the efficiency of photosynthesis, especially at more typical light intensities, by increasing absorption of 680-nm light and by extending the range of wavelengths of light that can be absorbed by other antenna pigments.

Photons can be absorbed by any of the pigment molecules in an LHC. The absorbed energy is then rapidly transferred (in $< 10^{-9}$ seconds) to one of the two "special-pair" chlorophyll *a* molecules in the associated reaction center, where it promotes the primary photosynthetic charge separation (see Figure 8-33). LHC proteins maintain the pigment molecules in the precise orientation and position optimal for light absorption and energy transfer, thereby maximizing the very rapid and efficient *resonance transfer* of energy from antenna pigments to reaction-center chlorophylls. Recent studies on one of the two photosystems in cyanobacteria, which are similar to those in higher plants, suggest that energy from absorbed light is funneled first to a "bridging" chlorophyll in each LHC and then to the special pair of reaction-center chlorophylls (Figure 8-34). Surprisingly, however, the molecular structures of LHCs from plants and cyanobacteria are completely different from those in green and purple bacteria, even though both types contain carotenoids and chlorophylls in a clustered geometric arrangement within the membrane.

Although LHC antenna chlorophylls can transfer light energy absorbed from a photon, they cannot release an electron. As we've seen already, this function resides in the two reaction-center chlorophylls. To understand their electron-releasing ability, we examine the structure and function of the reaction center in bacterial and plant photosystems in the next section.

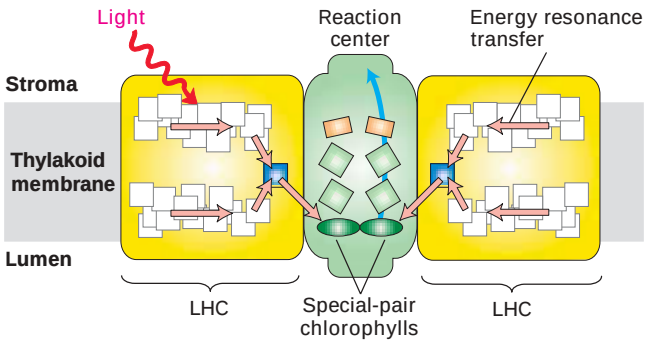

▲ FIGURE 8-34 **Energy transfer from light-harvesting complexes to associated reaction center in photosystem I of cyanobacteria.** The multiprotein light-harvesting complex binds 90 chlorophyll molecules (white and blue) and 31 other small molecules, all held in a specific geometric arrangement for optimal light absorption. Of the six chlorophyll molecules (green) in the reaction center, two constitute the special-pair chlorophylls (ovals) that can initiate photoelectron transport when excited (blue arrows). Resonance transfer of energy (red arrows) rapidly funnels energy from absorbed light to one of two "bridging" chlorophylls (blue) and thence to chlorophylls in the reaction center. [Adapted from W. Kühlbrandt, 2001, *Nature* **411**:896, and P. Jordan et al., 2001, *Nature* **411**:909.]

KEY CONCEPTS OF SECTION 8.4

Photosynthetic Stages and Light-Absorbing Pigments

- The principal end products of photosynthesis in plants are oxygen and polymers of six-carbon sugars (starch and sucrose).
- The light-capturing and ATP-generating reactions of photosynthesis occur in the thylakoid membrane located within chloroplasts. The permeable outer membrane and inner membrane surrounding chloroplasts do not participate in photosynthesis (see Figure 8-30).
- In stage 1 of photosynthesis, light is absorbed by chlorophyll *a* molecules bound to reaction-center proteins in the thylakoid membrane. The energized chlorophylls donate an electron to a quinone on the opposite side of the membrane, creating a charge separation (see Figure 8-33). In green plants, the positively charged chlorophylls then remove electrons from water, forming oxygen.
- In stage 2, electrons are transported from the reduced quinone via carriers in the thylakoid membrane until they reach the ultimate electron acceptor, usually $NADP^+$, reducing it to NADPH. Electron transport is coupled to movement of protons across the membrane from the stroma to the thylakoid lumen, forming a pH gradient (proton-motive force) across the thylakoid membrane.
- In stage 3, movement of protons down their electrochemical gradient through F_0F_1 complexes powers the synthesis of ATP from ADP and P_i.
- In stage 4, the ATP and NADPH generated in stages 2 and 3 provide the energy and the electrons to drive the fixation of CO_2 and synthesis of carbohydrates. These reactions occur in the thylakoid stroma and cytosol.

■ Associated with each reaction center are multiple light-harvesting complexes (LHCs), which contain chlorophylls *a* and *b*, carotenoids, and other pigments that absorb light at multiple wavelengths. Energy is transferred from the LHC chlorophyll molecules to reaction-center chlorophylls by resonance energy transfer (see Figure 8-34).

8.5 Molecular Analysis of Photosystems

As noted in the previous section, photosynthesis in the green and purple bacteria does not generate oxygen, whereas photosynthesis in cyanobacteria, algae, and higher plants does.* This difference is attributable to the presence of two types of photosystem (PS) in the latter organisms: PSI reduces $NADP^+$ to NADPH, and PSII forms O_2 from H_2O. In contrast, the green and purple bacteria have only one type of photosystem, which cannot form O_2. We first discuss the simpler photosystem of purple bacteria and then consider the more complicated photosynthetic machinery in chloroplasts.

The Single Photosystem of Purple Bacteria Generates a Proton-Motive Force but No O_2

The three-dimensional structures of the photosynthetic reaction centers from two purple bacteria have been determined, permitting scientists to trace the detailed paths of electrons during and after the absorption of light. Similar proteins and pigments compose photosystem II of plants as well, and the conclusions drawn from studies on this simple photosystem have proven applicable to plant systems.

The reaction center of purple bacteria contains three protein subunits (L, M, and H) located in the plasma membrane (Figure 8-35). Bound to these proteins are the prosthetic groups that absorb light and transport electrons during photosynthesis. The prosthetic groups include a "special pair" of bacteriochlorophyll *a* molecules equivalent to the reaction-center chlorophyll *a* molecules in plants, as well as several other pigments and two quinones, termed Q_A and Q_B, that are structurally similar to mitochondrial ubiquinone.

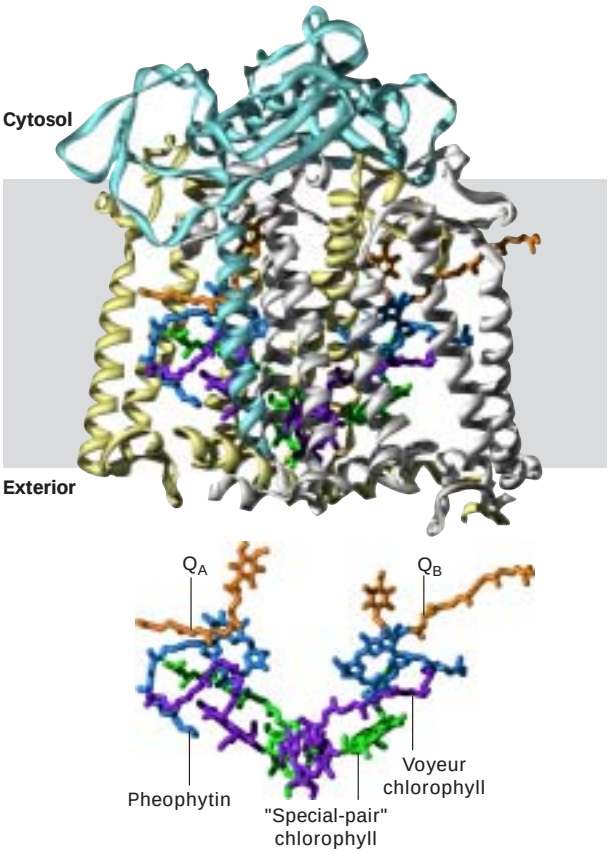

▲ FIGURE 8-35 **Three-dimensional structure of the photosynthetic reaction center from the purple bacterium *Rhodobacter spheroides*.** (*Top*) The L subunit (yellow) and M subunit (white) each form five transmembrane α helices and have a very similar structure overall; the H subunit (light blue) is anchored to the membrane by a single transmembrane α helix. A fourth subunit (not shown) is a peripheral protein that binds to the exoplasmic segments of the other subunits. (*Bottom*) Within each reaction center is a special pair of bacteriochlorophyll *a* molecules (green), capable of initiating photoelectron transport; two voyeur chlorophylls (purple); two pheophytins (dark blue), and two quinones, Q_A and Q_B (orange). Q_B is the primary electron acceptor during photosynthesis. [After M. H. Stowell et al., 1997, *Science* **276**:812.]

Initial Charge Separation The mechanism of charge separation in the photosystem of purple bacteria is identical with that in plants outlined earlier; that is, energy from absorbed light is used to strip an electron from a reaction-center bacteriochlorophyll *a* molecule and transfer it, via several different pigments, to the primary electron acceptor Q_B, which is loosely bound to a site on the cytosolic membrane face. The chlorophyll thereby acquires a positive charge, and Q_B acquires a negative charge. To determine the pathway traversed by electrons through the bacterial reaction center, researchers exploited the fact that each pigment absorbs light of only certain wavelengths, and its absorption spectrum changes when it possesses an extra electron. Because these electron movements are completed in less than 1 millisecond (ms), a special technique called *picosecond absorption spectroscopy* is required to monitor the changes in the absorption spectra of the various pigments as a function of time shortly after the absorption of a light photon.

When a preparation of bacterial membrane vesicles is exposed to an intense pulse of laser light lasting less than 1 ps, each

*A very different type of bacterial photosynthesis, which occurs only in certain archaebacteria, is not discussed here because it is very different from photosynthesis in higher plants. In this type of photosynthesis, the plasma-membrane protein bacteriorhodopsin pumps one proton from the cytosol to the extracellular space for every quantum of light absorbed. This small protein has seven membrane-spanning segments and a covalently attached retinal pigment (see Figure 5-13).

reaction center absorbs one photon. Light absorbed by the chlorophyll *a* molecules in each reaction center converts them to the excited state, and the subsequent electron transfer processes are synchronized in all reaction centers. Within 4×10^{-12} seconds (4 ps), an electron moves to one of the pheophytin molecules (Ph), leaving a positive charge on the chlorophyll *a*. It takes 200 ps for the electron to move to Q_A, and then, in the slowest step, 200μs for it to move to Q_B. This pathway of electron flow is traced in the left portion of Figure 8-36.

Subsequent Electron Flow and Coupled Proton Movement

After the primary electron acceptor, Q_B, in the bacterial reaction center accepts one electron, forming $Q_B^{-}\cdot$, it accepts a second electron from the same reaction-center chlorophyll following its absorption of a second photon. The quinone then binds two protons from the cytosol, forming the reduced quinone (QH_2), which is released from the reaction center (see Figure 8-36). QH_2 diffuses within the bacterial membrane to the Q_o site on the exoplasmic face of a cytochrome bc_1 complex, where it releases its two protons into the periplasmic space (the space between the plasma membrane and the bacterial cell wall). This process moves protons from the cytosol to the outside of the cell, generating a proton-motive force across the plasma membrane. Simultaneously, QH_2 releases its two electrons, which move through the cytochrome bc_1 complex exactly as depicted for the mitochondrial $CoQH_2$–cytochrome *c* reductase complex in Figure 8-21. The Q cycle in the bacterial reaction center, like the Q cycle in mitochondria, pumps additional protons from the cytosol to the intermembrane space, thereby increasing the proton-motive force.

The acceptor for electrons transferred through the cytochrome bc_1 complex is a soluble cytochrome, a one-electron carrier, in the periplasmic space, which is reduced from the Fe^{3+} to the Fe^{2+} state. The reduced cytochrome (analogous to cytochrome *c* in mitochondria) then diffuses to a reaction center, where it releases its electron to a positively charged chlorophyll a^+, returning the chlorophyll to the ground state and the cytochrome to the Fe^{3+} state. This *cyclic* electron flow generates no oxygen and no reduced coenzymes.

Electrons also can flow through the single photosystem of purple bacteria via a *linear* (noncyclic) pathway. In this case, electrons removed from reaction-center chlorophylls ultimately are transferred to NAD^+ (rather than $NADP^+$ as in plants), forming NADH. To reduce the oxidized reaction-center chlorophyll *a* back to its ground state, an electron is transferred from a reduced cytochrome *c;* the oxidized cytochrome *c* that is formed is reduced by electrons removed from hydrogen sulfide (H_2S), forming elemental sulfur (S), or from hydrogen gas (H_2). Since H_2O is not the electron donor, no O_2 is formed.

Both the cyclic and linear pathways of electron flow in the bacterial photosystem generate a proton-motive force. As

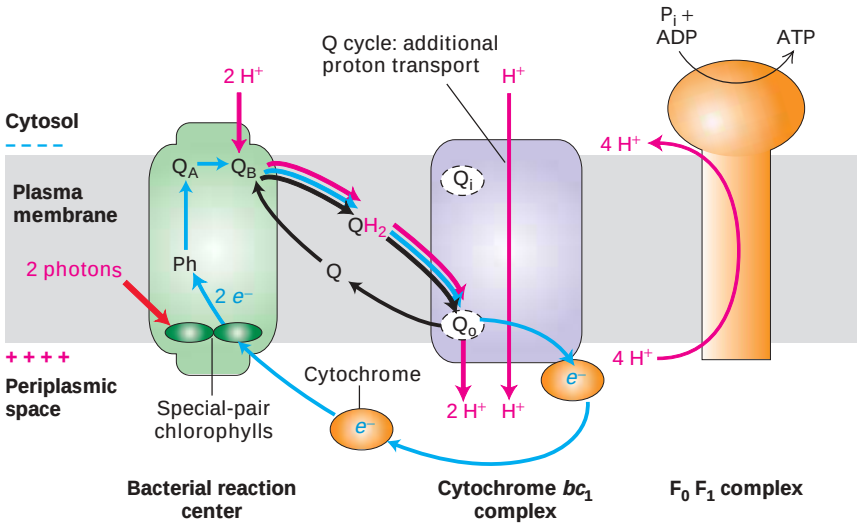

▲ FIGURE 8-36 **Cyclic electron flow in the single photosystem of purple bacteria.** Blue arrows indicate flow of electrons; red arrows indicate proton movement. *(Left)* Energy funneled from an associated LHC (not illustrated here) energizes one of the special-pair chlorophylls in the reaction center. Photoelectron transport from the energized chlorophyll, via pheophytin (Ph) and quinone A (Q_A), to quinone B (Q_B) forms the semiquinone $Q^{-}\cdot$ and leaves a positive charge on the chlorophyll. Following absorption of a second photon and transfer of a second electron to the semiquinone, it rapidly picks up two protons from the cytosol to form QH_2. *(Center)* After diffusing through the membrane and binding to the Q_o site on the exoplasmic face of the cytochrome bc_1 complex, QH_2 donates two electrons and simultaneously gives up two protons to the external medium, generating a proton-motive force ($H^+_{exoplasmic} > H^+_{cytosolic}$). Electrons are transported back to the reaction-center chlorophyll via a soluble cytochrome, which diffuses in the periplasmic space. Operation of a Q cycle in the cytochrome bc_1 complex pumps additional protons across the membrane to the external medium, as in mitochondria. The proton-motive force is used by the F_0F_1 complex to synthesize ATP and, as in other bacteria, to transport molecules in and out of the cell. [Adapted from J. Deisenhofer and H. Michael, 1991, *Ann. Rev. Cell Biol.* **7**:1]

in other systems, this proton-motive force is used by the F_0F_1 complex located in the plasma membrane to synthesize ATP and also to transport molecules across the membrane against a concentration gradient.

Chloroplasts Contain Two Functionally and Spatially Distinct Photosystems

In the 1940s, biophysicist R. Emerson discovered that the rate of plant photosynthesis generated by light of wavelength 700 nm can be greatly enhanced by adding light of shorter wavelength. He found that a combination of light at, say, 600 and 700 nm supports a greater rate of photosynthesis than the sum of the rates for the two separate wavelengths. This so-called *Emerson effect* led researchers to conclude that photosynthesis in plants involves the interaction of two separate photosystems, referred to as *PSI* and *PSII*. PSI is driven by light of wavelength 700 nm or less; PSII, only by light of shorter wavelength <680 nm.

As in the reaction center of green and purple bacteria, each chloroplast photosystem contains a pair of specialized reaction-center chlorophyll *a* molecules, which are capable of initiating photoelectron transport. The reaction-center chlorophylls in PSI and PSII differ in their light-absorption maxima because of differences in their protein environment. For this reason, these chlorophylls are often denoted P_{680} (PSII) and P_{700} (PSI). Like a bacterial reaction center, each chloroplast reaction center is associated with multiple light-harvesting complexes (LHCs); the LHCs associated with PSII and PSI contain different proteins.

The two photosystems also are distributed differently in thylakoid membranes: PSII primarily in stacked regions (grana) and PSI primarily in unstacked regions. The stacking of the thylakoid membranes may be due to the binding properties of the proteins in PSII. Evidence for this distribution came from studies in which thylakoid membranes were gently fragmented into vesicles by ultrasound. Stacked and unstacked thylakoid vesicles were then fractionated by density-gradient centrifugation. The stacked fractions contained primarily PSII protein and the unstacked fraction, PSI.

Finally, and most importantly, the two chloroplast photosystems differ significantly in their functions: only PSII splits water to form oxygen, whereas only PSI transfers electrons to the final electron acceptor, $NADP^+$. Photosynthesis in chloroplasts can follow a linear or cyclic pathway, again like green and purple bacteria. The linear pathway, which we discuss first, can support carbon fixation as well as ATP synthesis. In contrast, the cyclic pathway supports only ATP synthesis and generates no reduced NADPH for use in carbon fixation. Photosynthetic algae and cyanobacteria contain two photosystems analogous to those in chloroplasts.

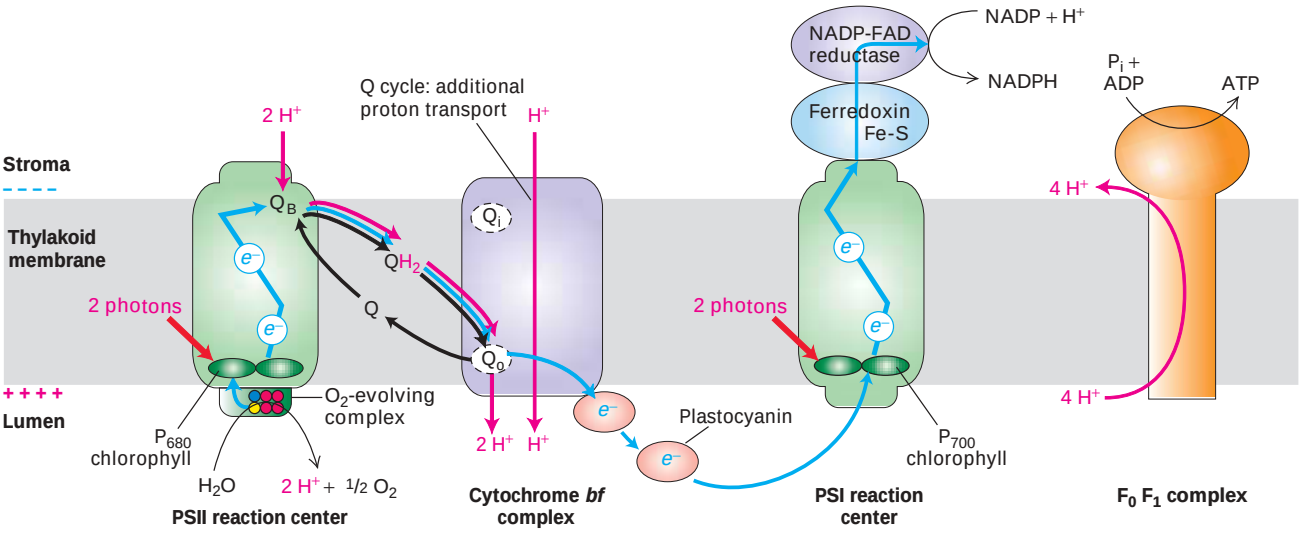

▲ FIGURE 8-37 **Linear electron flow in plants, which requires both chloroplast photosystems, PSI and PSII.** Blue arrows indicate flow of electrons; red arrows indicate proton movement. LHCs are not shown. *(Left)* In the PSII reaction center, two sequential light-induced excitations of the same P_{680} chlorophylls result in reduction of the primary electron acceptor Q_B to QH_2. On the luminal side of PSII, electrons removed from H_2O in the thylakoid lumen are transferred to P_{680}^+, restoring the reaction-center chlorophylls to the ground state and generating O_2. *(Center)* The cytochrome *bf* complex then accepts electrons from QH_2, coupled to the release of two protons into the lumen. Operation of a Q cycle in the cytochrome *bf* complex translocates additional protons across the membrane to the thylakoid lumen, increasing the proton-motive force generated. *(Right)* In the PSI reaction center, each electron released from light-excited P_{700} chlorophylls moves via a series of carriers in the reaction center to the stromal surface, where soluble ferredoxin (an Fe-S protein) transfers the electron to FAD and finally to $NADP^+$, forming NADPH. P_{700}^+ is restored to its ground state by addition of an electron carried from PSII via the cytochrome *bf* complex and plastocyanin, a soluble electron carrier. The proton-motive force generated by linear electron flow from PSII to NADP-FAD reductase powers ATP synthesis by the F_0F_1 complex.

Linear Electron Flow Through Both Plant Photosystems, PSII and PSI, Generates a Proton-Motive Force, O_2, and NADPH

Linear electron flow in chloroplasts involves PSII and PSI in an obligate series in which electrons are transferred from H_2O to $NADP^+$. The process begins with absorption of a photon by PSII, causing an electron to move from a P_{680} chlorophyll *a* to an acceptor plastoquinone (Q_B) on the stromal surface (Figure 8-37). The resulting oxidized P_{680}^+ strips one electron from the highly unwilling donor H_2O, forming an intermediate in O_2 formation and a proton, which remains in the thylakoid lumen and contributes to the proton-motive force. After P_{680} absorbs a second photon, the semiquinone $Q^{-}\cdot$ accepts a second electron and picks up two protons from the stromal space, generating QH_2. After diffusing in the membrane, QH_2 binds to the Q_o site on a cytochrome *bf* complex, which is analogous in structure and function to the cytochrome bc_1 complex in purple bacteria and the $CoQH_2$–cytochrome *c* reductase complex in mitochondria. As in these systems a Q cycle operates in the cytochrome *bf* complex in association with the PSII reaction center, thereby increasing the proton-motive force generated by electron transport.

Absorption of a photon by PSI leads to removal of an electron from the reaction-center chlorophyll *a*, P_{700} (see Figure 8-37). The resulting oxidized P_{700}^+ is reduced by an electron passed from the PSII reaction center via the cytochrome *bf* complex and *plastocyanin*, a soluble electron carrier that contains a single copper (Cu) atom. After the cytochrome *bf* complex accepts electrons from QH_2, it transfers them, one at a time, to the Cu^{2+} form of plastocyanin, reducing it to the Cu^+ form. Reduced plastocyanin then diffuses in the thylakoid lumen, carrying the electron to P_{700}^+ in PSI. The electron taken up at the luminal surface by P_{700} moves via several carriers to the stromal surface of the thylakoid membrane, where it is accepted by ferredoxin, an iron-sulfur (Fe-S) protein. Electrons excited in PSI can be transferred from ferredoxin via the electron carrier FAD to $NADP^+$, forming, together with one proton picked up from the stroma, the reduced molecule NADPH.

F_0F_1 complexes in the thylakoid membrane use the proton-motive force generated during linear electron flow to synthesize ATP on the stromal side of membrane. Thus this pathway yields both NADPH and ATP in the stroma of the chloroplast, where they are utilized for CO_2 fixation.

An Oxygen-Evolving Complex Is Located on the Luminal Surface of the PSII Reaction Center

Somewhat surprisingly, the structure of the PSII reaction center, which removes electrons from H_2O to form O_2, resembles that of the reaction center of photosynthetic purple bacteria, which does not form O_2. Like the bacterial reaction center, the PSII reaction center contains two molecules of chlorophyll *a* (P_{680}), as well as two other chlorophylls, two pheophytins, two quinones (Q_A and Q_B), and one nonheme iron atom. These small molecules are bound to two PSII proteins, called D1 and D2, whose sequences are remarkably similar to the sequences of the L and M peptides of the bacterial reaction center, attesting to their common evolutionary origins (see Figure 8-35). When PSII absorbs a photon with a wavelength of <680 nm, it triggers the loss of an electron from a P_{680} molecule, generating P_{680}^+. As in photosynthetic purple bacteria, the electron is transported via a pheophytin and a quinone (Q_A) to the primary electron acceptor, Q_B, on the outer (stromal) surface of the thylakoid membrane (Figures 8-37 and 8-38).

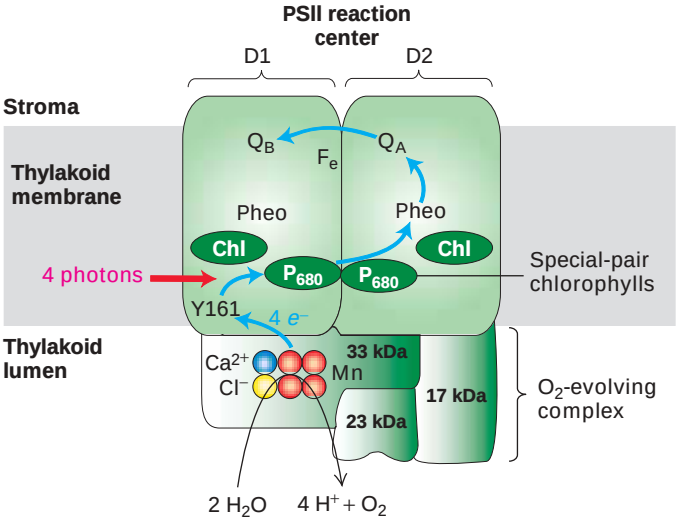

▲ FIGURE 8-38 **Electron flow and O_2 evolution in chloroplast PSII.** The PSII reaction center, comprising two integral proteins, D1 and D2, special-pair chlorophylls (P_{680}), and other electron carriers, is associated with an oxygen-evolving complex on the luminal surface. Bound to the three extrinsic proteins (33, 23, and 17 kDa) of the oxygen-evolving complex are four manganese ions (red), a Ca^{2+} ion (blue), and a Cl^- ion (yellow). These bound ions function in the splitting of H_2O and maintain the environment essential for high rates of O_2 evolution. Tyrosine-161 (Y161) of the D1 polypeptide conducts electrons from the Mn ions to the oxidized reaction-center chlorophyll (P_{680}^+), reducing it to the ground state P_{680}. See the text for details. [Adapted from C. Hoganson and G. Babcock, 1997, *Science* **277**:1953.]

The photochemically oxidized reaction-center chlorophyll of PSII, P_{680}^+, is the strongest biological oxidant known. The reduction potential of P_{680}^+ is more positive than that of water, and thus it can oxidize water to generate O_2 and H^+ ions. Photosynthetic bacteria cannot oxidize water because the excited chlorophyll a^+ in the bacterial reaction center is not a sufficiently strong oxidant. (As noted earlier, purple bacteria use H_2S and H_2 as electron donors to reduce chlorophyll a^+ in linear electron flow.)

The splitting of H_2O, which provides the electrons for reduction of P_{680}^+ in PSII, is catalyzed by a three-protein complex, the *oxygen-evolving complex*, located on the luminal surface of the thylakoid membrane. The oxygen-evolving complex contains four manganese (Mn) ions as well as

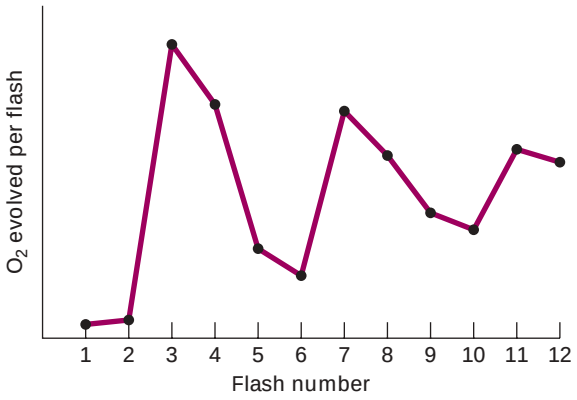

▲ EXPERIMENTAL FIGURE 8-39 **A single PSII absorbs a photon and transfers an electron four times to generate one O_2.** Dark-adapted chloroplasts were exposed to a series of closely spaced, short (5-μs) pulses of light that activated virtually all the PSIIs in the preparation. The peaks in O_2 evolution occurred after every fourth pulse, indicating that absorption of four photons by one PSII is required to generate each O_2 molecule. Because the dark-adapted chloroplasts were initially in a partially reduced state, the peaks in O_2 evolution occurred after flashes 3, 7, and 11. [From J. Berg et al., 2002, *Biochemistry,* 5th ed., W. H. Freeman and Company.]

bound Cl^- and Ca^{2+} ions (see Figure 8-38); this is one of the very few cases in which Mn plays a role in a biological system. These Mn ions together with the three extrinsic proteins can be removed from the reaction center by treatment with solutions of concentrated salts; this abolishes O_2 formation but does not affect light absorption or the initial stages of electron transport.

The oxidation of two molecules of H_2O to form O_2 requires the removal of four electrons, but absorption of each photon by PSII results in the transfer of just one electron. A simple experiment, described in Figure 8-39, resolved whether the formation of O_2 depends on a single PSII or multiple ones acting in concert. The results indicated that a single PSII must lose an electron and then oxidize the oxygen-evolving complex four times in a row for an O_2 molecule to be formed.

Manganese is known to exist in multiple oxidation states with from two to five positive charges. Subsequent spectroscopic studies indeed showed that the bound Mn ions in the oxygen-evolving complex cycle through five different oxidation states, S_0–S_4. In this S cycle, a total of two H_2O molecules are split into four protons, four electrons, and one O_2 molecule. The electrons released from H_2O are transferred, one at a time, via the Mn ions and a nearby tyrosine side chain on the D1 subunit, to the reaction-center P_{680}^+, where they regenerate the reduced chlorophyll, P_{680}. The protons released from H_2O remain in the thylakoid lumen. Despite a great deal of experimentation we still do not know the details of how O_2 is formed by this Mn-containing complex.

Herbicides that inhibit photosynthesis not only are very important in agriculture but also have proved useful in dissecting the pathway of photoelectron transport in plants. One such class of herbicides, the *s*-triazines (e.g., atrazine), binds specifically to D1 in the PSII reaction center, thus inhibiting binding of oxidized Q_B to its site on the stromal surface of the thylakoid membrane. When added to illuminated chloroplasts, *s*-triazines cause all downstream electron carriers to accumulate in the oxidized form, since no electrons can be released from PSII. In atrazine-resistant mutants, a single amino acid change in D1 renders it unable to bind the herbicide, so photosynthesis proceeds at normal rates. Such resistant weeds are prevalent and present a major agricultural problem. ▮

Cyclic Electron Flow Through PSI Generates a Proton-Motive Force but No NADPH or O_2

As we've seen, electrons from reduced ferredoxin in PSI are transferred to $NADP^+$ during linear electron flow (see Figure 8-37). Alternatively, reduced ferredoxin can donate two electrons to a quinone (Q) bound to a site on the stromal surface of PSI; the quinone then picks up two protons from the stroma, forming QH_2. This QH_2 then diffuses through the thylakoid membrane to the Q_o binding site on the luminal surface of the cytochrome *bf* complex. There it releases two electrons to the cytochrome *bf* complex and two protons to the thylakoid lumen, generating a proton-motive force. As in linear electron flow, these electrons return to PSI via plastocyanin. This cyclic electron flow, which does not involve PSII, is similar to the cyclic process that occurs in the single photosystem of purple bacteria (see Figure 8-36). A Q cycle operates in the cytochrome *bf* complex during cyclic electron flow, leading to transport of two additional protons into the lumen for each pair of electrons transported and a greater proton-motive force.

The proton-motive force generated during cyclic electron flow in chloroplasts powers ATP synthesis by F_0F_1 complexes in the thylakoid membrane. This process, however, generates no NADPH, and no O_2 evolves.

Relative Activity of Photosystems I and II Is Regulated

In order for PSII and PSI to act in sequence during linear electron flow, the amount of light energy delivered to the two reaction centers must be controlled so that each center activates the same number of electrons. If the two photosystems are not equally excited, then cyclic electron flow occurs in PSI, and PSII becomes less active. One mechanism for regulating the relative contribution of linear and cyclic electron flow in chloroplasts entails the reversible phosphorylation and dephosphorylation of the proteins associated with the PSII light-harvesting complex (LHCII).

According to this mechanism, a membrane-bound protein kinase senses the relative activities of the two photosys-

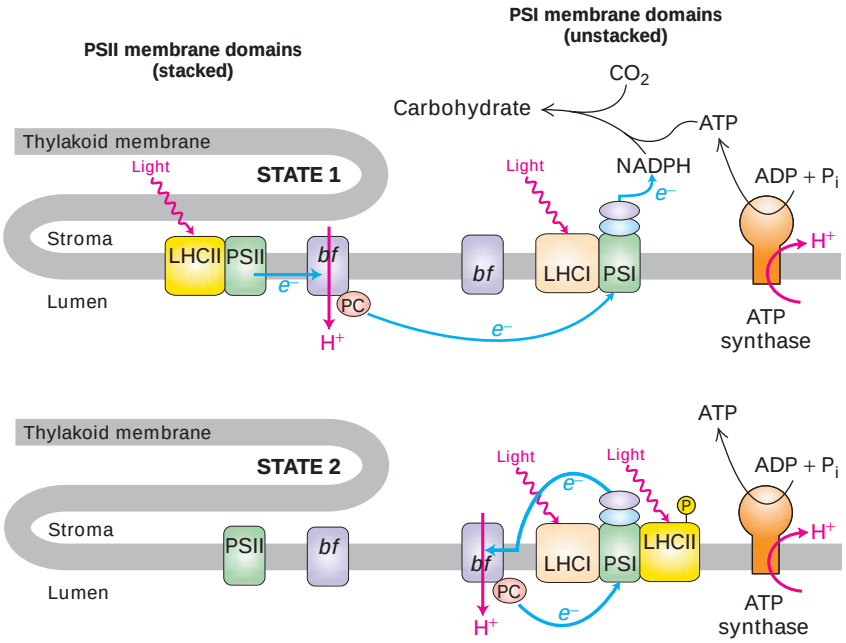

◀ FIGURE 8-40 **Distribution of multiprotein complexes in the thylakoid membrane and the regulation of linear versus cyclic electron flow.** *(Top)* In sunlight, PSI and PSII are equally activated, and the photosystems are organized in state I. In this arrangement, light-harvesting complex II (LHCII) is not phosphorylated and is tightly associated with the PSII reaction center in the grana. As a result, PSII and PSI can function in parallel in linear electron flow. *(Bottom)* When light excitation of the two photosystems is unbalanced, LHCII becomes phosphorylated, dissociates from PSII, and diffuses into the unstacked membranes, where it associates with PSI and its permanently associated LHCI. In this alternative supramolecular organization (state II), most of the absorbed light energy is transferred to PSI, supporting cyclic electron flow and ATP production but no formation of NADPH and thus no CO_2 fixation. PC = plastocyanin. [Adapted from F. A. Wollman, 2001, *EMBO J.* **20**:3623.]

tems. This monitoring may involve recognition of the oxidized-reduced state of the plastoquinone pool that transfers electrons from PSII to the cytochrome *bf* complex en route to PSI. Balanced excitation of the two photosystems is associated with linear electron flow (Figure 8-40, state I). However, if too much plastoquinone is reduced (indicating excessive activation of PSII relative to PSI), the kinase becomes activated and some LHCIIs are phosphorylated. These phosphorylated LHCIIs dissociate from PSII, which is preferentially located in the grana, and diffuse in the membrane to the unstacked thylakoid membranes, where they can activate PSI. This redistribution of LHCIIs, which decreases the antenna size of PSII and increases that of PSI, and the concomitant redistribution of cytochrome *bf* complexes from PSII-rich to PSI-rich membrane domains promote cyclic electron flow (Figure 8-40, state II).

The supramolecular organization of the photosystems in plants thus has the effect of directing them toward ATP production (state II) or toward generation of reducing equivalents (NADPH) and ATP (state I). Both NADPH and ATP are required to convert CO_2 to sucrose or starch, the fourth stage in photosynthesis, which we cover in the last section of this chapter.

KEY CONCEPTS OF SECTION 8.5

Molecular Analysis of Photosystems

- In the single photosystem of purple bacteria, cyclic electron flow from light-excited chlorophyll *a* molecules in the reaction center generates a proton-motive force, which is used mainly to power ATP synthesis by the F_0F_1 complex in the plasma membrane (Figure 8-36).
- Plants contain two photosystems, PSI and PSII, which have different functions and are physically separated in the thylakoid membrane. PSII splits H_2O into O_2. PSI reduces $NADP^+$ to NADPH. Cyanobacteria have two analogous photosystems.
- In chloroplasts, light energy absorbed by light-harvesting complexes (LHCs) is transferred to chlorophyll *a* molecules in the reaction centers (P_{680} in PSII and P_{700} in PSI).
- Electrons flow through PSII via the same carriers that are present in the bacterial photosystem. In contrast to the bacterial system, photochemically oxidized P_{680}^+ in PSII is regenerated to P_{680} by electrons derived from the splitting of H_2O with evolution of O_2 (see Figure 8-37, *left*).
- In linear electron flow, photochemically oxidized P_{700}^+ in PSI is reduced, regenerating P_{700}, by electrons transferred from PSII via the cytochrome *bf* complex and soluble plastocyanin. Electrons lost from P_{700} following excitation of PSI are transported via several carriers ultimately to $NADP^+$, generating NADPH (see Figure 8-37, *right*).
- In contrast to linear electron flow, which requires both PSII and PSI, cyclic electron flow in plants involves only PSI. In this pathway, neither NADPH nor O_2 is formed, although a proton-motive force is generated.
- The proton-motive force generated by photoelectron transport in plant and bacterial photosystems is augmented by operation of the Q cycle in cytochrome *bf* complexes associated with each of the photosystems.
- Reversible phosphorylation and dephosphorylation of the PSII light-harvesting complex control the functional organization of the photosynthetic apparatus in thylakoid membranes. State I favors linear electron flow, whereas state II favors cyclic electron flow (see Figure 8-40).

8.6 CO_2 Metabolism During Photosynthesis

Chloroplasts perform many metabolic reactions in green leaves. In addition to CO_2 fixation, the synthesis of almost all amino acids, all fatty acids and carotenes, all pyrimidines, and probably all purines occurs in chloroplasts. However, the synthesis of sugars from CO_2 is the most extensively studied biosynthetic pathway in plant cells. We first consider the unique pathway, known as the **Calvin cycle** (after discoverer Melvin Calvin), that fixes CO_2 into three-carbon compounds, powered by energy released during ATP hydrolysis and oxidation of NADPH.

CO_2 Fixation Occurs in the Chloroplast Stroma

The reaction that actually fixes CO_2 into carbohydrates is catalyzed by *ribulose 1,5-bisphosphate carboxylase* (often called *rubisco*), which is located in the stromal space of the chloroplast. This enzyme adds CO_2 to the five-carbon sugar ribulose 1,5-bisphosphate to form two molecules of 3-phosphoglycerate (Figure 8-41). Rubisco is a large enzyme (≈500 kDa) composed of eight identical large subunits and eight identical small subunits. One subunit is encoded in chloroplast DNA; the other, in nuclear DNA. Because the catalytic rate of rubisco is quite slow, many copies of the enzyme are needed to fix sufficient CO_2. Indeed, this enzyme makes up almost 50 percent of the chloroplast protein and is believed to be the most abundant protein on earth.

When photosynthetic algae are exposed to a brief pulse of ^{14}C-labeled CO_2 and the cells are then quickly disrupted, 3-phosphoglycerate is radiolabeled most rapidly, and all the radioactivity is found in the carboxyl group. This finding establishes that ribulose 1,5-bisphosphate carboxylase fixes the CO_2. Because CO_2 is initially incorporated into a three-carbon compound, the Calvin cycle is also called the *C_3 pathway* of carbon fixation.

The fate of 3-phosphoglycerate formed by rubisco is complex: some is converted to starch or sucrose, but some is used to regenerate ribulose 1,5-bisphosphate. At least nine enzymes are required to regenerate ribulose 1,5-bisphosphate from 3-phosphoglycerate. Quantitatively, for every 12 molecules of 3-phosphoglycerate generated by rubisco (a total of 36 C atoms), 2 molecules (6 C atoms) are converted to 2 molecules of glyceraldehyde 3-phosphate (and later to 1 hexose), while 10 molecules (30 C atoms) are converted to 6 molecules of ribulose 1,5-bisphosphate (Figure 8-42, *top*). The fixation of six CO_2 molecules and the net formation of two glyceraldehyde 3-phosphate molecules require the consumption of 18 ATPs and 12 NADPHs, generated by the light-requiring processes of photosynthesis.

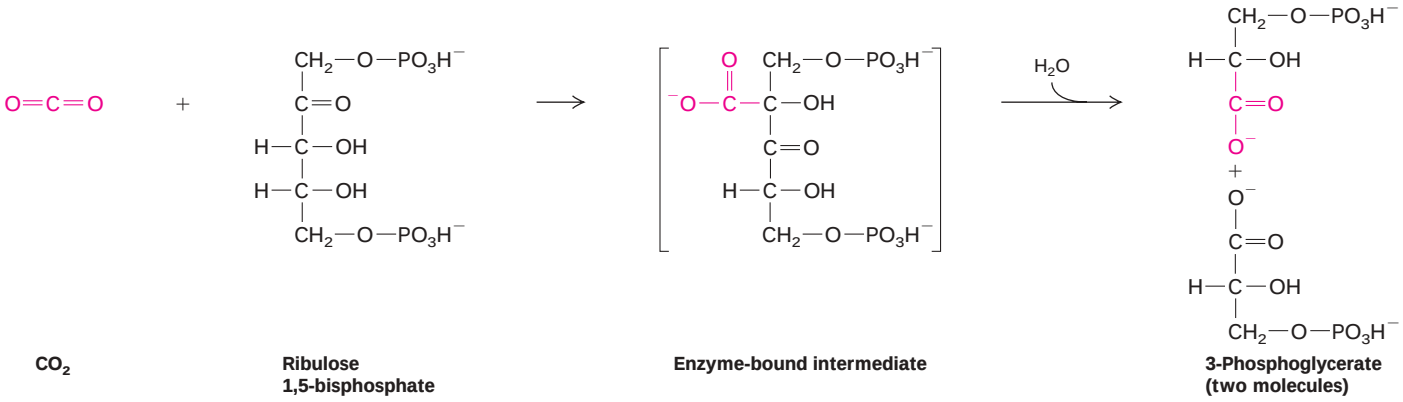

▲ FIGURE 8-41 **The initial reaction that fixes CO_2 into organic compounds.** In this reaction, catalyzed by ribulose 1,5-bisphosphate carboxylase, CO_2 condenses with the five-carbon sugar ribulose 1,5-bisphosphate. The products are two molecules of 3-phosphoglycerate.

▶ FIGURE 8-42 **The pathway of carbon during photosynthesis.** *(Top)* Six molecules of CO_2 are converted into two molecules of glyceraldehyde 3-phosphate. These reactions, which constitute the Calvin cycle, occur in the stroma of the chloroplast. Via the phosphate/triosephosphate antiporter, some glyceraldehyde 3-phosphate is transported to the cytosol in exchange for phosphate. *(Bottom)* In the cytosol, an exergonic series of reactions converts glyceraldehyde 3-phosphate to fructose 1,6-bisphosphate and, ultimately, to the disaccharide sucrose. Some glyceraldehyde 3-phosphate (not shown here) is also converted to amino acids and fats, compounds essential to plant growth.

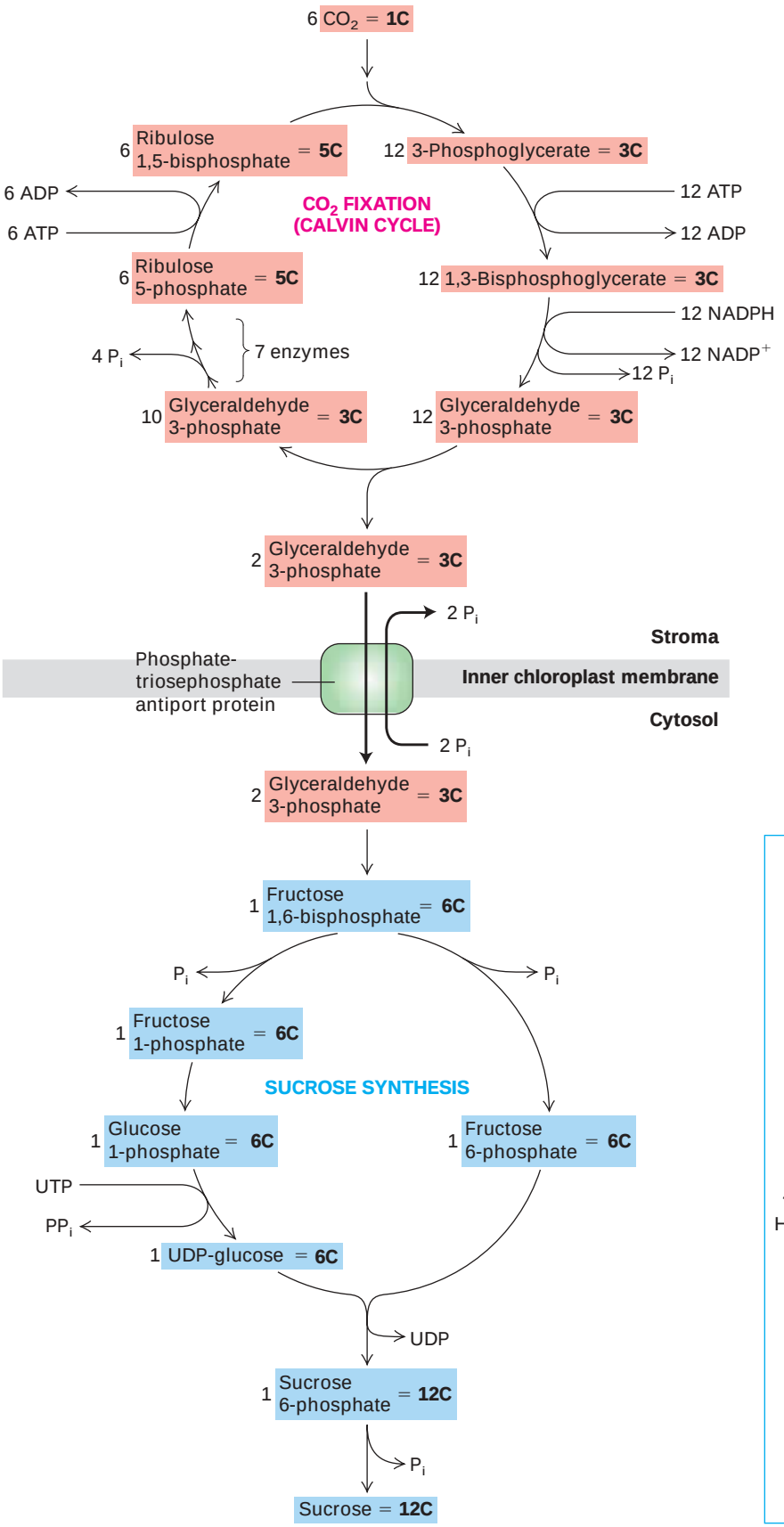
6 CO2 = 1C
6 Ribulose 1,5-bisphosphate = 5C
12 3-Phosphoglycerate = 3C
6 ADP
6 ATP
CO2 FIXATION (CALVIN CYCLE)
12 ATP
12 ADP
6 Ribulose 5-phosphate = 5C
12 1,3-Bisphosphoglycerate = 3C
12 NADPH
12 NADP+
12 Pi
4 Pi
7 enzymes
10 Glyceraldehyde 3-phosphate = 3C
12 Glyceraldehyde 3-phosphate = 3C
2 Glyceraldehyde 3-phosphate = 3C
2 Pi
Stroma
Phosphate-triosephosphate antiport protein
Inner chloroplast membrane
Cytosol
2 Pi
2 Glyceraldehyde 3-phosphate = 3C
1 Fructose 1,6-bisphosphate = 6C
Pi
Pi
1 Fructose 1-phosphate = 6C
SUCROSE SYNTHESIS
1 Glucose 1-phosphate = 6C
1 Fructose 6-phosphate = 6C
UTP
PPi
1 UDP-glucose = 6C
UDP
1 Sucrose 6-phosphate = 12C
Pi
Sucrose = 12C

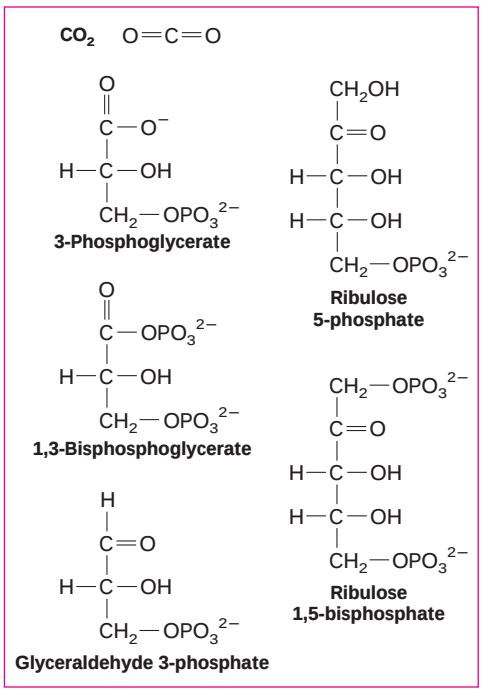
CO2
3-Phosphoglycerate
Ribulose 5-phosphate
1,3-Bisphosphoglycerate
Ribulose 1,5-bisphosphate
Glyceraldehyde 3-phosphate

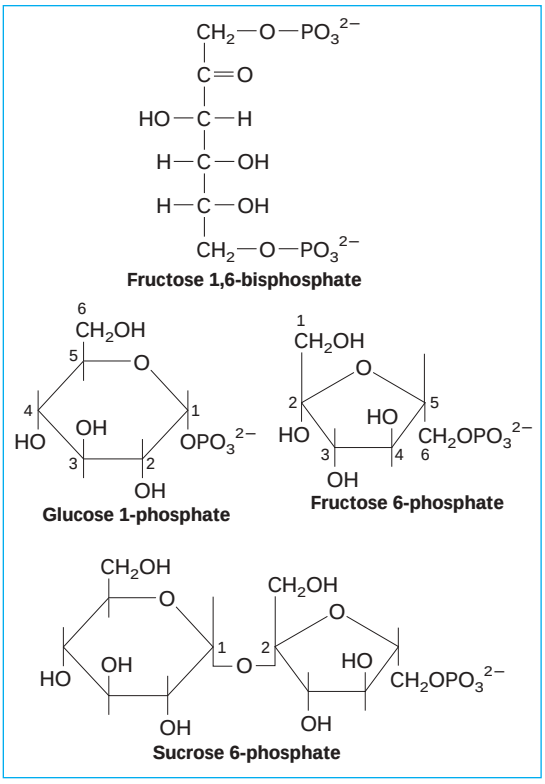
Fructose 1,6-bisphosphate
Glucose 1-phosphate
Fructose 6-phosphate
Sucrose 6-phosphate

Synthesis of Sucrose Incorporating Fixed CO_2 Is Completed in the Cytosol

After its formation in the chloroplast stroma, glyceraldehyde 3-phosphate is transported to the cytosol in exchange for phosphate. The final steps of sucrose synthesis occur in the cytosol of leaf cells. In these reactions, one molecule of glyceraldehyde 3-phosphate is isomerized to dihydroxyacetone phosphate. This compound condenses with a second molecule of glyceraldehyde 3-phosphate to form fructose 1,6-bisphosphate, which is the reverse of the aldolase reaction in glycolysis (see Figure 8-4, step 4). Fructose 1,6-bisphosphate is converted primarily to sucrose by the reactions shown in the bottom portion of Figure 8-42.

The transport protein in the chloroplast membrane that brings fixed CO_2 (as glyceraldehyde 3-phosphate) into the cytosol when the cell is exporting sucrose vigorously is a strict antiporter: No fixed CO_2 leaves the chloroplast unless phosphate is fed into it. The phosphate is generated in the cytosol, primarily during the formation of sucrose, from phosphorylated three-carbon intermediates. Thus the synthesis of sucrose and its export from leaf cells to other cells encourages the transport of additional glyceraldehyde 3-phosphate from the chloroplast to the cytosol.

Light and Rubisco Activase Stimulate CO_2 Fixation

The Calvin cycle enzymes that catalyze CO_2 fixation are rapidly inactivated in the dark, thereby conserving ATP that is generated in the dark for other synthetic reactions, such as lipid and amino acid biosynthesis. One mechanism that contributes to this control is the pH dependence of several Calvin cycle enzymes. Because protons are transported from the stroma into the thylakoid lumen during photoelectron transport (see Figure 8-37), the pH of the stroma increases from ≈7 in the dark to ≈8 in the light. The increased activity of several Calvin cycle enzymes at the higher pH promotes CO_2 fixation in the light.

A stromal protein called *thioredoxin (Tx)* also plays a role in controlling some Calvin cycle enzymes. In the dark, thioredoxin contains a disulfide bond; in the light, electrons are transferred from PSI, via ferredoxin, to thioredoxin, reducing its disulfide bond:

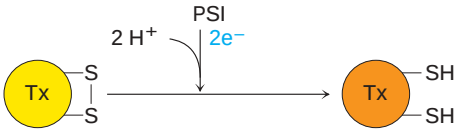

Reduced thioredoxin then activates several Calvin cycle enzymes by reducing disulfide bonds in them. In the dark, when thioredoxin becomes reoxidized, these enzymes are reoxidized and thus inactivated.

Rubisco is spontaneously activated in the presence of high CO_2 and Mg^{2+} concentrations. The activating reaction entails covalent addition of CO_2 to the side-chain amino group of lysine-191, forming a carbamate group that then binds a Mg^{2+} ion. Under normal conditions, however, with ambient levels of CO_2, the reaction requires catalysis by rubisco activase, an enzyme that simultaneously hydrolyzes ATP and uses the energy to attach a CO_2 to the lysine. This enzyme was discovered during the study of a mutant strain of *Arabidopsis thaliana* that required high CO_2 levels to grow and that did not exhibit light activation of ribulose 1,5-bisphosphate carboxylase; the mutant had a defective rubisco activase.

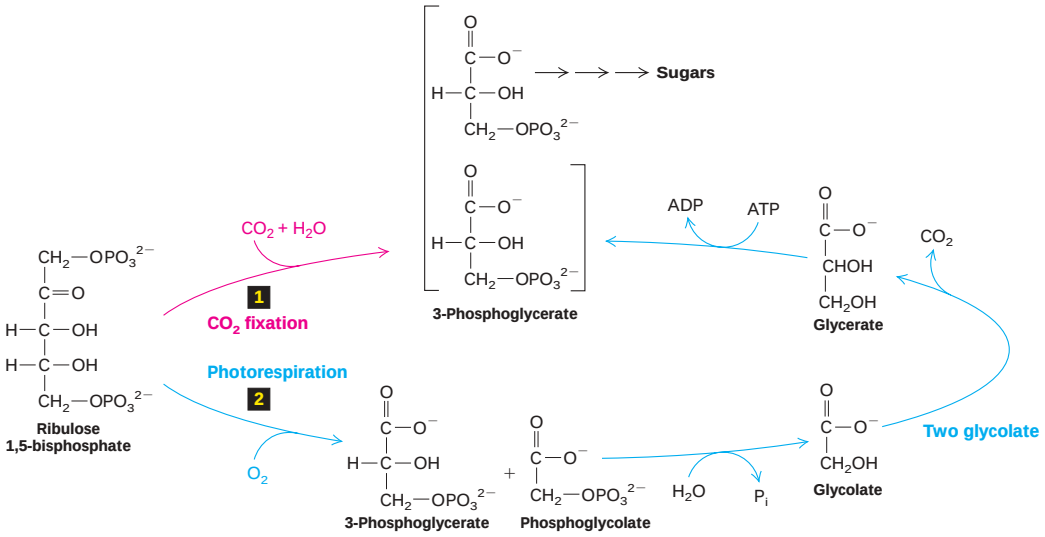

▲ FIGURE 8-43 **CO_2 fixation and photorespiration.** These competing pathways are both initiated by ribulose 1,5-bisphosphate carboxylase (rubisco), and both utilize ribulose 1,5-bisphosphate. CO_2 fixation, pathway (1), is favored by high CO_2 and low O_2 pressures; photorespiration, pathway (2), occurs at low CO_2 and high O_2 pressures (that is, under normal atmospheric conditions). Phosphoglycolate is recycled via a complex set of reactions that take place in peroxisomes and mitochondria, as well as chloroplasts. The net result: for every two molecules of phosphoglycolate formed by photorespiration (four C atoms), one molecule of 3-phosphoglycerate is ultimately formed and recycled, and one molecule of CO_2 is lost.

Photorespiration, Which Competes with Photosynthesis, Is Reduced in Plants That Fix CO_2 by the C_4 Pathway

Photosynthesis is always accompanied by **photorespiration**—a process that takes place in light, consumes O_2, and converts ribulose 1,5-bisphosphate in part to CO_2. As Figure 8-43 shows, rubisco catalyzes two competing reactions: the addition of CO_2 to ribulose 1,5-bisphosphate to form two molecules of 3-phosphoglycerate and the addition of O_2 to form one molecule of 3-phosphoglycerate and one molecule of the two-carbon compound phosphoglycolate. Photorespiration is wasteful to the energy economy of the plant: it consumes ATP and O_2, and it generates CO_2. It is surprising, therefore, that all known rubiscos catalyze photorespiration. Probably the necessary structure of the active site of rubisco precluded evolution of an enzyme that does not catalyze photorespiration.

In a hot, dry environment, plants must keep the gas-exchange pores (stomata) in their leaves closed much of the time to prevent excessive loss of moisture. This causes the CO_2 level inside the leaf to fall below the K_m of rubisco for CO_2. Under these conditions, the rate of photosynthesis is slowed and photorespiration is greatly favored. Corn, sugar cane, crabgrass, and other plants that can grow in hot, dry environments have evolved a way to avoid this problem by utilizing a two-step pathway of CO_2 fixation in which a CO_2-hoarding step precedes the Calvin cycle. The pathway has been named the *C_4 pathway* because [^{14}C] CO_2 labeling showed that the first radioactive molecules formed during photosynthesis in this pathway are four-carbon compounds, such as oxaloacetate and malate, rather than the three-carbon molecules that begin the Calvin cycle (C_3 pathway).

The C_4 pathway involves two types of cells: *mesophyll cells,* which are adjacent to the air spaces in the leaf interior, and *bundle sheath cells,* which surround the vascular tissue (Figure 8-44a). In the mesophyll cells of C_4 plants, phosphoenolpyruvate, a three-carbon molecule derived from pyruvate, reacts with CO_2 to generate oxaloacetate, a four-

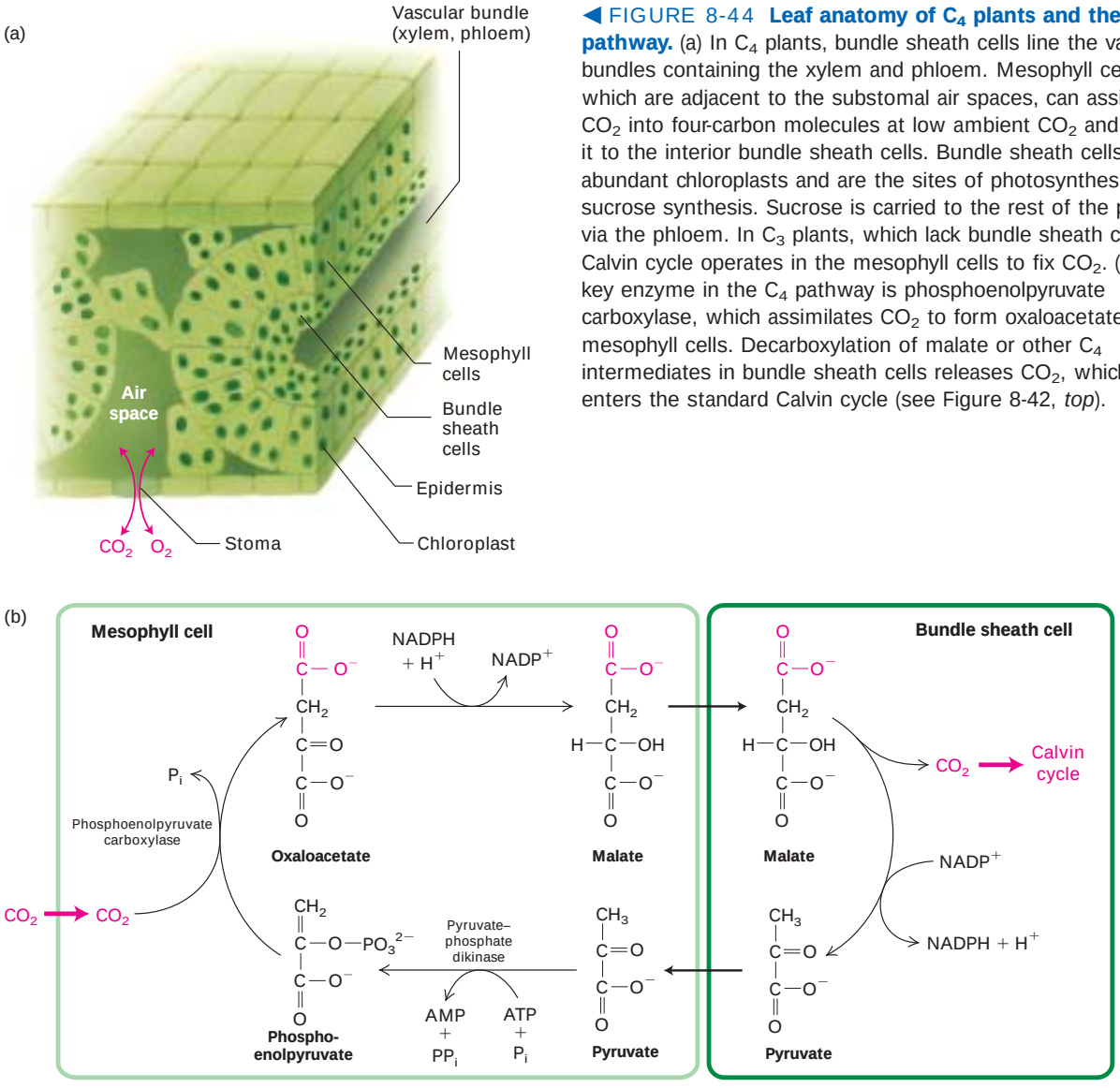

◀ FIGURE 8-44 **Leaf anatomy of C_4 plants and the C_4 pathway.** (a) In C_4 plants, bundle sheath cells line the vascular bundles containing the xylem and phloem. Mesophyll cells, which are adjacent to the substomal air spaces, can assimilate CO_2 into four-carbon molecules at low ambient CO_2 and deliver it to the interior bundle sheath cells. Bundle sheath cells contain abundant chloroplasts and are the sites of photosynthesis and sucrose synthesis. Sucrose is carried to the rest of the plant via the phloem. In C_3 plants, which lack bundle sheath cells, the Calvin cycle operates in the mesophyll cells to fix CO_2. (b) The key enzyme in the C_4 pathway is phosphoenolpyruvate carboxylase, which assimilates CO_2 to form oxaloacetate in mesophyll cells. Decarboxylation of malate or other C_4 intermediates in bundle sheath cells releases CO_2, which enters the standard Calvin cycle (see Figure 8-42, *top*).

carbon compound. The enzyme that catalyzes this reaction, *phosphoenolpyruvate carboxylase,* is found almost exclusively in C_4 plants and unlike rubisco is insensitive to O_2. The overall reaction from pyruvate to oxaloacetate involves the hydrolysis of one phosphoanhydride bond in ATP and has a negative ΔG. Therefore, CO_2 fixation will proceed even when the CO_2 concentration is low. The oxaloacetate formed in mesophyll cells is reduced to malate, which is transferred, by a special transporter, to the bundle sheath cells, where the CO_2 is released by decarboxylation and enters the Calvin cycle (Figure 8-44b).

Because of the transport of CO_2 from mesophyll cells, the CO_2 concentration in the bundle sheath cells of C_4 plants is much higher than it is in the normal atmosphere. Bundle sheath cells are also unusual in that they lack PSII and carry out only cyclic electron flow catalyzed by PSI, so no O_2 is evolved. The high CO_2 and reduced O_2 concentrations in the bundle sheath cells favor the fixation of CO_2 by rubisco to form 3-phosphoglycerate and inhibit the utilization of ribulose 1,5-bisphosphate in photorespiration.

In contrast, the high O_2 concentration in the atmosphere favors photorespiration in the mesophyll cells of C_3 plants (pathway 2 in Figure 8-43); as a result, as much as 50 percent of the carbon fixed by rubisco may be reoxidized to CO_2 in C_3 plants. C_4 plants are superior to C_3 plants in utilizing the available CO_2, since the C_4 enzyme phosphoenolpyruvate carboxylase has a higher affinity for CO_2 than does rubisco in the Calvin cycle. However, one phosphodiester bond of ATP is consumed in the cyclic C_4 process (to generate phosphoenolpyruvate from pyruvate); thus the overall efficiency of the photosynthetic production of sugars from NADPH and ATP is lower than it is in C_3 plants, which use only the Calvin cycle for CO_2 fixation. Nonetheless, the net rates of photosynthesis for C_4 grasses, such as corn or sugar cane, can be two to three times the rates for otherwise similar C_3 grasses, such as wheat, rice, or oats, owing to the elimination of losses from photorespiration.

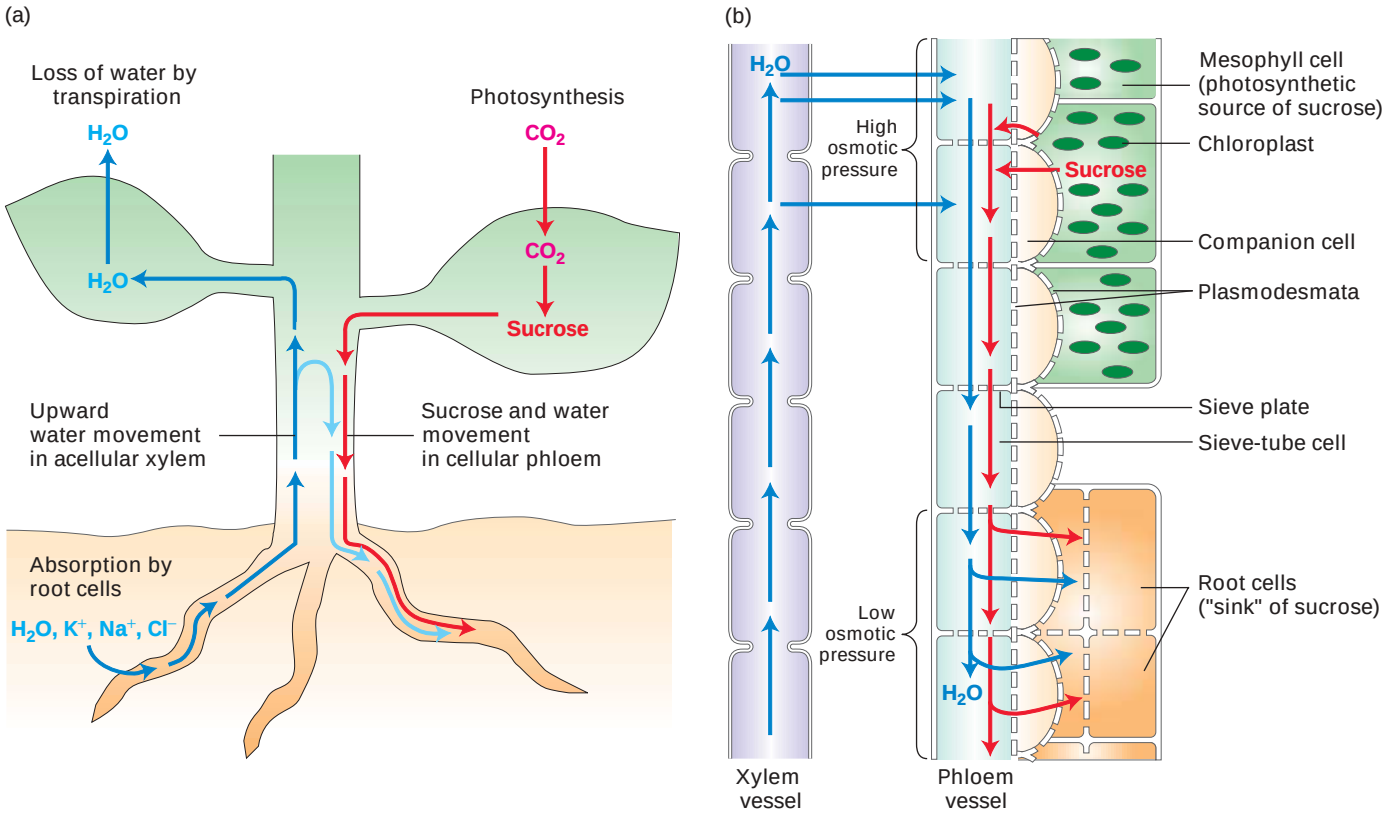

▲ FIGURE 8-45 **Schematic diagrams of the two vascular systems—xylem and phloem—in higher plants, showing the transport of water (blue) and sucrose (red).** (a) Water and salts enter the xylem through the roots. Water is lost by evaporation, mainly through the leaves, creating a suction pressure that draws the water and dissolved salts upward through the xylem. The phloem is used to conduct dissolved sucrose, produced in the leaves, to other parts of the plant. (b) Enlarged view illustrates the mechanism of sucrose flow in a higher plant. Sucrose is actively transported from mesophyll cells into companion cells, and then moves through plasmodesmata into the sieve-tube cells that constitute the phloem vessels. The resulting increase in osmotic pressure within the phloem causes water carried in xylem vessels to enter the phloem by osmotic flow. Root cells and other nonphotosynthetic cells remove sucrose from the phloem by active transport and metabolize it. This lowers the osmotic pressure in the phloem, causing water to exit the phloem. These differences in osmotic pressure in the phloem between the source and the sink of sucrose provide the force that drives sucrose through the phloem.

Sucrose Is Transported from Leaves Through the Phloem to All Plant Tissues

Of the two carbohydrate products of photosynthesis, starch remains in the mesophyll cells of C_3 plants and the bundle sheaf cells in C_4 plants. In these cells, starch is subjected to glycolysis, mainly in the dark, forming ATP, NADH, and small molecules that are used as building blocks for the synthesis of amino acids, lipids, and other cellular constituents. Sucrose, in contrast, is exported from the photosynthetic cells and transported throughout the plant. The vascular system used by higher plants to transport water, ions, sucrose, and other water-soluble substances has two components: the *xylem* and the *phloem*, which generally are grouped together in the *vascular bundle* (see Figure 8-44).

As illustrated in Figure 8-45a, the xylem conducts salts and water from the roots through the stems to the leaves. Water transported upward through the xylem is lost from the plant by evaporation, primarily from the leaves. In young plants the xylem is built of cells interconnected by plasmodesmata, but in mature tissues the cell body degenerates, leaving only the cell walls. The phloem, in contrast, transports dissolved sucrose and organic molecules such as amino acids from their sites of origin in leaves to tissues throughout the plant; water also is transported downward in the phloem.

A phloem vessel consists of long, narrow cells, called *sieve-tube cells*, interconnected by *sieve plates*, a type of cell wall that contains many **plasmodesmata** and is highly perforated (Figure 8-45b). Numerous plasmodesmata also connect the sieve-tube cells to *companion cells*, which line the phloem vessels, and mesophyll cells to companion cells. Sieve-tube cells have lost their nuclei and most other organelles but retain a water-permeable plasma membrane and cytoplasm, through which sucrose and water move. In effect, the sieve-tube cells form one continuous tube of cytosol that extends throughout the plant. Differences in osmotic strength cause the movement of sucrose from the photosynthetic mesophyll cells in the leaves, through the phloem, to the roots and other nonphotosynthetic tissues that catabolize sucrose.

KEY CONCEPTS OF SECTION 8.6

CO_2 Metabolism During Photosynthesis

- In the Calvin cycle, CO_2 is fixed into organic molecules in a series of reactions that occur in the chloroplast stroma. The initial reaction, catalyzed by rubisco, forms a three-carbon intermediate. Some of the glyceraldehyde 3-phosphate generated in the cycle is transported to the cytosol and converted to sucrose (see Figure 8-42).
- The light-dependent activation of several Calvin cycle enzymes and other mechanisms increases fixation of CO_2 in the light.
- In C_3 plants, much of the CO_2 fixed by the Calvin cycle is lost as the result of photorespiration, a wasteful reaction catalyzed by rubisco that is favored at low CO_2 and high O_2 pressures (see Figure 8-43).
- In C_4 plants, CO_2 is fixed initially in the outer mesophyll cells by reaction with phosphoenolpyruvate. The four-carbon molecules so generated are shuttled to the interior bundle sheath cells, where the CO_2 is released and then used in the Calvin cycle. The rate of photorespiration in C_4 plants is much lower than in C_3 plants.
- Sucrose from photosynthetic cells is transported through the phloem to nonphotosynthetic parts of the plant. Osmotic pressure differences provide the force that drives sucrose transport (see Figure 8-45).

PERSPECTIVES FOR THE FUTURE

Although the overall processes of photosynthesis and mitochondrial oxidation are well understood, many important details remain to be uncovered by a new generation of scientists. For example, little is known about how complexes I and IV in mitochondria couple proton and electron movements to create a proton-motive force. Similarly, although the binding-change mechanism for ATP synthesis by the F_0F_1 complex is now generally accepted, we do not understand how conformational changes in each β subunit are coupled to the cyclical binding of ADP and P_i, formation of ATP, and then release of ATP. Many questions also remain about the structure and function of transport proteins in the inner mitochondrial and chloroplast membranes that play key roles in oxidative phosphorylation and photosynthesis. Molecular analysis of such membrane proteins is difficult, and new types of techniques will be needed to elucidate the details of their structure and operation.

We now know that release of cytochrome *c* and other proteins from the intermembrane space of mitochondria into the cytosol plays a major role in triggering apoptosis (Chapter 22). Certain members of the Bcl-2 family of apoptotic proteins and ion channels localized in part to the outer mitochondrial membrane participate in this process. Yet much remains to be learned about the structure of these proteins in the mitochondrial membrane, their normal functions in cell metabolism, and the alterations that lead to apoptosis.

KEY TERMS

aerobic oxidation *301*
ATP synthase *302*
C_4 pathway *345*
Calvin cycle *342*
cellular respiration *307*
chemiosmosis *302*
chlorophylls *331*
chloroplasts *302*
citric acid cycle *309*
cytochromes *318*
electron carriers *302*
endosymbiont hypothesis *302*
F_0F_1 complex *302*
glycolysis *301*
mitochondria *301*

oxidative phosphorylation *316*
photoelectron transport *334*
photorespiration *345*
photosynthesis *301*
photosystems *333*
proton-motive force *302*
Q cycle *323*
respiratory (electron-transport) chain *310*
respiratory control *330*
rubisco *342*
substrate-level phosphorylation *304*
thylakoids *331*
uncouplers *330*

REVIEW THE CONCEPTS

1. The proton motive force (pmf) is essential for both mitochondrial and chloroplast function. What produces the pmf, and what is its relationship to ATP?

2. The mitochondrial inner membrane exhibits all of the fundamental characteristics of a typical cell membrane, but it also has several unique characteristics that are closely associated with its role in oxidative phosphorylation. What are these unique characteristics? How does each contribute to the function of the inner membrane?

3. Maximal production of ATP from glucose involves the reactions of glycolysis, the citric acid cycle, and the electron transport chain. Which of these reactions requires O_2, and why? Which, in certain organisms or physiological conditions, can proceed in the absence of O_2?

4. Describe how the electrons produced by glycolysis are delivered to the electron transport chain. What role do amino acids play in this process? What would be the consequence for overall ATP yield per glucose molecule if a mutation inactivated this delivery system? What would be the longer-term consequence for the activity of the glycolytic pathway?

5. Each of the cytochromes in the mitochondria contains prosthetic groups. What is a prosthetic group? Which type of prosthetic group is associated with the cytochromes? What property of the various cytochromes ensures unidirectional electron flow along the electron transport chain?

6. It is estimated that each electron pair donated by NADH leads to the synthesis of approximately three ATP molecules, while each electron pair donated by $FADH_2$ leads to the synthesis of approximately two ATP molecules. What is the underlying reason for the difference in yield for electrons donated by $FADH_2$ versus NADH?

7. Much of our understanding of ATP synthase is derived from research on aerobic bacteria. What makes these organisms useful for this research? Where do the reactions of glycolysis, the citric acid cycle, and the electron transport chain occur in these organisms? Where is the pmf generated in aerobic bacteria? What other cellular processes depend on the pmf in these organisms?

8. An important function of the mitochondrial inner membrane is to provide a selectively permeable barrier to the movement of water-soluble molecules and thus generate different chemical environments on either side of the membrane. However, many of the substrates and products of oxidative phosphorylation are water-soluble and must cross the inner membrane. How does this transport occur?

9. The Q cycle plays a major role in the electron transport chain of mitochondria, chloroplasts, and bacteria. What is the function of the Q cycle, and how does it carry out this function? What electron transport train components participate in the Q cycle in mitochondria, in purple bacteria, and in chloroplasts?

10. Write the overall reaction of oxygen-generating photosynthesis. Explain the following statement: the O_2 generated by photosynthesis is simply a by-product of the reaction's generation of carbohydrates and ATP.

11. Photosynthesis can be divided into multiple stages. What are the stages of photosynthesis, and where does each occur within the chloroplast? Where is the sucrose produced by photosynthesis generated?

12. The photosystems responsible for absorption of light energy are composed of two linked components, the reaction center and an antenna complex. What is the pigment composition and role of each in the process of light absorption? What evidence exists that the pigments found in these components are involved in photosynthesis?

13. Photosynthesis in green and purple bacteria does not produce O_2. Why? How can these organisms still use photosynthesis to produce ATP? What molecules serve as electron donors in these organisms?

14. Chloroplasts contain two photosystems. What is the function of each? For linear electron flow, diagram the flow of electrons from photon absorption to NADPH formation. What does the energy stored in the form of NADPH synthesize?

15. The Calvin cycle reactions that fix CO_2 do not function in the dark. What are the likely reasons for this? How are these reactions regulated by light?

ANALYZE THE DATA

A proton gradient can be analyzed with fluorescent dyes whose emission intensity profiles depend on pH. One of the most useful dyes for measuring the pH gradient across mitochondrial membranes is the membrane-impermeant, water-soluble fluorophore 2′,7′-bis-(2-carboxyethyl)-5(6)-carboxyfluorescein (BCECF). The effect of pH on the emission intensity of BCECF, excited at 505 nm, is shown in the accompanying figure. In one study, sealed vesicles containing this compound were prepared by mixing unsealed, isolated

inner mitochondrial membranes with BCECF; after resealing of the membranes, the vesicles were collected by centrifugation and then resuspended in nonfluorescent medium.

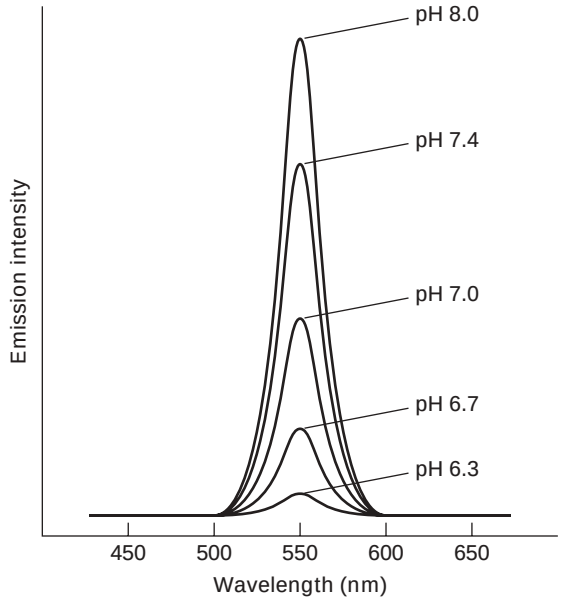

a. When these vesicles were incubated in a physiological buffer containing NADH, ADP, P_i, and O_2, the fluorescence of BCECF trapped inside gradually decreased in intensity. What does this decrease in fluorescent intensity suggest about this vesicular preparation?

b. How would you expect the concentrations of ADP, P_i, and O_2 to change during the course of the experiment described in part a? Why?

c. After the vesicles were incubated in buffer containing ADP, P_i, and O_2 for a period of time, addition of dinitrophenol caused an increase in BCECF fluorescence. In contrast, addition of valinomycin produced only a small transient effect. Explain these findings.

d. Predict the outcome of an experiment performed as described in part a if brown-fat tissue was used as a source of unsealed, isolated inner mitochondrial membranes. Explain your answer.

REFERENCES

Oxidation of Glucose and Fatty Acids to CO_2

Berg, J., J. Tymoczko, and L. Stryer. 2002. *Biochemistry,* 5th ed. W. H. Freeman and Company, chaps. 16 and 17.

Depre, C., M. Rider, and L. Hue. 1998. Mechanisms of control of heart glycolysis. *Eur. J. Biochem*. **258**:277–290.

Fell, D. 1997. *Understanding the Control of Metabolism*. Portland Press.

Fersht, A. 1999. *Structure and Mechanism in Protein Science: A Guide to Enzyme Catalysis and Protein Folding.* W. H. Freeman and Company. Contains an excellent discussion of the reaction mechanisms of key enzymes.

Fothergill-Gilmore, L. A., and P. A. Michels. 1993. Evolution of glycolysis. *Prog. Biophys. Mol. Biol.* **59**:105–135.

Guest, J. R., and G. C. Russell. 1992. Complexes and complexities of the citric acid cycle in *Escherichia coli. Curr. Top. Cell Reg.* **33**:231–247.

Krebs, H. A. 1970. The history of the tricarboxylic acid cycle. *Perspect. Biol. Med.* **14**:154–170.

Mannaerts, G. P., and P. P. Van Veldhoven. 1993. Metabolic pathways in mammalian peroxisomes. *Biochimie* **75**:147–158.

Nelson, D. L., and M. M. Cox. 2000. *Lehninger Principles of Biochemistry.* Worth, chaps. 14–17, 19.

Pilkis, S. J., T. H. Claus, I. J. Kurland, and A. J. Lange. 1995. 6-Phosphofructo-2-kinase/fructose-2,6-bisphosphatase: a metabolic signaling enzyme. *Ann. Rev. Biochem*. **64**:799–835.

Rasmussen, B., and R. Wolfe. 1999. Regulation of fatty acid oxidation in skeletal muscle. *Ann. Rev. Nutrition* **19**:463–484.

Velot, C., M. Mixon, M. Teige, and P. Srere. 1997. Model of a quinary structure between Krebs TCA cycle enzymes: a model for the metabolon. *Biochemistry* **36**:14271–14276.

Electron Transport and Generation of the Proton-Motive Force

Babcock, G. 1999. How oxygen is activated and reduced in respiration. *Proc. Nat'l. Acad. Sci. USA* **96**:12971–12973.

Beinert, H., R. Holm, and E. Münck. 1997. Iron-sulfur clusters: nature's modular, multipurpose structures. *Science* **277**:653–659.

Brandt, U., and B. Trumpower. 1994. The protonmotive Q cycle in mitochondria and bacteria. *Crit. Rev. Biochem. Mol. Biol.* **29**:165–197.

Darrouzet, E., C. Moser, P. L. Dutton, and F. Daldal. 2001. Large scale domain movement in cytochrome bc1: a new device for electron transfer in proteins. *Trends Biochem. Sci.* **26**:445–451.

Grigorieff, N. 1999. Structure of the respiratory NADH:ubiquinone oxidoreductase (complex I). *Curr. Opin. Struc. Biol.* **9**:476–483.

Michel, H., J. Behr, A. Harrenga, and A. Kannt. 1998. Cytochrome *c* oxidase. *Ann. Rev. Biophys. Biomol. Struc.* **27**:329–356.

Mitchell, P. 1979. Keilin's respiratory chain concept and its chemiosmotic consequences. *Science* **206**:1148–1159. (Nobel Prize Lecture.)

Ramirez, B. E., B. Malmström, J. R. Winkler, and H. B. Gray. 1995. The currents of life: the terminal electron-transfer complex of respiration. *Proc. Nat'l. Acad. Sci. USA* **92**:11949–11951.

Ruitenberg, M., et al. 2002. Reduction of cytochrome *c* oxidase by a second electron leads to proton translocation. *Nature* **417**:99–102.

Saraste, M. 1999. Oxidative phosphorylation at the fin de siecle. *Science* **283**:1488–1492.

Scheffler, I. 1999. *Mitochondria.* Wiley.

Schultz, B., and S. Chan. 2001. Structures and proton-pumping strategies of mitochondrial respiratory enzymes. *Ann. Rev. Biophys. Biomol. Struc.* **30**:23–65.

Tsukihara, T., et al. 1996. The whole structure of the 13-subunit oxidized cytochrome *c* oxidase at 2.8 Å. *Science* **272**:1136–1144.

Walker, J. E. 1995. Determination of the structures of respiratory enzyme complexes from mammalian mitochondria. *Biochim. Biophys. Acta* **1271**:221–227.

Xia, D., et al. 1997. Crystal structure of the cytochrome bc_1 complex from bovine heart mitochondria. *Science* **277**:60–66.

Zaslavsky, D., and R. Gennis. 2000. Proton pumping by cytochrome oxidase: progress and postulates. *Biochim. Biophys. Acta* **1458**:164–179.

Zhang, Z., et al. 1998. Electron transfer by domain movement in cytochrome bc_1. *Nature* **392**:677–684.

Harnessing the Proton-Motive Force for Energy-Requiring Processes

Bianchet, M. A., J. Hullihen, P. Pedersen, and M. Amzel. The 2.8-Å structure of rat liver F1-ATPase: configuration of a critical intermediate in ATP synthesis/hydrolysis. *Proc. Nat'l. Acad. Sci. USA* **95**:11065–11070.

Boyer, P. D. 1989. A perspective of the binding change mechanism for ATP synthesis. *FASEB J.* **3**:2164–2178.

Boyer, P. D. 1997. The ATP synthase—a splendid molecular machine. *Ann. Rev. Biochem.* **66**:717–749.

Capaldi, R., and R. Aggeler. 2002. Mechanism of the F_0F_1-type ATP synthase—a biological rotary motor. *Trends Biochem. Sci.* **27**:154–160.

Elston, T., H. Wang, and G. Oster. 1998. Energy transduction in ATP synthase. *Nature* **391**:510–512.

Kinosita, K., et al. 1998. F_1-ATPase: a rotary motor made of a single molecule. *Cell* **93**:21–24.

Klingenberg, M., and S. Huang. 1999. Structure and function of the uncoupling protein from brown adipose tissue. *Biochim. Biophys. Acta* **1415**:271–296.

Tsunoda, S., R. Aggeler, M. Yoshida, and R. Capaldi. 2001. Rotation of the **c** subunit oligomer in fully functional F_0F_1 ATP synthase. *Proc. Nat'l. Acad. Sci. USA* **98**:898–902.

Yasuda, R., et al. 2001. Resolution of distinct rotational substeps by submillisecond kinetic analysis of F1- ATPase. *Nature* **410**:898–904.

Photosynthetic Stages and Light-Absorbing Pigments

Blankenship, R. E. 2002. *Molecular Mechanisms of Photosynthesis.* Blackwell.

Deisenhofer, J., and J. R. Norris, eds. 1993. *The Photosynthetic Reaction Center,* vols. 1 and 2. Academic Press.

Govindjee, and W. J. Coleman. 1990. How plants make oxygen. *Sci. Am.* **262**(2):50–58.

Harold, F. M. 1986. *The Vital Force: A Study of Bioenergetics.* W. H. Freeman and Company, chap. 8.

McDermott, G., et al. 1995. Crystal structure of an integral membrane light-harvesting complex from photosynthetic bacteria. *Nature* **364**:517.

Prince, R. 1996. Photosynthesis: the Z-scheme revisited. *Trends Biochem. Sci.* **21**:121–122.

Wollman, F. A. 2001. State transitions reveal the dynamics and flexibility of the photosynthetic apparatus. *EMBO J.* **20**:3623–3630.

Molecular Analysis of Photosystems

Allen, J. F. 2002. Photosynthesis of ATP—electrons, proton pumps, rotors, and poise. *Cell* **110**:273–276.

Aro, E. M., I. Virgin, and B. Andersson. 1993. Photoinhibition of photosystem II. Inactivation, protein damage, and turnover. *Biochim. Biophys. Acta* **1143**:113–134.

Deisenhofer, J., and H. Michel. 1989. The photosynthetic reaction center from the purple bacterium *Rhodopseudomonas viridis*. *Science* **245**:1463–1473. (Nobel Prize Lecture.)

Deisenhofer, J., and H. Michel. 1991. Structures of bacterial photosynthetic reaction centers. *Ann. Rev. Cell Biol.* **7**:1–23.

Golbeck, J. H. 1993. Shared thematic elements in photochemical reaction centers. *Proc. Nat'l. Acad. Sci. USA* **90**: 1642–1646.

Haldrup, A., P. Jensen, C. Lunde, and H. Scheller. 2001. Balance of power: a view of the mechanism of photosynthetic state transitions. *Trends Plant Sci.* **6**:301–305.

Hankamer, B., J. Barber, and E. Boekema. 1997. Structure and membrane organization of photosystem II from green plants. *Ann. Rev. Plant Physiol. Plant Mol. Biol.* **48**:641–672.

Heathcote, P., P. Fyfe, and M. Jones. 2002. Reaction centres: the structure and evolution of biological solar power. *Trends Biochem. Sci.* **27**:79–87.

Horton, P., A. Ruban, and R. Walters. 1996. Regulation of light harvesting in green plants. *Ann. Rev. Plant Physiol. Plant Mol. Biol.* **47**:655–684.

Jordan, P., et al. 2001 Three-dimensional structure of cyanobacterial photosystem I at 2.5 Å resolution. *Nature* **411**:909–917.

Kühlbrandt, W. 2001. Chlorophylls galore. *Nature* **411**:896–898.

Martin, J. L., and M. H. Vos. 1992. Femtosecond biology. *Ann. Rev. Biophys. Biomol. Struc.* **21**:199–222.

Penner-Hahn, J. 1998. Structural characterization of the Mn site in the photosynthetic oxygen-evolving complex. *Struc. and Bonding* **90**:1–36.

Tommos, C., and G. Babcock. 1998. Oxygen production in nature: a light-driven metalloradical enzyme process. *Accounts Chem. Res.* **31**:18–25.

CO_2 Metabolism During Photosynthesis

Bassham, J. A. 1962. The path of carbon in photosynthesis. *Sci. Am.* **206**(6):88–100.

Buchanan, B. B. 1991. Regulation of CO_2 assimilation in oxygenic photosynthesis: the ferredoxin/thioredoxin system. Perspective on its discovery, present status, and future development. *Arch. Biochem. Biophys.* **288**:1–9.

Portis, A. 1992. Regulation of ribulose 1,5-bisphosphate carboxylase/oxygenase activity. *Ann. Rev. Plant Physiol. Plant Mol. Biol.* **43**:415–437.

Rawsthorne, S. 1992. Towards an understanding of C_3-C_4 photosynthesis. *Essays Biochem.* **27**:135–146.

Rokka, A., I. Zhang, and E.-M. Aro. 2001. Rubisco activase: an enzyme with a temperature-dependent dual function? *Plant J.* **25**:463–472.

Sage, R., and J. Colemana. 2001. Effects of low atmospheric CO_2 on plants: more than a thing of the past. *Trends Plant Sci.* **6**:18–24.

Schneider, G., Y. Lindqvist, and C. I. Branden. 1992. Rubisco: structure and mechanism. *Ann. Rev. Biophys. Biomol. Struc.* **21**:119–153.

Wolosiuk, R. A., M. A. Ballicora, and K. Hagelin. 1993. The reductive pentose phosphate cycle for photosynthetic CO_2 assimilation: enzyme modulation. *FASEB J.* **7**:622–637.